EXPLORING FIBRONECTIN'S INTEGRIN BINDING DOMAIN EFFECTS ON LUNG FIBROBLAST INTEGRIN SPECIFICITY AND DOWNSTREAM PHENOTYPIC DIFFERENCES

A Dissertation
Presented to
The Academic Faculty

by

Haylee N. Bachman

In Partial Fulfillment
of the Requirements for the Degree
Doctor of Philosophy in the
School of Chemistry and Biochemistry

Georgia Institute of Technology
December 2017

EXPLORING FIBRONECTIN'S INTEGRIN BINDING DOMAIN EFFECTS ON LUNG FIBROBLAST INTEGRIN SPECIFICITY AND DOWNSTREAM PHENOTYPIC DIFFERENCES

Approved by:

Dr. Thomas H. Barker, Advisor
Department of Biomedical Engineering
University of Virginia

Dr. Bridgette Barry
School of Chemistry and Biochemistry
Georgia Institute of Technology

Dr. M.G. Finn, Co-Advisor
School of Chemistry and Biochemistry
Georgia Institute of Technology

Dr. Wilbur Lam
Wallace H. Coulter Department of Biomedical Engineering
Georgia Institute of Technology and Emory School of Engineering

Dr. Loren Williams
School of Chemistry and Biochemistry
Georgia Institute of Technology

Date Approved: July 14, 2017

This thesis is dedicated to my Grandma. I never could have done this without your support and love. I miss you dearly.

ACKNOWLEDGEMENTS

This work could not have been accomplished without the love, encouragement, guidance, and involvement for a number of people. I would first like to thank my advisor Dr. Thomas H. Barker for letting me become a part of the Matrix Biology and Engineering Lab. My experience in graduate school has been exciting and challenging and I've been thankful to have had guidance and support that allowed me to pursue the science that I found interesting and for allowing me to make contributions that were impactful for the field and for the future work in the lab. I especially want to thank Tom for bringing me into the lab when I was not his student and making me feel welcome and then for taking me on officially and helping me to pursue something out of my comfort zone. I would secondly like to thank my committee members Dr. M. G. Finn who became my co-PI when Tom departed GT for UVA and allowed me the support I needed to finish up this work, Dr. Loren Williams for being both a teacher and confidant through some of the tough years, Dr. Wilbur Lam for always showing up to meetings and for being flexible with my ever changing project, and Dr. Bridgette Barry who was supportive of me by leading the Molecular Biophysics GAANN that I was supported under and for dedicating time to talk with me about my work and keeping up with me for several years. I am deeply appreciative that my committee has been so supportive and understanding of my personal experience through graduate school and has always had helpful insight and been a wonderful sounding board. I'd also like to thank Andrew Lyon for taking me on during my first year and for supporting my transition to the Barker Lab. I'd like to thank both Phil Santangelo and Mark Styczynski for allowing me space and supplies to work this spring and summer. I'd also

like to thank some other faculty who have been responsive to my emails, questions, and have been there for me through many different challenges (Nael McCarty, Michele McGibony, Kimberly Schurmeier, and Shannon Davis). I'd also like to thank Tami Hutto from the BEST program for helping me learn about myself and for exposure to exciting professional development opportunities.

I would next like to thank the members of the lab that have supported me in my work and in helping me to keep my sanity over the last several years. I honestly could not have done this without your help. I would like to thank the members of Dr. Andrew Lyon's lab who first took me under their wing to make me feel welcome particularly Dr. Emily Harden and Dr. Kim Clarke who have always been responsive and helpful. I would next like to thank the previous members of the Barker Lab who contributed to my training and were an essential source of reminding me that this was something I could do, Dr. Ashley Brown, Dr. Marilyn Dysart, Dr. Vince Fiore, Dr. Lizhi Cao, Dr. Alison Douglas, and Dr. Michelle Gaines. Thank you for laying the foundations to the lab and to the work I was able to carry forward and for being receptive to my naïve understanding and helping to train me in so many different ways.

Next, I would like to thank my fellow lab mates who have helped with crazy long experiments, who entertained me, picked me up when I felt lost, created a sense of comradery and who were nothing but the very best! Dwight Chamber was a constant companion and is a kickass scientist who was always the most giving of his time and energy to help me with my project. Between the many walks and talks, through hugs and tears and many good breakfasts, lunches, dinners and watching shows together you have been the very best work husband I could have asked for. John Nicosia has always tagged along on

my external journeys (business classes and BEST) and has been a wonderful emotional support when I felt lost about the abyss of the future. I could never thank either of you enough for ALL that you have done for me. Others in the lab (Vicky Stefanelli, Leandro Moretti, Riley Hannen, Wei Li, Ping Hi, Vincent Yeh, and the many new members who I haven't gotten to know) who were supportive for many years and will continue to be supportive of these projects in the future. I appreciate everything from feedback to sassy attitudes to pranks to potlucks and so much more. I'd like to thank Gulcin Azizoglu Arslan who helped to further this work and was supportive and always a positive spirit during some trying times. I'd also like to thank the undergraduate students who have worked with me over the years (Jane Watts, Evan Teng, and Kushal Shankar). As far as "labbies" go, y'all have been the best.

Next I'd like to acknowledge my family for their support. My Mom, Dad, and brother, Chris, have all been so supportive throughout this process and I'm thankful to have had them behind me always ready to be there when I needed it. I'd also like to thank Andrew's family for making me a part of your family and being so encouraging. I'd like to mention how much I appreciate so many of my friends who have listened to me many times and also who have let me blow them off and be late to dinners and who have just been the best friends a girl could ask for (Kait, Jessica, Rachel, and Tracy). I'd like to thank my roommate Caroline for listening to my whining and letting me know that this is do-able and for doing the last 5 years with me, thank you! Thank you to my many couple friends who have helped keep Andrew busy when I couldn't entertain him and for always creating a space where I could de-stress (Austin/Morgan, Sarah/Juan, Justin/Sarah, Chris/Fran).

Thank you to my many other friends not mentioned here from the neighborhood and from college, I would never have gotten this far without your encouragement early on.

Next, I'd like to thank my grandparents for creating a beautiful family for me to have been brought up with. Thank you to my Grandma for loving me and listening to me and pushing me to follow this dream.

Finally, I'd like to thank my loving boyfriend, Andrew, for your everyday support and love. You are my rock, my safe place, and my love. Thank you to you and Lucy for providing me so much love that the rest didn't seem to matter. Your constant encouragement, reassurance, and complete belief in me has made the hard days easier and the better days the best.

TABLE OF CONTENTS

LIST OF FIGURES

LIST OF SYMBOLS AND ABBREVIATIONS

α	alpha
αSMA	alpha smooth muscle actin
APTES	(3-aminopropyl) triethoxy silane
BSA	bovine serum albumin
CCL-210	normal human lung fibroblast
DMEM	Dulbecco's modified eagle's minimum essential medium
ECM	extracellular matrix
FBS	fetal bovine serum
Fn	Fibronectin
FnIII9-4G-10	fibronectin 9^{th} and 10^{th} type III domain with 4-glycine insertion
FnIII9-10	fibronectin 9^{th} and 10^{th} type III domain
FnIII9*10	fibronectin 9^{th} and 10^{th} type III domain with stabilizing point mutation
FPLC	fast protein liquid chromatography
HRP	Horse radish peroxidase
IPF	idiopathic pulmonary fibrosis
IPTG	isopropyl β-D-1-thiogalactopyranoside
MRTF	myocardin related transcription factor
MTT	3-(4,5-dimethykthiazol-2-yl)-2,5-diphenyltetrazolium bromide
MW	molecular weight
OD	optical density
PBS	phosphate buffered saline
PBST	phosphate buffered saline, with 0.1% Tween-20

PCR	polymerase chain reaction
SDS-PAGE	sodium dodecyl sulfate polyacrylamide gel electrophoresis
TBS	tris buffered saline
TBST	tris buffered saline, with 0.1% Tween-20
TGF-β	transforming growth factor beta
WB	western blot

SUMMARY

The extracellular matrix (ECM) is a complex, interactive, and dynamic protein mesh which provides support for cells through physical scaffolding and affords essential biochemical and mechanical cues about the surrounding environment. This non-cellular component of tissues can be maintained via cell regulation and recruitment of activated fibroblasts as well as from other contributing factors associated with the ECM. When there is dysregulation of the biochemical and mechanical (biophysical) cues the ECM provides to cells, fibrosis, a scar-like disease, can occur.

Idiopathic Pulmonary Fibrosis (IPF) is a disease where scar tissue forms in the lungs and the organ thickens and becomes rigid or stiff. In IPF the wound healing process is initiated and excessive matrix is assembled into a fibrotic state, excessive fibrous connective tissue and the cause for dysregulation of the normal wound healing process is unknown. As required cell-derived forces initiate remodeling the dynamics of the ECM turnover rate are increase within a fibrotic tissue. Increased stiffness in the direct environment could prevent mechanical deformation of protein in the local matrix; however, based on unpublished work from Thomas Barker's lab it is suggested that in the fibroblastic foci the tissue is soft and elastic. It is believed that the ECM proteins here may become strained and deformed, spatially changing conformation and providing different mechanical and biochemical cues to the cells in this environment and constitutive activity of the fibroblasts present at the site of injury. The IPF disorder is pervasive, affecting 5 million people worldwide[1]. Treatment is limited and life expectancy is short resulting in grave impacts on quality of life for patients. Tissue fibrosis is a necessary process important

to tissue repair. Fibrotic diseases are characterized by the dysregulation of matrix deposition that occurs leading to a disruption to matrix architecture and function which further leads to the characteristic excessive scar tissue formation. Fibroblasts become activated in the fibrotic environment which causes them to proliferate and secrete excessive amounts of ECM proteins, which then causes the environment to stiffen. Once the environment is stiff, then the fibroblasts may respond by becoming even further "activated" with increased contraction and other myofibroblast phenotype characteristics. Myofibroblast differentiation, activated fibroblasts, and cell contraction based cell-derived forces lead to physical unfolding and stiffening of the ECM. Within the diseased state a feed-forward is established where the wound healing responses and fibrobasts never revert from their activated state even after healing has occurred.

Proteins which comprise the matrix structure can become displaced and undergo cell traction force mediated partial unfolding. A stable intermediate is believed to be present which provides integrin selectivity for cells. These strained states of Fn will influence cell-ECM interactions ultimately leading to effects on cell phenotype. Cell-ECM interactions through cell-surface receptors, integrins, are greatly impacted when matrix alterations cause integrin preferences to change affecting many downstream signaling events which influence cell phenotype. FAK and Src are both integrin associated focal adhesion complex proteins that can influence cell migration, mechano-sensing, and proliferation.

One ECM protein that is especially interesting is fibronectin (Fn) because its expression and deposition in tissues following injury are distinctly increased. During repair there is an excess deposition of fibronectin into the ECM associated with fibrosis. It is

believed that polymerized fibronectin may serve as a precursor to collagen deposition. A more thorough understanding of the role of Fn's IBD in regulating cell activities which contribute to the development of fibrosis is necessary and explored in this work. Elucidating the impacts of Fn's IBD on fibroblasts is central to being able to mimic naïve and fibrotic environments for cell studies and for identifying key targets for therapeutic options. As such, the overall aim of this work is to identify cell responses to changes in the integrin binding domain of Fn to be able to determine which cell behaviors are resultant from the change in biochemical cues.

Integrin engagement can affect cell behaviors such as adhesion, migration and differentiation, as well as direct more coordinated behaviors like wound remodeling. Over the past decade, several groups have developed recombinant Fn fragments that engage specific integrins leading to distinct cellular responses. The mechanics of the Fn molecule are thought to be an important regulator of integrin specificity. Integrin-switch behavior has been introduced as a likely hypothesis. This theorizes that integrin engagement can be controlled based on the conformation of the integrin binding domain of Fn evidenced in the engagement of α5β1 on relaxed Fn fibers and equivalent engagement of αvβ3 on both relaxed and strained Fn matrices. The integrin α5β1 appears to be turned "off" when presented with "strained" conformations of Fn indicating that it engages with the promiscuous RGD integrin binding site as well as the spatially coordinated "synergy" site, PHSRN. Moving forward, the field will benefit from experimental evidence of this mechano-sensitive integrin switch hypothesis as well as further engineering advances in Fn-based tissue engineering strategies[2].

Biochemically, Fn fragments displaying the synergistic RGD and PHSRN binding sites facilitate cell binding through α5β1 integrins. Presentation of these domains in a specific conformation can lead to the influence on fibroblast phenotype. Smith *et al.* showed that extended Fn fibers can decrease cell spreading and adhesion[3]. Cells have the ability to bind RGD if they have access to this region contained in FnIII10. Fn fragments that display the RGD and PHSRN site with 4 Glycine linker, removing the presence and orientation of these synergistic sites and therefore the synergistic effect of the two sites, facilitates cell binding primarily through αv integrins. This work indicates that there are differential responses in cell behavior based on if cells engage αvβ3 or α5β1 integrins. Since these integrins are the two key integrins known to bind to Fn they are of particular interest; however, their direct influence on cell behavior within lung fibroblasts has not been studied extensively. Steered molecular dynamics simulations have been performed in order to predict the structural states of Fn's integrin binding domain under force which indicate that "extended" conformation displaces the RGD and "synergy" sites[4]. It is believed that by mimicking the extended conformation of FnIII9-10 (IBD) with a recombinant fragment by spatially separating the sites with a 4 Glycine linker designed to engage only αvβ3 integrins. Engagement of this integrin alone is believed to lead to enhanced activation of fibroblasts and ultimately a more myo-like fibroblastic profile. It has been shown by Liu *et al.* and others that β1 integrins are implicated in activated fibroblasts necessary for tissue repair *in vivo*[5,6]. Specifically, enhanced β1 binding is associated with increased cell contractility through the rho-ROCK pathway. These effects are not solely on or off but presentation of variations between RGD and PHSRN distance

can have influence on integrin engagement. Certain pathways can be activated based on integrin engagement.

An in depth investigation into integrin-switch behavior and the downstream phenotypic changes that are affected in fibroblasts is examined. There are biochemical cues that we have previously explored with epithelial cells, that can direct cell behavior and I want to explore this effect of a normal human lung fibroblast to act more myo-like if directed with preferential integrin engagement. Biophysically, mechanical stiffness can also be an influencing factor sufficient to cause myofibroblast transition. The results explored through analyzing the cellular response to micro-mechanical environment and matrix presentation could likely be attributed to phenotypic changes of lung fibroblasts, particularly those often associated with fibrotic disease progression.

It is important to further understand the physiological processes that result in normal wound remodeling vs. progressive fibrosis. In this thesis the biochemical and biophysical cues that influence cell response to environmental changes will be explored. We examine Fn's IBD as recombinant peptides that mimic the protein in a relaxed or strained conformation and find that there is an influence on cell behavior based on presentation of RGD and PHSRN. The work in this Thesis provided a clearer understanding of how the fate of a fibroblast can be defined and regulated based on biochemical changes in cell microenvironment. This work in combination with biophysical regulation through substrate stiffness could provide testing environments to determine the total effects that the cell microenvironment can have on cell fate.

CHAPTER 1. INTRODUCTION

1.1 Specific Aims

Fibrosis predominantly occurs in soft tissues through fibroblast proliferation and deposition of extracellular matrix (ECM)[7,8]. Pulmonary fibrosis is a disease involving advanced scarring of the lung tissue resulting in the thickening and ultimately stiffening of the lung. Chronic fibrotic disorders are plagued by unrelenting fibrotic remodeling which disrupts normal microenvironment structure and can ultimately impair organ function. Idiopathic pulmonary fibrosis (IPF) is a progressive and terminal fibrotic disorder affecting 50 of every 100,000 Americans with an average survival rate of 3 years post diagnosis[9,10]. The current understanding of the causes of this condition are not known, and there is no present cure or widely accepted treatments[9-11]. In IPF, recruitment and constitutive activity of fibroblasts causes the excessive deposition of ECM proteins resulting in scar formation and lung stiffness. Fibrogenesis is thought to be driven by excessive matrix deposition and abnormal myofibroblast contractility and results in alterations to the mechanical properties of tissues[12]. Pathologically this is relevant because alterations in extracellular mechanics can modify cell behavior such that rigid ECM leads to fibroblast activation towards a state of increased matrix synthesis and proliferation[13-15]. Cells are able to sense and respond to the ECM as it is a biochemical and mechanical environment. It is known that specific integrin signaling is present within stiff cellular environments[16]. Integrin-switch behavior is a hypothesized mechanism regulated by the spatial relationship of RGD and "synergy" site, PHSRN, on the Fn integrin binding domain. It has been implicated that through separation of these two integrin binding sites engagement of α5β1 integrin is switched "off"

opposed to αvβ3 integrins which engage RGD alone or when the two sites are confomationally stable. Specific integrin signaling leads to enhanced fibroblast activation (i.e. enhanced proliferation, resistance to apoptosis, migration/invasion, and ECM synthesis); however, the details of the effects of differential integrin engagement on downstream signaling are still largely unknown. Underlying matrix stiffness also influences cell fate because it has been proven that cells will alter their internal stiffness to match their surroundings as a response to substrate stiffness which can ultimately lead to increased cell contractility and ultimately a more myofibroblastic phenotype[17]. Discovering new therapeutic targets that could inhibit the progressive nature of this disease is critical for patient survival and quality of life.

Myofibroblasts are the primary effector cell in IPF. Fibrosis is evident by increased deposition of extracellular matrix proteins and myofibroblast presence. Myofibroblastic cells will have a contractile phenotype and are characterized by the appearance of α-smooth muscle actin[18]. Myofibroblasts are likely to be derived by activation/proliferation of local lung fibroblasts, though their origins are still debated. Therapeutic treatments of IPF could benefit by interfering with the pathways that lead to myofibroblast expansion; however, it is important to first understand the differential engagement of the lung fibroblast integrin-switch and how it leads to potentiation of myofibroblast phenotype differentiation. Since fibroblasts are responsible for and sensitive to changes in ECM rigidity, understanding how fibroblasts "sense" and "respond" to their environment is of key importance to understand the pathology of IPF. Fibroblasts are responsible for Fn IBD conformational changes and this work seeks to explore their sensitive to these changes.

Fibronectin, an ECM protein that is assembled into fibers serving as a provisional matrix is important in would healing. Fibronectin interacts with cells via cell surface receptors called integrins. Molecular dynamic simulations have suggested that under tensile force there is a conformational change within the integrin binding domain of fibronectin that is hypothesized to skew the affinity of specific integrin heterodimers to Fn[19-23]. This partial unfolding of Fn's type III repeats under tensile force outlines a possible mechanism for the mechanical force of the extracellular environment to have influence on intracellular signaling. We have developed recombinant fragments of Fn's integrin binding domain that mimic the predicted "relaxed" and "strained" states.

1.1.1 Hypothesis

Loss of fibroblast engagement of Fn via the α5β1 integrin drives myofibroblast differentiation

This approach seeks a deeper understanding of the biochemical effects on cell behavior which can ultimately lead to IPF. Current treatment options are widely unavailable (lung transplant) or only slow disease progression (pirfenidone and nintedanib)[24-26]. Since we know that myofibroblasts are a primary effector in IPF we hope to better understand the influence that integrin engagement has on determining myofibroblast phenotype in order to explore therapeutic options that could selectively inhibit αvβ3 integrin and not α5β1 integrin interaction with fibronectin[27]. Investigating the assembly of stress fibers and focal adhesion structures can provide insight into the biochemical signaling, mechano-transduction, as cells transduce rigidity cues[28]. Further

understanding of the cell-matrix interaction will allow us to understand how a potential therapeutic could affect cell behaviors.

In this thesis, my objective was to further understand the cellular responses based on differential integrin engagement through exploration of cell signaling events and myofibroblast characteristics. This was accomplished using qualitative standard cell biological practices and phenotypic characterization methods with these (2) aims:

1.1.2 Specific Aim 1

Observe how fibronectin's integrin binding domain (reflected by recombinant fibronectin fragments) triggers differential integrin engagement (integrin-switch) in lung fibroblasts and affects focal adhesion associated signaling proteins

*1.1.2.1 Characterize "integrin switch" with α5 and αv integrin immunostaining on FnIII9-4G-10 and FnIII9*10*

*1.1.2.2 Investigate the quality of focal adhesions on FnIII9-4G-10 and FnIII9*10 over time*

*1.1.2.3 Determine force-mediated focal adhesion components (FAK and Src) associated with FnIII9-4G-10 and FnIII9*10*

1.1.3 Specific Aim 2

Characterize phenotype due to conformational bias of recombinant fibronectin integrin binding domain.

*1.1.3.1 Evaluate lung fibroblast cell contractility (via size and shape) on FnIII9-4G-10 and FnIII9*10*

*1.1.3.2 Asses cell proliferation and metabolism on FnIII9-4G-10 and FnIII9*10*

1.1.3.3 *Calculate MRTF nuclear localization on FnIII9-4G-10 and FnIII9*10*

To evaluate the influence of the integrin binding domain of Fn, recombinant protein fragments which were previously designed will be used. Design of an optimized protein production system was performed for ease of use for evaluation efforts of human lung fibroblasts and their pathway through myofibroblast differentiation. Spatial decoupling of the cell binding motifs (RGD and PHSRN) within the cell binding domain of fibronectin are expected to produce phenotypic shifts in lung fibroblasts in important wound healing phenotypes.

Early analysis of integrin binding by SPR and lung fibroblast adhesion on these substrates indicated a switch in the integrins engaged for attachment and spreading; fibroblasts engage a greater ratio of α5β1 integrin on FnIII9*10, whereas they display an increased shift in ratio towards integrin αvβ3 on FnIII9-4G-10[29]. Analysis of the influence of this differential integrin engagement should be completed through further evaluation of focal adhesion markers, resistance to apoptosis and myofibroblast differentiation markers. Through our previous work on Fn's hypothesized integrin switch effects on epithelial-to-mesenchymal transition we were led to hypothesize that the extended conformation of Fn's integrin binding domain will enhance myo-like differentiation (myofibroblastic) and resistance to apoptosis. In the work looking at epithelial cells it was shown that these engineered integrin-specific recombinant Fn fragments can be used to guide cell

phenotype[30]. It was hypothesized that a similar approach could be taken to explore if fibroblast to myofibroblast transition occurred in normal human lung fibroblasts.

The innovative nature of this project comes from the exploration of the relationship of the integrin- switch behavior with cell fate. Current studies of Fn conformational change have been limited to molecular dynamics simulations and AFM studies. These experiments have supported theories about Fn conformation change but they have not explored the physiological relevance or examination of these changes in native ECM. Exploration of these recombinant Fn integrin binding domain proteins on differential integrin engagement and impact on lung fibroblast behavior is a novel pursuit. Based on previous work and our expertise we expect that when the synergistic effect of RGD and PHSRN is reduced and α5β1 is no longer engaged and the primary integrin engaged is αvβ3 there will be a change in fibroblast fate leading to differential focal adhesion component association and downstream internal cell signals that results in a more myofibroblastic phenotype. This work is impactful because it associates specific stimuli (mechanical and biochemical) with myofibroblast differentiation and ultimately events that are related to lung fibrosis.

This project has the potential to advance the field by furthering our understanding of the integrin engagement behavior that likely contributes to the recruitment of fibroblasts and the phenotypic characteristics of lung fibroblasts associated with Fn presentation, both of which could lead to the excessive deposition of extracellular matrix which is ultimately the primary contributor to fibrosis and in particular the relevance we see for specific lung diseases, such as idiopathic lung fibrosis. Current research focuses on therapeutic targets to inhibit further fibrosis. While this is useful information, it is advantageous to also understand if the specific integrin engagement can be a potential target for therapeutics and

if αvβ3 can be solely responsible for myofibroblast phenotype. Here, we explore these recombinant Fn fragments to probe important wound healing phenotypes of fibroblasts, such as proliferation, mechano-transduction and myofibroblastic differentiation. The potential of a detailed comprehension of fibrotic integrin mechano-switch interactions could greatly expand the way that IPF is treated.

1.1.4 Significance

The extracellular matrix (ECM) comprises the non-cellular component of tissues, including water, proteins, and polysaccharides. Although the basic components remain the same, the ECM of each tissue has a unique composition and organization that leads to a wide diversity of ECM arrangement and structure in the body. Additionally, the ECM of a tissue is highly dynamic, and undergoes remodeling by cells through both enzymatic and non-enzymatic processes. Fibrous ECM proteins such as collagen and fibronectin (Fn), form complex 3D scaffolds that mechanically support cells and form the basis of tissue shape[31]. This support can exert signaling cues through a process known as mechano-transduction. For example, varying the rigidity of ECM substrates can influence cell behaviors such as adhesion, migration, and differentiation[32-34]. However, the role of the ECM is not limited to mechanical support. ECM components also provide numerous biochemical cues to cells through the presentation of specific amino acid binding sequences. Cells bind to ECM proteins primarily through ECM receptors called, integrins[35-37], which then directly initiate signaling responses that can affect cell behavior and direct coordinated physiological responses[38].

Fn is an excellent example of an ECM protein that is intricately involved in cell behavior. With binding sites for integrins, other ECM proteins, growth factors, and other Fn molecules, Fn is a mediator in many cellular interactions with the ECM[39]. As a result, Fn plays a key role in cell behaviors such as adhesion, migration, and differentiation, as well as more coordinated tissue behaviors such as morphogenesis and wound healing. Fn is capable of binding a number of different integrins, and growing evidence suggests that the selectivity of integrin engagement can drive distinct cell responses. In this thesis, I discuss in detail the fundamentals of Fn-integrin interactions, the mechanical properties of Fn that may contribute to the specificity of integrin engagement, and the physiological consequences of integrin specificity.

In response to injury the wound healing process is initiated and can for unknown reasons enter into overdrive with potential feed-back loops accelerating without restraint resulting in fibrosis. Progressive loss of lung elasticity and respiratory capacity can be the result of this scar tissue build up. Particularly in idiopathic lung fibrosis, the exact causes of fibroblast dysregulated continuous activation are still unclear but there is reason to believe that minor injury occurs in the lungs caused by irritants such as smoke inhalation or particulate matter present in many smoggy environments in combination with genetic pre-disposition to react adversely which trigger resident fibroblasts to synthesize, assemble, and remodel their ECM through excessive protein deposition. This diagnosis is fatal with a prognosis of approximately 3-5 years. Pulmonary fibrosis is known to be result of the cells constitutive activation and excessive matrix deposition. This matrix deposition is signaled by specific cell surface receptors. Evidence of active fibrosis is exhibited by

increased number of activated fibroblasts, many of which have the phenotypic characteristics of myofibroblasts.

Specifically in IPF, the extracellular matrix (ECM) is constitutively produced resulting in scar formation and lung stiffness. It is known that specific integrin signaling is present within stiff cellular environments which in turn lead to enhanced fibroblast activation (i.e. enhanced proliferation, resistance to apoptosis, migration/invasion, and ECM synthesis).

Further understanding the effects that matrix mechanics and triggered signaling can have on cell fate and disease pathophysiology can be used to understand the mechanobiology of the lungs and the pathological implications of tissue stiffness and strain[40-42]. Since fibroblasts are the drivers of fibrotic progression understanding how they sense and respond to biochemical and mechanical cues is essential to better understand lung physiology *in vivo*. This work is aimed towards discovering novel molecular pathways for therapeutic targets in IPF.

Cells communicate with the ECM protein Fn through integrin receptors on the cell surface. Controlling integrin-Fn interactions offers a promising approach to directing cell behavior such as adhesion, migration, and differentiation, as well as coordinated tissue behaviors such as morphogenesis and wound healing. Several different groups have developed recombinant fragments of Fn that can control epithelial to mesenchymal transition, sequester growth factors, and promote wound healing[43]. It is thought that these physiological responses are in part due to specific integrin engagement.

Furthermore, it has been postulated that the integrin-binding domain of Fn is a mechanically sensitive "switch" that drives binding of one integrin heterodimer over another. Although computational simulations have predicted the mechano-switch hypothesis and recent evidence supports the existence of varying strain states of Fn *in vivo*, experimental evidence of the Fn integrin switch is still lacking but through the publication of our work in Cao *et al.* the evidence is more clear *in vitro*[29]. This work indicates that there is influence of Fn presentation on initial cell integrin engagement, focal adhesion formation and signaling, downstream cell behavior, and eventual influence on cell phenotype. Evidence of the integrin mechano-switch will enable the development of new Fn-based peptides in tissue engineering and wound healing, as well as deepen our understanding of ECM pathologies, such as fibrosis.

Cell interactions with the extracellular matrix (ECM) can drive not only cell behaviors such as adhesion and migration, but also contribute to wound healing. Fibronectin (Fn), a cell-adhesive ECM protein, has been studied for several decades, yet still offers a rich variety of new information regarding its interaction with cells and other components of the extracellular environment. This thesis focuses on Fn-integrin interactions, and their subsequent effect on cell and tissue behavior. Recent advances in engineering recombinant Fn-based protein fragments are also discussed.

Engineer fragments are used to mimic work that was initially explore *in* silico. Molecular dynamics simulations have suggested that when applied forces are present Fn's 10th III repeat can partially unfold. The intermediate state that is then represented has a distance between the 9th and 10th type III repeat leading to downstream effects on cell behavior. The indicated spatial separation of the two key binding sites RGD and PHSRN

present in FnIII9-10 can implicate mechano-transduction effects. Engineered recombinant Fn fragments are attractive as a guide for cell phenotype because they could help interpret effects sensitive to force mediated translocation.

To interpret effects of ECM proteins effects on cell behavior recombinant peptides are utilized to track the downstream effects based on differential integrin engagement. Fn is known to be present in the ECM of injured tissues undergoing regeneration. Latent wound healing can be promoted by controlling Fn's integrin binding domain. Fn's integrin-binding domain has been studied and recombinant Fn fragments that contain this region are of particular interest due to the relevance to cellular response. Engineered Fn fragments have also been shown to inhibit growth factors, control epithelial to mesenchymal transition. This makes Fn fragments a desirable candidate for tissue engineering.

Understanding cell-integrin interactions and their role in directing cellular processes can be useful for tissue engineering approaches that aim to study *in vitro* cell behaviors. Further understanding how cell-Fn interactions play a role in cell behavior within wound healing is central to determining therapeutic targets that may aim to inhibit constitutive fibroblast activation leading to pathological, fibrotic disorders. Being able to understand the role that integrins play in fibroblast activation and in their overall phenotype can be useful and eventual combination with therapeutic options can provide insight for eventual *in vivo* implications that may occur. In this thesis we show how Fn's IBD influences cell adhesions and cell behavior through engineered Fn fragments that have been previously utilized to direct endothelial phenotype and mimic the "strained" spatial conformation present during lung stiffening.

CHAPTER 2. BACKGROUND AND LITERATURE REVIEW

Portions of this chapter are adapted from previously published work: "**Haylee Bachman**, John Nicosia, Marilyn Dysart, Thomas H. Barker, *Utilizing fibronectin integrin-binding specificity to control cellular responses.* **Advances in Wound Care. August 2015 4(8) pp. 501-511** Publication date: July 2, 2015 DOI: 10.1089/wound.2014.0621"[2]. The author of this document contributed to this work primarily through overall literature review and writing of the manuscript.

2.1 IPF and Fibrosis

Idiopathic pulmonary fibrosis is a disease that affects roughly 200,000 Americans and is a terminal disorder which lacks therapeutic options that can prevent disease progression[25,44]. This disease is one of several fibrotic disorders that are characterized by excessive matrix deposition and tissue scarring. In this disorder the activated fibroblasts, termed myofibroblasts, are initiated into a wound healing process and extracellular matrix is excessively deposited. Connective tissue then thickens and becomes more rigid, triggering a positive force feedback loop and dysregulated bidirectional signaling between cell and matrix. In this environment the matrix deposition is uncontrolled and myofibroblasts will become constitutively active, leading to thickening of the matrix. Cues from enhanced stiffness will continue to drive the myofibroblast phenotype. It is understood that mechanical forces can drive biochemical signals and that the fibrotic matrix is providing information to cells that drives fibrosis[15].

2.2 The ECM:

The extracellular matrix (ECM) is an essential non-cellular component of tissues that is made up of protein scaffolding, which defines the extracellular microenvironment, and provides support to the surrounding cells[31]. ECM proteins provide important cues for cells through both composition and structure which can ultimately influence cell adhesion and signaling. Cells can bind via integrins, heterodimeric cell-surface receptors, which bind to specific sequences on their ECM proteins[45,46]. These interactions between cells and their microenvironment can ultimately direct cellular fate. Cell adhesion and signaling can be influenced by protein composition and structure within the ECM. Cellular fate in the sense of survival, proliferation, migration, and differentiation can be dictated by the complex and dynamic nature of cell-ECM interactions[47]. Specifically, biological tissues are heterogeneous mixtures of various ECM proteins including collagens, laminins, proteoglycans and many other components which can bind and sequester growth factors that control spatial and sequential cellular process control.[48] All of these components explain the complexity of the native ECM's dynamic ability to control cell fate. This diverse set of constituents results in a highly complex and dynamic ECM environment that must be regulated to direct cell and tissue fate.

The ECM is naturally in a state in which cells are constantly synthesizing new protein components and remodeling the ECM both mechanically, through deformations induced by cell contractile forces, and proteolytically through secretion of numerous proteases and new matrix molecules. Larger scale tissue composition can be impacted by these remodeling events to the ECM. Some lung cells, particularly fibroblasts, over-produce extracellular matrix when they are in a strained environment which further leads to fibrosis. The wound healing environment is believed to be induced by breakages and

tears possibly due to environmental factors such as smoking or pollution. Understanding this environment and how we can control the activity of fibroblasts and their regulation of matrix proteins is imperative to expanding therapeutic treatments in this field.

Many different ECM proteins play a pivotal role in controlling cell fate within larger scale tissues. During development, repair, and regeneration of epithelial tissues, cells must interact with the fibronectin-rich matrix of granulation tissue.[39] In epithelial tissues including the lung, breast, and kidney, epithelial cells interact with an underlying matrix composed predominantly of collagen and elastin. However, in response to injury and during repair the matrix shifts from predominantly collagen and elastin to a provisional matrix composed predominantly of fibrin and fibronectin. This biochemical shift has been shown to skew integrin engagement from α3β1 to αvβ3, which in turn leads to changes in cell behavior and phenotype.[30] This matrix composition is mimicked in the lungs during IPF and similarly shifts integrin engagement from α5β1 to αvβ3[37,49]. This fibronectin matrix may have a role in directing cells to a more migratory/repair phenotype. Specifically, in pulmonary tissue, the underlying vasculature is damaged and results in the initiation of the clotting cascade and the creation of a fibrin rich intermediate ECM with areas of cross-linked fibronectin.[50]

2.3 Fibrosis Directed Microenvironment Changes

These changes in the matrix result in signaling changes to the cells to direct healing and regeneration. Specifically, this provisional fibronectin matrix has been shown to direct cells to a more migratory/repair phenotype. Fibrosis Directed Microenvironment Changes

The local cellular microenvironment consists mainly of the ECM but also contains soluble signals and substrate-bound macromolecules (ie. neighboring cells). Cells will consistently and continuously synthesize, assemble, and remodel the extracellular matrix. Cells are known to have the ability to communicate bidirectionally with the ECM by being both sensitive to changes in the ECM and influencing the modulation of the local ECM[51]. The inside-out and outside-in signaling is regulated by integrins. During fibrosis the abundance and ligand presentation of connective tissue deposited by fibroblasts changes creating effects on biochemical and biophysical properties of the ECM[15]. As shifts are made towards a fibrotic matrix tissue rigidity responds comparatively and tensile strain occurs further providing signals for disease progression.

Pro-fibrotic cell responses occur in response to ECM stiffness. Fibroblasts experiencing matrix stiffening increase α-SMA expression which then constitutively promotes further activation of cytoskeletal features[52,53]. It is known that α-SMA gene expression is driven by MRTF nuclear localization[41]. Other important features such as cytoskeletal contractility are indicated based on pro-fibrotic changes to fibroblasts. Matrix stiffening also promotes fibroblast proliferation and increased matrix synthesis. This relationship between the microenvironment and fibroblasts demonstrates the feedback loop in which there is bi-directional regulation of the cell's remodeling ECM and the sensitive response of the cell to its local microenvironment. During normal tissue regulation the local rigidity of the environment is bi-directionally regulated and when fibrotic disease is present the cytoskeletal-ECM adhesion complexes provide indication to the fibroblasts that they should activate. When the biophysical state of the ECM indicates activation of fibroblast

cytoskeleton the balanced relationship of this feedback loop may become unstable and chronic fibrotic remodeling can occur.

2.4 Fundamentals of Integrin Binding to Fibronectin

2.4.1 Fn Structure

Fibronectin (Fn) is a dimeric glycoprotein containing two identical ~220kDa subunits that are covalently linked through a pair of disulfide bonds near their C-termini. Each subunit is composed of three types of repeating modules: Type I (12 modules), II (2 modules), and III (15-17 modules) (Figure 1). Type I and Type II modules contain two intra-chain disulfide bridges, not present within Type III modules. Type I modules have a hydrophobic core made up of highly conserved aromatic residues and a disulfide bond which is enclosed by stacked β sheets[54]. Type II repeats are made up of perpendicular anti-parallel β-sheets linked together through the previously described disulfide bonds[55]. Type III repeats are approximately 90 amino acids long and do not contain intra-chain disulfide bonds. These repeats are made up of anti-parallel β-sheets linked together with flexible loops, and only hydrogen bonding stabilizes them[56,57]. As a result, Type III repeats are highly sensitive to force-mediated unfolding[58]. These functional domains mediate interactions amongst Fn itself, with integrins, and with other ECM components. In particular there are 15-18 type III repeats which each are approximately 90 residues long and do not contain any disulfide bonds.

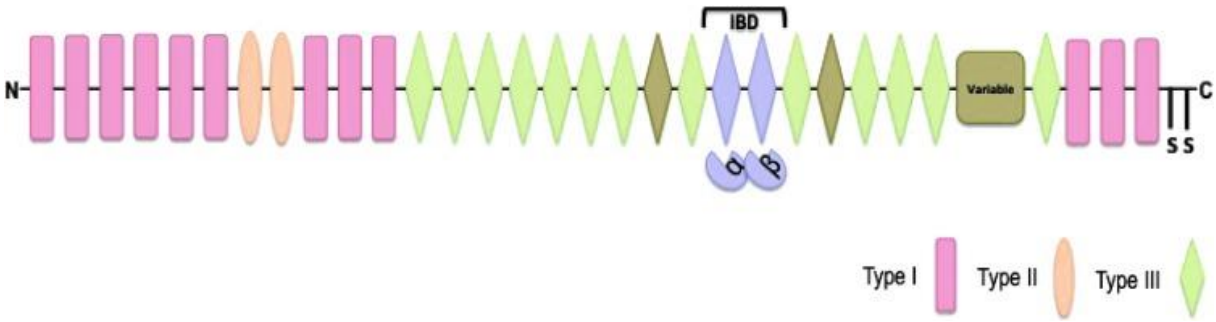

Figure 1: Modular structure schematic of full-length fibronectin molecule

Fn is a known ligand for many integrin receptors, linking the extracellular matrix with the intracellular cytoskeleton. Although there are many different integrins that bind to Fn, the classic receptor is the α5β1 integrin receptor. Specific integrin-recognition sites have been identified within the Fn molecule[39]. Identification of integrin-specific recognition sites was preceded by the characterization of Fn's interaction with cells and it was determined that the Fn-receptor interaction has only moderate affinity (Kd= $8*10^{-7}$ M) relative to other extracellular matrix protein receptors[59,60]. An isolated peptide sequence arginine-glycine-aspartic acid-serine (RGDS) has been identified as a key cell-binding site within fibronectin as well as a second, distant synergistic site within the cell-binding domain provides recognition effectively mediating adhesion and cytoskeletal organization[61]. Cellular Fn which is secreted in fibroblasts and many other cell types, is then incorporated into a fibrillar matrix on the cell surface. The cell-binding domain of Fn is comprised of an Arg-Gly-Asp (RGD) and synergy Pro-His-Ser-Arg-Asn (PHSRN) sequences.

2.4.2 Background on Integrins

Cells interact with their surrounding extracellular matrix (ECM), including Fn, via transmembrane cell surface receptors known as integrins. Integrins are heterodimeric

proteins consisting of one α subunit and one β subunit.[37]. A variety of ECM protein ligands can be bound by integrin receptors and these are studied elsewhere[62]. Integrins serve as the link between structural intracellular protein complexes and the extracellular environment, effectively physically coupling the intracellular and extracellular physical network.

The α and β subunits of integrins combine to form at least 24 unique heterodimers. Certain integrins can bind multiple ECM proteins, and some ECM proteins can interact with several different integrin heterodimers[63,64]. The presentation of specific adhesive ligands direct which integrins bind and correspondingly alter intracellular signaling events[64]. The ligand-binding sites within integrins, particularly for the ligand Fn, can be classified into two different groups of ligands: RGD-binding and LDV-binding type integrins. The active site pocket located between the α and β subunits binds ligand peptides and provides ligand specificity[37]. Integrin binding to Fn's cell binding domain offers an excellent example of the complexity of controlling integrin specificity and is a continuing area of investigation both from the perspective of how biochemical specificity is determined as well as the cell biological consequences of that specificity.

2.4.3 RGD and synergy sites in integrin binding interactions

The major cell-binding site for many integrins is the three amino acid sequence arginine-glycine-aspartic acid (RGD). This tripeptide, originally identified in Fn in 1983 by Erkki Rouslatti, is an integrin binding site present in many adhesive ECM, blood, and cell surface proteins[65]. Importantly, RGD is the primary cell attachment site for fibronectin binding by integrins[66]. Integrins that engage fibronectin via RGD include αIIbβ3, αVβ3, αVβ6, αVβ1, α5β1, and α8β1[37]. Mimicking adhesion proteins with RGD peptides has been a useful way to enable cell adhesion; however, RGD peptides alone are not selective for

specific integrins as they mimic sites in a number of adhesion proteins and are capable of binding to numerous different integrins[66].

The recognition of this simple tripeptide sequence can be quite complex and greatly depends on flanking residues, its three dimensional presentation, and individual features of the integrin-binding pockets For example, neighboring residues can inhibit or suppress the activity of RGD due to conformational restrictions that shield integrin binding[67]. Integrin binding can also be modulated by the activity of peptide sequences on neighboring domains. The best example of this is α5β1 integrin binding to Fn, in which RGD in combination with a second recognition sequence (PHSRN), the so-called "synergy" site, in the adjacent 9th type III repeat which when in synergy with RGD is known to promote the specific interaction of α5β1 integrin binding to Fn through interactions with the α5 subunit[20,21]. The synergy site is located approximately 32 Å from the 10th type III repeat RGD loop. The type III repeats show great elasticity in the loops between their F- and G-β strands, known as the FG loop, which allows the 9th and 10th type III repeats to present multiple conformations. Steered molecular dynamics (SMD) simulations suggest that under small applied forces (on the order of 10 pN) Fn's 10th type III repeat is susceptible to partial unfolding, resulting in an intermediate state in which the RGD loop within the 10th type III repeats begins to translocate away from the 9th type III repeat, resulting in an increase in the distance between the RGD and synergy sites from approximately 32 Å to approximately 55 Å[58]. The integrin α5β1 is the initial receptor mediating assembly of Fn into its fibrillar matrix. Due to the elasticity of type III repeats, the 9th and 10th type III repeats together present multiple conformations that direct integrin specificity to this region.[19] Fn is known to be highly sensitive to force-mediated unfolding in which these

two sites can be distanced from one another.[68] The best Fn unfolding model shows significant impact on integrin engagement and ultimately cell fate because of the domain unfolding of the Fn 9th and 10th type III repeats. This capacity to present multiple spatial orientations of the 9th and 10th type III repeats has great implications on cell binding and subsequent cell phenotype because the relative positioning of these two domains has been shown to influence integrin α5β1 binding. Integrin α5β1 binds by simultaneously engaging the RGD and synergy sites and is known to be highly involved in epithelial tissue repair. As these sites translocate away from one another, they can no longer be bound simultaneously, and integrin α5β1 no longer binds resulting in changes in the normal tissue repair process. These results suggest that the conformation of these two domains may be used to drive which integrins cells use to bind Fn. For example, by stabilizing the 9th type III repeat by a Leu-Pro mutation at amino acid 1408, there is an increased affinity for α5β1 over integrin αvβ3. Alternatively, by increasing the linker region between the RGD and synergy sites there is a reduction in α5β1 binding. Furthermore, α3β1 integrin binding to Fn may also be promoted by the 9th type III repeat (unpublished data). Integrins that do not bind the synergy site, such as αvβ3, are not affected by this separation in adhesive domains[30]. This is of particular interest because it suggests that the ratio of α5β1 binding to αvβ3 binding can be modulated by changing the conformation of these sites of Fn. This hypothesis forms the basis of Fn conformation-driven integrin specificity, and has significant implications in cell behavior, discussed later.

2.5 Molecular Dynamics of the Integrin-Binding Domain

Fn was first noted as a structurally dynamic protein by Erickson *et al.* in 1983. These researchers used electron microscopy and sedimentation analysis to observe the effect of

ionic strength on Fn conformation. At low ionic strength (0.05 M KCl), Fn was observed as a more compact, irregularly coiled strand. At increasing ionic strength (0.2 KCl), Fn was found to take on a more extended conformation with fewer intra-chain bends[69]. These observations suggested that electrostatic interactions influence Fn molecule conformation and introduced the possibility that other forces, such as mechanical tension on Fn fibers, may alter Fn structure as well. This discussion focuses primarily on the force-induced changes in the integrin-binding domain of Fn, composed of FnIII repeats.

2.5.1 Mechanics of the FnIII domain

About a decade later, the elasticity of another large protein, titin, was explored after observing that titin molecules extend up to four times their length at their I-band region. Titin is composed of many immunoglobulin and FnIII-like domains, and the extraordinary elasticity of titin is in part due to unfolding of these FnIII-like domains[70]. FnIII domains are composed of 7 β-strands arranged into 2 sheets, and are connected in series in an Fn molecule. Inspired by these findings, a structural model for the unfolding of FnIII domains was proposed in 1994 (Figure 2), but this was not directly validated on Fn fibers[71]. The comparisons to titin continued when researchers studied the intramolecular dynamics of FnIII10 (where the integrin-binding RGD motif is located) and an analogous FnIII-like domain on titin. Using ^{15}N nuclear spin relaxation, Carr *et al*. found that FnIII10 is more flexible than the corresponding titin domain, especially on the loop containing the RGD sequence. At the time, these results were discussed in the context of an "induced fit" model for Fn-integrin binding reactions, and were used as support for the idea that the RGD motif on FnIII10 was not as specific to distinct integrins as the analogous RGD motif on titin was[72]. If this idea were correct, we wouldn't expect to see specific integrins engaged with

Fn in different structural contexts. Yet previous work has shown that mutations affecting the mechanical stability and structure of FnIII9-10 can cause distinct integrins to bind[73]. An alternative explanation to these results might be that the flexibility of FnIII10 allows for greater mechanical sensitivity, through which Fn can tailor tension-modulated integrin specificity.

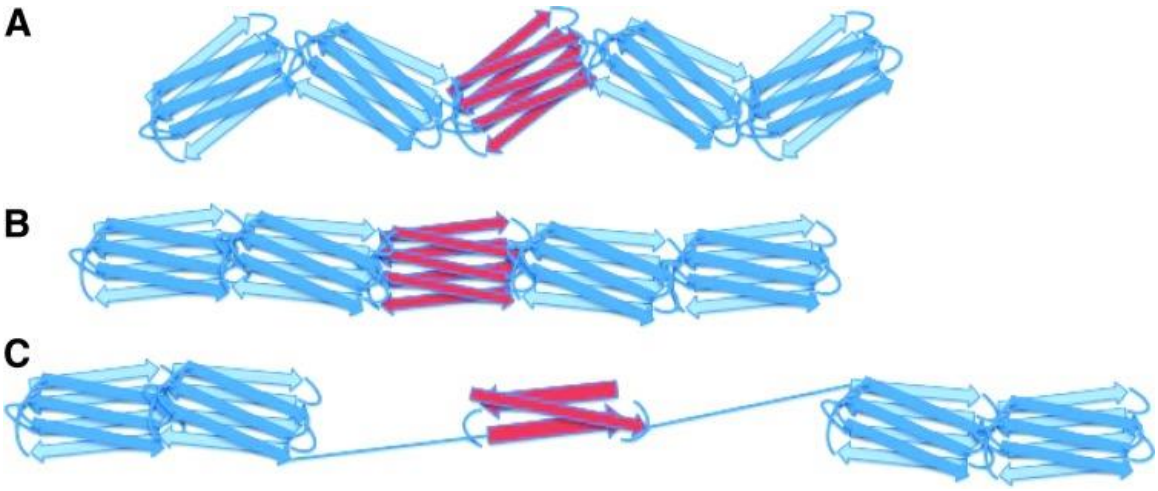

Figure 2. Proposed model of FnIII domain unfolding by Erickson in 1994[71]. As tension is applied to the relaxed molecule (A), the domains first align (B), followed by unfolding of certain domains (C), particularly the beta-sheet domains of the 9th and 10th type III repeats.

Knowledge on the molecular dynamics of FnIII domains was accelerated by the use of atomic force microscopy (AFM). AFM allows for single molecule measurements of force versus extension, providing myriad insights into the mechanical properties of fibrous proteins. The first protein with FnIII repeats to be investigated by AFM was Tenascin. Tenascin is an ECM protein important in embryonic development and tissue repair. Notably, tenascin contains multiple FnIII repeats along its chain. Single-molecule AFM was used to study the modular elasticity of tenascin, and suggested that unfolding of FnIII

domains was responsible for the sawtooth pattern of force versus extension curves observed in tenascin hexabrachions[74]. While this work focused on tenascin elasticity, the importance of FnIII domain unfolding has applications to other ECM molecules, especially fibronectin. The first study to specifically investigate the molecular dynamics of FnIII10 utilized steered molecular dynamics (SMD) simulations to describe the sequence of events of FnIII10 unfolding and the resulting effects on RGD loop accessibility to integrin binding. This study predicted that the β-strand attached to the RGD loop would be the first to break away from the module under tension, and would therefore pull the RGD loop, which is normally located between two β-strands, closer to the surface of the β-sheet structure that comprises the bulk of the module (Figure 3). This conformational change was suggested to decrease the affinity of the loop for integrin receptors on the cell surface. The authors discussed that this property of Fn may be a mechanism of mechanosensitive control of ligand recognition[75]. Further work with SMD showed that when compared to other FnIII domains such as FnIII7, FnIII8, and FnIII9, FnIII10 has the lowest force threshold for the early stages of unfolding. This conclusion is important when discussing the dynamics of the integrin-binding domain since it predicts that FnIII10 will be one of the first domains to unfold under tension[76]. This simulation was later confirmed by AFM measurements of FnIII domain unfolding[77]. The incorporation of the neighboring synergy site in SMD simulations of FnIII10 provided a structural model for the increase in distance between the synergy site (PHSRN, on FnIII9) and RGD and its effect on integrin binding[58]. These simulations gave structural confirmation to earlier studies, which noted that an increase in the linker region between synergy and RGD led to a decrease in α5β1 binding

in favor of αvβ3 binding[78]. These findings form the basis of the theories on the conformational sensitivity of integrin specificity to Fn.

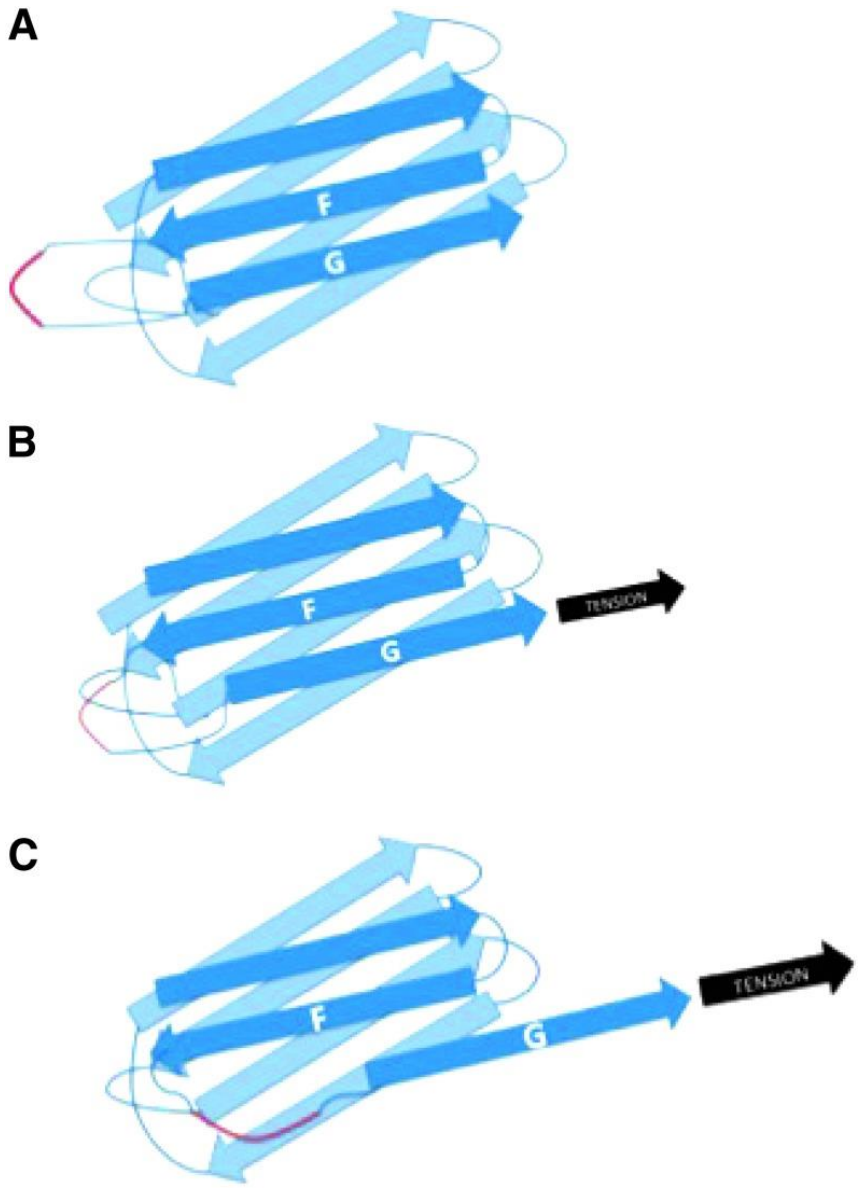

Figure 3. SMD simulations of early stages of FNIII10 unfolding under force. RGD loop is shown in red between the F and G strands. As the G strand of FnIII10 (shown in (A)) is pulled (B), the RGD loop is brought closer to the bulk of the module (C). SMD, steered molecular dynamics.

Simulations on the unfolding of FnIII domains were supported by *in vitro* experiments involving fluorescence resonance energy transfer (FRET). This technique

involves labeling fibronectin with two fluorophores: one donor, and one acceptor. Excitation energy from the donor fluorophore is transferred to the acceptor fluorophore, resulting in excitation of the acceptor. Energy transfer decays rapidly with increasing distance between the fluorophores, resulting in a signal that varies in strength directly with increasing distance. In fibronectin, the FnIII7 and FnIII15 domains are labeled with donor fluorophores, which encompass the integrin binding domain (FnIII9-10). The domains are labeled on cysteines and nonspecific labeling of exposed amino groups (lysines) with acceptor fluorophores so the Fn FRET probes will only indicate relative extension not which parts are extended; therefore, Fn FRET probe comparison across multiple batches cannot be compared because of the somewhat random nature of lysine labeling. This technique was first utilized to suggest unfolding of Fn in response to varying concentrations of a denaturant, and was then applied to show this effect in response to cytoskeletal tension[79,80]. Together with the SMD simulations discussed earlier, these results strongly suggest that cell-mediated forces can partially unfold the integrin binding domain of Fn. The first experimental proof proving this is evidenced in Cao *et al*[29].

Until recently, the existence of varying strain states in Fn fibers had not been observed in native tissue Previously bacterial adhesins were used to identify Fn fiber destruction of binding epitopes[81]. Therefore, phage display identified probes against fragments of Fn that mimic different spatial orientations of the Fn integrin-binding domain, peptide-based molecular probes were developed that could distinguish between "low-strain" and "high-strain" regions of Fn fibers[82]. These probes were used to stain *ex vivo* mouse lung slices, and discriminate between varying strain states in the tissue[83]. These results give strong evidence to the hypothesis that distinct force-induced structural states

of Fn exist *in vivo.* It is tempting to think of the integrin-binding domain of Fn as a mechanically sensitive "switch" for specific integrin engagement, and the SMD simulations discussed earlier support this idea. Moving forward, the challenge will be experimental detection of the conformational changes to the integrin-binding domain that confirm the validity of the switch model and its relevance to mammalian physiology.

Fn is known to be highly sensitive to force-mediated unfolding in which these two sites can be distanced from one another[68]. The best Fn unfolding model shows significant impact on integrin engagement and ultimately cell fate because of the domain unfolding of the RGD site, one of the most famous recognition sites, which is incorporated in the 10th type III repeat (FnIII10). This RGD loop promotes interaction via the αvβ3 subunit independent of the second recognition site. The second recognition sequence, 32Å away from the RGD loop, the "synergy site" PHSRN, is incorporated into the 9th type III repeat which allows these two motifs to synergistically promote α5β1 integrin binding to Fn. The integrin α5β1 is the initial receptor mediating assembly of Fn into its fibrillar matrix. Due to the elasticity of type III repeats, the 9th and 10th type III repeats together present multiple conformations that direct integrin specificity to this region[19].

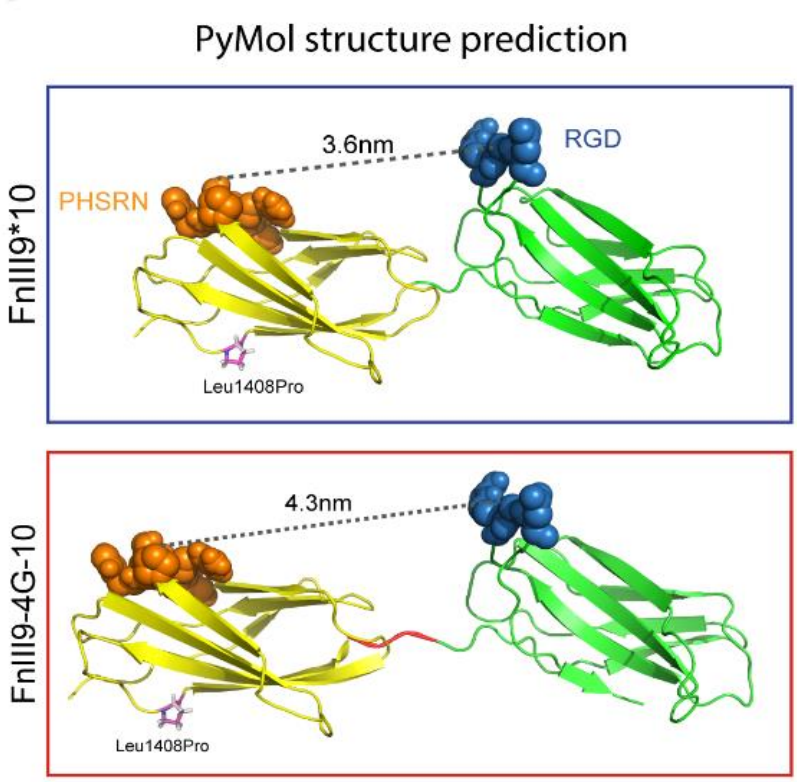

Figure 4. Fibronectin strain drives differential integrin affinity. PyMol structure predictions of engineered recombinant fragments of Fn's integrin binding domain. FnIII9*10, represents a stabilized native structure through a Leu-to-Pro point mutation at position 1408. In this conformation, the PHSRN-to-RGD distance is approximately 36 Å. FnIII9-4G-10 is a mutation of the FnII9*10 variant that contains a 4xGly insertion between the 9th and 10th type III repeats. This mutation increases domain separation and the PHSRN-to-RGD distance to approximately 43 Å. These fragments have been employed in the past to predict potential biological consequences of the theorized integrin switch.

2.5.2 Exposure of Cryptic Binding Sites

It is known that specific integrin signaling is present within stiff cellular environments which in turn leads to enhanced fibroblast activation (i.e. enhanced proliferation, resistance to apoptosis, migration/invasion, and ECM synthesis).

Concurrent with the advances in knowledge of FnIII unfolding, researchers had begun to investigate the process of Fn matrix assembly, which involves the polymerization

of multiple Fn molecules together into fibers. This process requires the accessibility of Fn-Fn binding sites on the Fn molecule. Treatment of Fn with Fn fragments containing a cleaved form of the first type III repeat (FnIII-1C) was found to stimulate spontaneous disulfide crosslinking of Fn molecules into multimers resembling matrix fibrils. It was hypothesized that III-1C represented a binding site within native Fn that became revealed during matrix assembly[84]. Shortly after, another group demonstrated that heat-denaturing III-1 allowed for it to bind the amino-terminal portion of Fn, as in matrix assembly. The authors noted that since Fn matrix assembly is a cell-dependent process, the exposure of the Fn binding site in III-1 could result from tension generated by the cytoskeleton through integrin-Fn connections[85]. These sites, exposed through cleavage of FnIII domains, heat denaturation, or tension, became known as cryptic binding sites. In the following years, other cryptic self-association sites were discovered in Fn[86]. Further research into this area confirmed that Rho-mediated cell contractility exposes cryptic binding sites in Fn and can induce Fn matrix assembly. Interestingly, it was also discovered that even III-10 contains a cryptic binding site for III-1, and could potentially serve as an assembly site for stretched Fn fibrils in focal adhesions[87,88]. About a decade later, it was shown that tension-mediated exposure of cryptic binding sites on Fn leads to an increase in fiber rigidity due to increased Fn-Fn binding. This strain-hardening property allows Fn fibers to limit how much they can be extended by cell-forces, and accordingly alter local ECM environments by increasing fiber rigidity, which can be sensed by cells[89].

2.6 Engineering approaches to control Fn-integrin interactions

2.6.1 FnIII9 and FnIII10 affect integrin specificity

It is believed that integrin specificity is related to the binding domains within Fn and their spatial relationships, which are controlled by the flexibility between the two sites of integrin binding within the FnIII9 and III10 domains. It has been directly observed that integrin specificity between the RGD and the "synergy" site, PHSRN, within the cell binding domain of fibronectin can direct cells down a migratory/repair phenotype necessary for wound healing processes[30]. These critical sites regulate epithelial cell phenotype by their ability to direct integrin specificity. Some ECM proteins contain the ability to specifically engage certain integrins, while other sequences within ECM proteins are known to be promiscuous for multiple integrins. It has been indicated that RGD, for example, engages αv integrins; however, due to the ability of several ECM proteins, particularly fibronectin, to be responsive to cellular and environmental changes such as cell adhesion and spreading forces, the distance between these two synergistic sites can have downstream effects on cellular expression. For example, peptides incorporating FnIII10 only (containing just the RGD site) lead lung epithelial cells down a path of epithelial to mesenchymal transition (EMT); whereas, peptides including the synergy site, such as FnIII9-10, maintain the epithelial phenotype of the same cells. Interestingly, substrate mechanics play an important role in this interaction. Stiff substrates (~32 kPa) spontaneously induce EMT in lung epithelial cells, but this response can be overcome by engagement with FnIII9-10. Taken together with the studies of RGD and synergy as they relate to specific integrin engagement (discussed earlier in section 5.1.3), these results suggest interplay between substrate rigidity sensing, stiffness-mediated cell phenotypes, and integrin specificity[43].

The 12th through 14th type III repeats of Fn serve an important role in the delivery of growth factors to cells. FnIII12-14 has been shown to bind most growth factors from the platelet-derived growth factor (PDGF), vascular endothelial growth factor (VEGF), and fibroblast growth factor (FGF) families in the nanomolar range, without inhibiting growth factor activity[90]. Building on this finding, the Hubbell group designed Fn fragments incorporating both the integrin-binding domain (FnIII9-10) and the growth factor binding domain (FnIII12-14), along with a Factor XIIIa substrate fibrin-binding sequence as a method of enhancing the effects of various growth factors in wound and bone healing strategies[91]. Coupling the cell-binding and growth factor-binding domains of Fn shows promise in tissue engineering and wound healing approaches.

2.6.2 Engineering Fn fragments

Particular Fn fragments have thus far been designed to initiate desired responses from cells such as cell adhesion, motility, spreading, proliferation and differentiation. In particular, it has been noted that these ECM protein changes can engage different integrin "switches" which is guided by integrin specificity. These fragments have been designed with different length and flexibility in order to induce the desired cellular outcomes. It could be proposed that by engaging even more drastically different conformations there could be unique cellular responses that may not be as predictable.

Small inputs of force (<100pN), within the range of cellular contractile forces, affect the 10th type III repeat prior to complete unfolding by exposing it to an intermediate state characterized by the RGD loop translocating away from 9th type III repeat. Within this state the RGD and synergy site distance is increased from 32Å to approximately 55Å, a distance

too large for both sites to co-bind the same receptor. A small cell contractile force can regulate this distance, or these force mediated conditions can be mimicked by engineering peptides that have increased linker chain length or through point mutations. These changes in the distance between the RGD and synergy sites have been shown to reduce α5β1 integrin binding.[78] This information suggests that α5β1 integrin binding can be mediated mechanically by forces that result in an intermediate lengthened state or beyond.

Mardon *et al.*'s work has focused on further understanding integrin specificity within the cell binding domain of Fn[21]. This work has outlined the initial cell attachment and downstream cell adhesion events as significantly affected by the addition of short flexible linkers between the 9th and 10th type III domains. These short linkers are primarily designed with a series of glycine residues in order to provide a tensile character and distance between the two synergistic sites[78]. This work inspired further exploration of recombinant Fn III 9 and 10 domains explored by Martino *et al.*. Engineered integrin-specific Fn fragments were designed from Fn's 9th and 10th type III repeats since this is a known cell-binding domain. A stabilized fragment FnIII9*10 is designed with a Leu to Pro mutation which provides greater α5β1-integrin specificity based on the conformational stability of the RGD and synergy sites[58,73,92,93]. This recombinant Fn fragment, FnIII9*10 has a greater degree of α5 clustering than the wild-type FnIII9-10 fragment, which due to conformational change is believed to contribute to specificity alternatively to the wild-type fragment, which has poor specificity for intergrin binding type. Another engineered Fn fragment displaying spatially displaced RGD and PHSRN (FnIII9-4G-10) has been explored for its preference for αvβ3 integrin engagement. These engineered fragments can be utilized since the presence of force or mutational distanced type III repeats could result in preferential engagement of

certain integrins over others. It has been seen that ECM protein conformations affect integrin binding to the same protein, with different integrin binding leading to differential cellular responses.

The role of alterations in Fn conformations have been explored through recombinant Fn fragments that were designed to model these different conformational states by mutating the integrin specific binding sites within the fragments. The downstream cell phenotypes including adhesion and spreading were investigated in order to confirm the hypothesis concerning the role of these conformations and their role in tissue regeneration. It is clear that when mechanical forces are applied to an ECM rich in fibronectin, conformation changes to the protein can have significant impact on integrin specificity and can in turn modulate cellular behavior through intracellular signaling events. It has been shown that through mutations within the integrin binding domains of Fn 9^{th} and 10^{th} type III repeats the conformational changes can be mimicked.

2.7 Physiological relevance of integrin specificity

As discussed in section 2.4.3 of this thesis, Fn can bind multiple integrins, dependent on the conformation of two adjacent FnIII domains. Integrin α5β1 has a high affinity for RGD (located on FnIII10) when the synergy site (PHSRN, located on FnIII9) is conformationally close. As distance between RGD and synergy increases, the affinity for α5β1 is decreased, while affinity for synergy-independent integrins, such as αvβ3, remains unchanged. As a result, Fn conformational change can drive integrin specificity. To illustrate the importance of this mechanism, it is useful to consider the consequences of integrin specificity within the context of more organized cell behaviors and even diseases.

2.7.1 Cell adhesion, spreading, migration, and growth

Evidence for integrin-specific cell behaviors was first noted in the ability of α5β1 integrins to promote migration to a greater degree than α4β1[61,94]. This concept was bolstered by research performed by the Ruoslahti group in 1993. Starting with a cell type that lacks the α5 subunit, Zhang *et al.* expressed αv subunits in these cells to obtain an αvβ1 integrin. Cells with the αvβ1 integrin adhered to a Fn substrate, but did not migrate or assemble a fibronectin matrix. Transfecting the cells to produce the α5 subunit rescued these two behaviors[95]. These results were particularly striking because the β subunit remained the same in both heterodimers (β1), suggesting that changing one subunit of the integrin is sufficient to affect cell behavior. Two years later, the same group took the experiment one step further and showed that cells lacking α5 undergo apoptosis under conditions of serum starvation, whereas re-introducing α5 protected against apoptosis under these same conditions[96]. Taken together, these studies show the dramatic effect of integrin specificity on basic cell behavior. It is known that integrin specificity is clearly linked to cell fate differentiation and proliferation processes. For example, the β1 integrin subunit enhances the progression of differentiation of precursor cells, while αv integrins, like αvβ3, correlate with increased cell adhesion, enhanced cell proliferation, and decreased differentiation.[97-100]

About a decade later, researchers explored the effects of varying biomaterial surface chemistry on integrin specificity. While α5β1 integrins preferentially bound to surfaces rich in hydroxyl groups (-OH), αvβ3 integrins preferred surfaces with carboxyl groups (-COOH). Interestingly, this variation in surface chemistry not only influenced which integrins cells use to adhere, but also modulated the composition of the resulting

focal adhesion complex[101]. These results were strong evidence that integrin specificity could drive distinct cellular behaviors by altering focal adhesion composition. Integrin specificity has recently been shown to influence the assembly of ECM proteins such as collagen and fibronectin[102].

Integrin specificity is highly sensitive to the conformation of RGD and PHSRN. Having identified these sequences as important for α5β1 ligation, it is tempting to reduce bioadhesive material design strategies to incorporate solely these two binding epitopes. Yet research has shown that the structural context of these sites in Fn is beneficial for cell adhesion, focal adhesion assembly, and cell proliferation. All of these behaviors were enhanced in cells exposed to FnIII7-10, a fragment of Fn containing both RGD and PHSRN in their native form, versus cells exposed to an RGD-PHSRN oligopeptide with a polyglycine linker between the two sites. Importantly, FnIII7-10 also promoted specificity for integrin α5β1 over αvβ3 to a much greater degree than the RGD-PHSRN oligopeptide[103]. Other work in this area has suggested that RGD-containing peptides such as GRGDSP can direct integrin specificity depending on the presentation of the peptide. Linear GRGDSP was bound primarily by α5β1 integrins, whereas binding to GRGDSP in a loop conformation was mediated by αvβ3[104].

The influence of recombinant Fn integrin binding domain alterations can have significant influence on cell fate. Fn fragments displaying stabilized synergy site, RGD (FnIII9'10), or RGD alone (FnIII10) can be analyzed for cell phenotype and cell-cell contacts. It has been indicated that epithelial cells engage integrins demonstrating the importance of synergy in regulation of epithelial cell phenotype behavior relevant to tissue

engineering as well as the use of engineered integrin-specific ECM fragments in directing cell phenotype.[30]

2.7.2 Stem Cell Differentiation and Renewal

The binding of α5β1 to Fn was shown to be critical for the proliferation and differentiation of progenitor cells into both osteoblasts and myoblasts[105,106]. Using the biomaterial surface chemistry modification technique described in section 2.7.1, it was found that integrin specificity for the β1 subunit over the β3 subunit was critical for osteoblastic differentiation of progenitor cells[107]. Further studies on mesenchymal stem cells (MSCs) revealed similar results regarding the importance of the α5 subunit in promoting osteoblast differentiation[108].

Combining these results with knowledge of FnIII unfolding events, researchers have engineered approaches to tailor MSC differentiation using FnIII9-10 variants with different mechanical stabilities. Variants that specifically promoted α5β1 binding over αvβ3 resulted in enhanced osteogenic differentiation of MSCs[92].

Integrin specificity has also been explored as a method of promoting stem cell self-renewal. By designing a defined, synthetic three-dimensional matrix, researchers stimulated specific combinations of integrins to promote the renewal of embryonic stem cells[109].

2.7.3 Wound Healing

The process of cutaneous wound healing involves a close coordination between cells and the surrounding matrix. Fn is abundantly present in the ECM of regenerating

injured tissues. After the initial fibrin clot forms a provisional matrix, inflammatory cells and fibroblasts migrate to the wound area. Fibroblasts proliferate and assemble ECM proteins before differentiating into myofibroblasts to contract and organize the new ECM. This example of matrix assembly and remodeling has the potential to expose cryptic binding sites, as discussed in section 2.5.2. The importance of β1 integrins in wound healing was first noted in keratinocyte migration during cutaneous wound repair in mice[110]. Later, the β1 integrin was found to be critical for wound closure and ECM deposition in cutaneous wounds[5]. Recently, the Hocking group designed fibronectin matrix mimetic proteins that preferentially engage either α5β1 or αvβ3 integrins, or an equal contribution of both[102]. Initial testing of these proteins in a diabetic mouse wound model has shown the capability of fibronectin matrix mimetics to promote wound healing, though the impact of integrin specificity is uncertain[111].

2.8 Tissue Engineering

To date, many groups have aimed to develop biomaterials that are capable of mimicking the behavior of the complex micro-environment through synthetic or biosynthetic hybrids for tissue regeneration applications. In order to develop new, novel biomaterials, this dynamic environment must be further explored to ultimately lead to therapeutic options for tissue regeneration.[112] . Development of model systems used to investigate cell behavior and fate under a multitude of different environmental conditions is of particular interest.

Integrin-specific peptide sequences are an obvious candidate for tissue engineering approaches, due to their ability to modulate cell behavior. One example of these approaches

is the use of FnIII7-10, an α5β1-specific fragment, as a coating on titanium bone implants to improve osseointegration[113]. Augmentation of bone regeneration has also been achieved by delivering bone morphogenetic protein-2 (BMP-2) in a hyaluronic acid hydrogel modified with FnIII9*-10, a fragment known to bind α5β1[114].

Biomaterials that are capable of mimicking the behavior of desired environments in synthetic or biosynthetic hybrids have been a desired goal in the field of tissue engineering and regenerative medicine. Specifically, during tissue development, repair, and regeneration of epithelial tissues; cells must interact with the structural scaffold of tissues comprised of a fibronectin (Fn)-rich matrix[39]. For example, in the case of wound healing, biochemically the ECM is known to shift from a predominantly laminin/elastin matrix to the emergence of a provisional matrix majorly comprised of fibrin and fibronectin. This shift leads to changes in cell behavior and phenotype. This concentrated Fn matrix may aid in directing cells to a more migratory/repair phenotype. Specifically, in pulmonary tissue, underlying vasculature is damaged and results in the initiation of the clotting cascade and the creation of a fibrin rich intermediate ECM with areas of cross-linked fibronectin. Controlling cell behavior within engineered tissues is essential for tissue repair and regulation mechanisms for organ function. Cellular process left uncontrolled that enhance the progression of fibrosis can be an ideal candidate for regenerative medicine strategies. Mechanical signals influenced by matrix rigidity are known to drive fibrosis but it is important to explore these effects in combination with biochemical cues provided in strained matrices as well. Exploration into potential therapeutic inhibitors of certain cell processes could be useful in limiting the progression of fibrotic disease, particularly IPF.

2.9 Mechano-transduction

Mechano-transduction is a sensory transduction mechanism by which cells sense and respond to mechanical stimuli by translating into electrochemical biochemical signals that can prompt specific cellular responses. As cells secrete, assemble, and remodel their matrix the biophysical properties of the matrix can alter based on stiffness, binding site conformation, and other crosslinking properties. As these properties change a feedback to cell response is mediated through cell signaling which can then further create a force-feedback loop[115]. These effects can result in cell functions like proliferation, resistance to apoptosis, adhesion, cytoskeletal structure, cell contractility, and motility[116]. Cells will remodel themselves and their environment based on different cell-ECM force signals[117].

Integrins are implicated in sensing mechanical forces at site between the cell and ECM at a physical attachment site, integrin-based adhesion[64]. Integrins are mechanosensitive and take mechanistically relevant information into the cell. The physical association between cytoskeleton and ECM, focal adhesions, can propagate biochemical signals and is dynamic in response to mechanical force[118,119]. Complexes around focal adhesions which are scaffolding molecules such as paxillin and vinculin can provide information about the maturation of these adhesion complexes[120-122]. Mechanical tension at the sites of these adhesion complexes can lead to activation of downstream signaling molecules such as focal adhesion kinase (FAK), Src, and others[123,124]. As focal adhesions assemble following ECM ligation of cells other integrin-specific signals can be paved and exogenous force applied at these sites can mimic signals generated by internal force. Cytoskeletal rearrangements can result in site specific stiffening of the cell at the cell-ECM adhesion sites[125]. Cryptic binding motifs may be exposed as force alters the matrix which may change the downstream signaling pathways associated with carious structural FA and

cytoskeletal proteins (ie integrin) leading to signal transduction[126,127]. The multifaceted architecture and abundance of proteins, and binding interactions make the study mechanotransduction perplexing although key for understanding the relationship of mechanical stimuli to biochemical signal.

Key focal adhesion components are analyzed in this work. Src family kinases (SFKs) are a grouping of nine related tyrosine kinases with homology to c-Src[128]. It is known that the simple regulation of integrin clusters (when ligation or force is absent) downstream signaling molecules necessary for signal generation such as SFKs are recruited[129]. Alternate scaffolding molecules are necessary to bridge the interactions (binding) between early signaling intermediates and integrin receptors. Adaptor proteins that bind to the β-integrin cytoplasmic tail are outlined in Legate *et al.* and it is previously known that Src binds β3 and FAK binds β1 and β3 which should ultimately have an effect on downstream events important for phenotype[130,131].

Adhesion-associated signaling molecules such a FAK and Src play a critical role in integrin signaling a focal adhesion formation. Shattil *et al*. work shows that Src Family Kinases (SFKs) play a critical role in adhesion assembly and integrin-mediated regulation of multiple downstream pathways such as FAK and Src and corresponding phosphorylation[129,132]. The mechanosensitive signaling molecule FAK is activated in response to force. The complex formations of SFKs with previously activated FAK results in phosphorylation of additional tyrosine residues in FAK serving as a binding site for subsequent proteins[129]. Examples of how enhanced ECM deposition and crosslinking via fibroblasts enhances integrin signaling in nascent cells through extracellular-related kinase and focal adhesion kinase is explored in mammary tumorgenesis through work by Levental

et al[133]. Modulation of intracellular signaling pathways via SFKs (ie. Src and FAK explored in this work) can be critical for fibroblast phenotype both *in vitro* and *in vivo* (Figure 5). Fn-binding integrin-associated SFK, c-Src is also fibroblast expressed so understanding the relationship between the Fn IBD and the downstream effects on signaling can be key to interpreting phenotype changes.

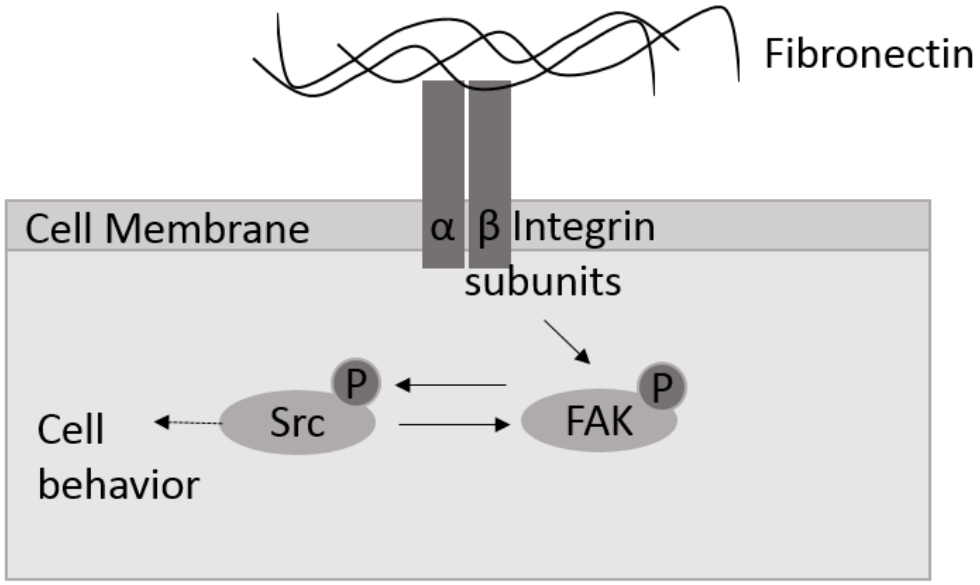

Figure 5. Schematic of FAK and Src phosphorylation and output on cell behavior.

2.10 Myofibroblast Characterization

Fibroblasts are a type of cell which synthesize, assemble, and remodel the protein matrix that make up the stroma of connective tissues. Fibroblasts can be defined as cells that create a meshwork of structural (collagen and fibronectin) and nonstructural (matricellular molecules) ECM molecules through synthesis and secretion. These cells will also organize and remodel the ECM with proteinases they produce. These fibroblast cells will also interact with neighboring cells through autocrine, paracrine, and other forms of

communication[134]. Mechanotransduction also helps to define fibroblasts through their ability to respond to directional cues within their local mechanical environment. Fibroblasts sense mechanical stress and translate this information into the remodeling of the ECM. Understanding the mechanism of this adaptive process is imperative for the future of tissue regeneration and engineering designs.

In IPF the presence of myofibroblasts, activated fibroblasts, are located at fibroblastic foci and are indicated by expression of α-smooth muscle actin[135]. It is known that within the alveolar wall myofibroblasts will proliferate and deposit ECM furthering disease progression. As fibroblasts are native to healthy lung tissue it is important to diagnose the unique phenotypic differences responsible for IPF versus the normal pathological features associated with essential normal lung repair[136,137]. Myofibroblasts continue to drive the fibrotic nature of disease because their functional role in IPF is the *de novo* assembly of fibrotic tissue. It is noted in other work that fibroblasts noted in IPF display a unique phenotype that is still uncharacterized[136,137]. Since fibroblasts in the lung are both responsible for and sensitive to changes towards IPF understanding how fibroblasts sense and respond to changes in the ECM. Activated fibroblast can be characterized by their increased cytoskeletal contractility, the upregulation of genetic biochemical signals that support this cell contractility, expression of α-SMA, increased proliferation, migration/invasion, increased ECM synthesis, and resistance to apoptosis[138-140].

Unanswered questions about which events are triggered in normal human lung fibroblast that may lead to fibrosis is further explored in this thesis. Characterizing the shifts in phenotype based on biochemical cues and the integrin associated events that may

lead to these changes will be addressed. Identification of the "integrin-switch" in normal human lung fibroblast when they are presented with engineered variations of Fn's IBD and focal adhesion components associated with such events in the presence of force are explored. Classification of the fibroblast to myofibroblast phenotype changes is observed by analyzing myo-type phenotype indicators like α-SMA expression and MRTF nuclear translocalization. The data in this review will cover these unanswered question by establishing a process for which engineer Fn fragments can be optimally produced and then further used to understand the relationship between Fn IBD spatial presentation and lung fibroblast cellular response.

2.11 Summary

To summarize; this comprehensive examination discussed fibrosis and IPF, the ECM, the microenvironment and fibrotic progression, integrin binding to Fn, molecular dynamics of the integrin binding domain, engineering approaches to control Fn-integrin specificity, physiological relevance, mechanotransduction, and the characteristics of myofibroblasts. Fibrotic disease lacks many options for treatment. Since the space around the ECM and fibroblast interaction has limited understanding it is important to continue to explore the phenotypes associated with fibrosis. It is also useful to expand the knowledge of the bidirectional mechanotransduction and how it becomes uncontrolled within fibrotic tissue. Investigating the biochemical and biophysical relationship between the matrix and fibroblasts is of great importance to better understand how fibrosis occurs and what therapeutic options there could be for the treatment of these disorders and of particular interest to us IPF.

CHAPTER 3. ENGINEERED SYSTEM FOR FIBRONECTIN FRAGMENT EXPRESSION, PRODUCTION, AND PURIFICATION

Portions of this chapter are adapted from previously published work: "Shuoran Li, Lina Nih, **Haylee Bachman**, Peng Fei, Yilei Li, Eunwoo Nam, Robert Dimatteo, S. Carmichael, Thomas Barker, and Tatiana Segura, *Hydrogels with precisely controlled integrin activation dictate vascular patterning and permeability*. **Nature Materials. July 12, 2017** DOI: 10.1038/nmat4954"[141]. The author of this document contributed to this work primarily through contribution of FnIII9-10 variants, optimization of protein expression system and writing of the manuscript.

Portions of this chapter are adapted from previously published work: "**Haylee Bachman**, John Nicosia, Marilyn Dysart, Thomas H. Barker, *Utilizing fibronectin integrin-binding specificity to control cellular responses.* **Advances in Wound Care. August 2015 4(8) pp. 501-511** Publication date: July 2, 2015 DOI: 10.1089/wound.2014.0621"[2]. The author of this document contributed to this work primarily through overall literature review and writing of the manuscript.

3.1 Introduction

Fibronectin (Fn), an EMC protein, is a good candidate for exploring the wound healing processes. The Fn molecule is a high molecular weight (~440kDa) glycoprotein that participates in a wide array of important cellular interactions such as adhesion, migration, growth and differentiation. Fibronectin is an essential component of the provisional matrix

and is a template for collagen deposition. Typically Fn is purchased for a high price from a life science retailer or through an extensive process it is isolated from human plasma. After decades of investigation of the complexity of the full-length Fn, various binding sites and interaction motifs are indicated contributing to its intricate nature. Another key difficulty results as aggregation of this large molecule occurs during the purification process. These components indicated the difficulty of using full-length protein even though it's an attractive option for creating bio-functional surfaces for cell adhesion and regulation. The complex nature of this molecule and the desire to specifically engage a specific interaction to determine site-specific makes a clear argument for using recombinant proteins to mimic the integrin binding site.

In Martino *et al.* isolated fragments containing the integrin binding domain of Fn was isolated and manipulated for further studies[92]. This region is of particular interest because the effects that integrin signaling has on cell phenotype would be indicative to therapeutic targets that aim to inhibit the fibrotic process. Using the integrin binding domain (located within Fn's 9^{th} and 10^{th} type III repeats) we can observe very distinct influences that are guided by differential integrin engagement. Further these recombinant Fn fragments can be used specifically to present biochemical cues that mimic strained and relaxed Fn conformations. Previously, the Barker Lab designed several Fn mimics based on the understanding of Fn unfolding (founded on MD simulations from Erickson *et al.*[71]). Small inputs of force (<100pN) affect the 10^{th} type III repeat prior to complete unfolding by exposing it to an intermediate state characterized by the RGD loop translocating away from the 9^{th} type III repeat (containing PHSRN "synergy" site). Within this state the RGD and

synergy site distance increases from 32Å to roughly 55Å, a distance too large for both sites to co-bind the same receptor.

While cell contractile forces can regulate this distance between FnIII9 and FnIII10 *in vitro* and *in vivo*, these force mediated conditions, FnIII10 extended from III9 and FnIII9-10 together, can be mimicked by engineering peptides that have increased linker chain length or through point stabilizing point mutations, respectively.

Integrins are heterodimeric cell surface receptors that link the cytoskeleton of a cell to the ECM with at least 12 distinct integrin pairs capable of linkage to Fn[142]. Integrins are well-studied receptors for Fn and they play a critical role in the assembly of Fn into fibrils within the ECM[143]. Fn matrix assembly into Fn fibrils is regulated by α5 and αv integrin subunits even though other subunits can regulate ECM protein secretion[144]. The integrin α5β1 is the major Fn binding integrin that cells use to engage and assemble Fn molecules into the matrix[145,146]. These two key studied Fn-binding integrins, α5β1 and αvβ3, both engage the RGD recognitions motif within FnIII10. However, α5β1 can also engage the PHSRN "synergy" site within FnIII9, presumably by binding to the α5 subunit and altering its conformation, for high affinity Fn-integrin interactions[92,147]. Recent evidence suggested that integrins α5β1 and αvβ3 can work together to optimize fibroblast rigidity sensing on a Fn-based substrate, and may have implications for cell migration and invasion in fibrotic pathologies and cancer[148]. It was hypothesized that spacing between the RGD and PHSRN site may result in differential integrin engagement and potentially mediation of different signaling events. Because of this hypothesis, recombinant fragments were designed which mediated the molecular conformation of the FnIII9-10 region to mimic force-actuated changes.

Recombinant fibronectin fragments of the 9th type III repeat (FnIII9) and 10th type III repeat (FnIII10) were designed to preferentially bind α3/α5β1 or αvβ3 integrin respectively. The mutation, FnIII9*10, has been previously shown to stabilize the integrin-binding domain of fibronectin and enhance its binding selectivity to synergy-dependent β1 integrins, including both α5β1 and α3β1[92,149,150]. To achieve αvβ3 integrin specificity, 4 glycine residues were then inserted into the linker region between FnIII9 and FnIII10 (mutation called FnIII9-4G-10)[43]. The 4 glycine insertion (FnIII9-4G-10) both physically separates the synergy (PHSRN) and RGD sites located on FnIII9 and FnIII10, respectively, and introduces torsional flexibility between the two domains, resulting in a complete disruption of α3/α5β1 integrin binding and promoting a αvβ3 integrin preference. These changes in the distance between the RGD and synergy sites have been shown to reduce α5β1 integrin binding.[78] Though both recombinant fragments can theoretically bind αvβ3 integrin via the RGD sequence, we and others consistently observe a preference of the stabilized mutant (FnIII9*10) to bind synergy-dependent integrins, like α5β1 integrin[30,43,141]. This information suggests that α5β1 integrin binding can be mediated mechanically by forces that result in an intermediate lengthened state of FnIII9-10 or beyond. Through previous work indicated FnIII9*10 is believed to mimic a relaxed integrin binding domain of Fn and FnIII9-4G-10 mimics the strained matrix environment. These Fn fragments are a useful way to explore the cell phenotypic responses specific to integrin engagement with ECM protein fibronectin.

These previously developed recombinant fragments of Fn's integrin binding domain that mimic the predicted "relaxed" and "strained" states and, within this dissertation, their

use to probe important wound healing phenotypes of fibroblasts, such as proliferation, mechano-transduction and myofibroblastic differentiation will be further explored.

In Brown *et al.* epithelial cells were found to engage RGD only with αv integrins demonstrating the importance of synergy in regulation of epithelial cell phenotype behavior relevant to the use of engineered integrin-specific ECM fragments in directing cell phenotype[30]. Consideration of similar effects for fibroblasts due to their known activation and known myofibroblast differentiation during the wound healing process is relevant. Within IPF there are specific myofibroblast-like phenotypes such as excessive matrix deposition (lung architecture remodeling), resistance to apoptosis, and increased contractility, spreading, and motility. These could be related to the changes seen in integrin binding because various integrins can promote different activities within the cell. This relationship between integrin engagement and myofibroblast phenotype in human lung cells hasn't been directly explored up until this point. Through previous work it has been indicated that differential integrin engagement occurs when cells are exposed to these recombinant Fn fragments (FnIII9-10). These fragments need to be produced efficiently so that they can be used to probe these phenotypes easily by presenting variable conformations that may trigger integrin selectivity that ultimately influences to downstream cell behavior. Using these fragments that solely contain the Fn integrin binding domain, we are able to attribute differences that are observed to the integrins that we recognize as being engaged with each fragment respectively.

The FnIII9-10 constructs were originally highly susceptible to plasmid mutation and overall plasmid and peptide degradation. Issues with mutations to the DNA, nt-sequence and low copy number have caused alterations in protein expression levels as well as

misfolding and incorrect protein expression. These mutations cause chronic issues with production, purification, and use for cellular experiments. Metabolic stress is exerted on the bacterial cells as they are engineered to express recombinant proteins; therefore, careful consideration of plasmid design is necessary to reduce the many difficulties seen within the original expression platform. Through freeze-thaw cycles and generation expansion, these previously engineered constructs lost viability and production/quality was unreliable; therefore, an improved construct was designed to maximize protein expression, allow for ease of protein tracking, and improve the purification process. Optimization was completed to produce maximal amounts of protein. Various growth temperatures were explored due to the temperature effect on growth rate of the bacteria and this facet could be easily optimized. Media conditions can provide different ratios of amino acids, sugars, and other nutrients for cells so it is useful to maximize expression of proteins but evaluating various mediums for growth. Induction regulator (IPTG) concentration can be maximized for peak induction rate and total amount. Careful consideration to the design of the engineered protein was given and new strategies were outlined to monitor the quality of each batch of protein after purification.

3.2 Materials and Methods

3.2.1 Redesign Protein Expression Plasmid

Engineered, recombinant Fn fragments were designed to observe the integrin binding domain (9^{th} and 10^{th} type III repeats) and the effects they can have on cell signaling. Two specific recombinant peptides were observed that can provide different cell signals based on the integrins they engage. The original protein production process used was inefficient

due to dysregulation of cell metabolism causing DNA mutations; therefore, the system was re-engineered in order to optimize protein expression and simplify the purification process. The expression system for these recombinant Fn fragments was optimized from prior publications (Markowski *et al.*) to create a high throughput production process[43]. New plasmid constructs were designed with new multipart features added. A 10-His tag was added on the C-terminal end and is used for purification in an AKTA start system. A thrombin-cleavable tdTomato fusion protein for real-time production feedback and optimization of protein production conditions was also included (Figure 6).

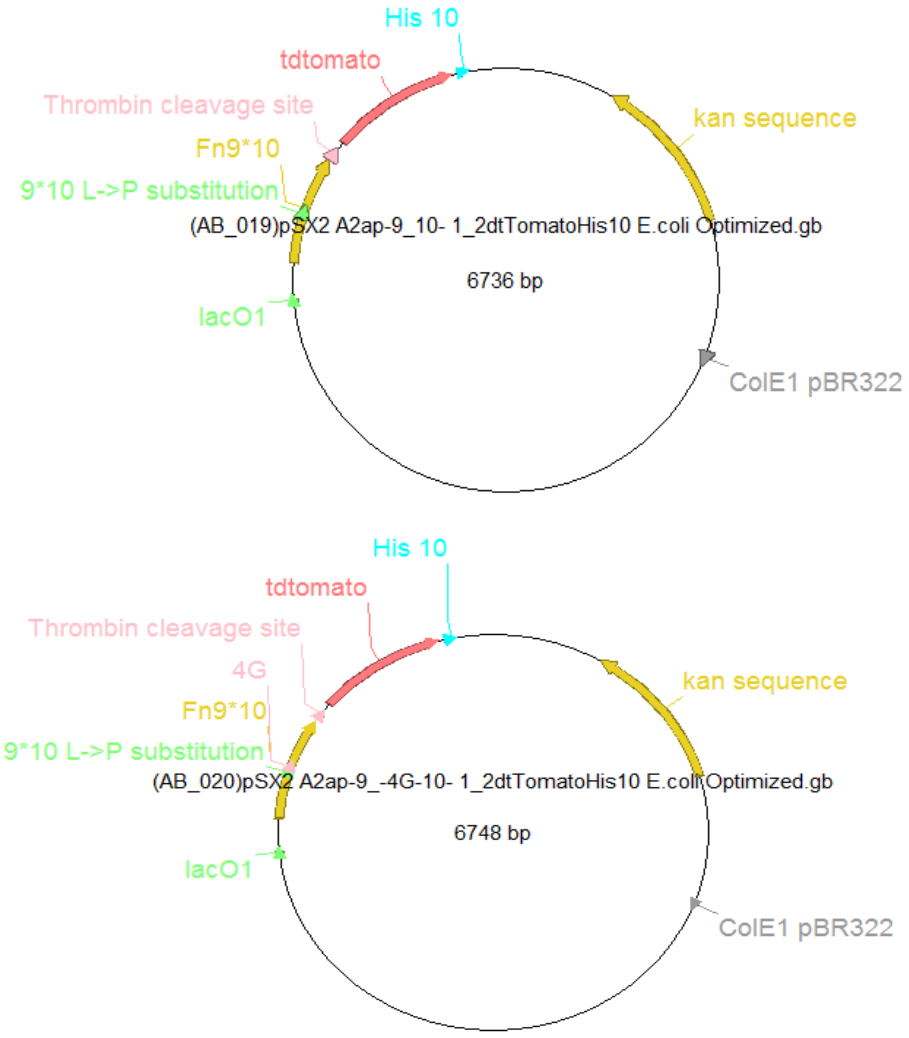

Figure 6. ***Vector Maps of FnIII9*10 and FnIII9-4G-10. Indicated are the design elements of significance for expression and purification purposes (recombinant changes for conformational bias, fluorescent protein, thrombin cleavage site, and 10 His residues).***

Nucleotide Sequence of FnIII9*10+Thrombin digest site+tdTomato +His10	atgggatcttgtaatcaagaacaagtcagtccccttggcttagattctccgactggaattgacttctca gacattacggccaattccttcacagtgcactggatcgcaccccgcgcaaccattactggataccgta ttcgtcatcaccctgaacacttttcaggacgtccccgcgaggaccgcgtaccacattcgcgcaaca gtatcactcttactaatttgacccctggtactgagtatgtagtttccatcgtcgctctgaacgggcgcga ggaatccccaccgttaattggtcaacaatctaccgtttcagatgttccccgtgatttagaagttgtagc agctactccgacatctttactgatttcttgggacgcaccagctgtcacagttcgctattaccgcatcac atacggtgaaaccggtgggaactcgcctgttcaggaatttactgtgccaggtagtaagtcgaccgc aacaatctccggcttaaagccgggcgtggattatacaattactgtctatgcagttaccggccgcggc gattccccggcgtcgtcaaagccgatcagtatcaattatcgcaccggtggtggagatcatccgccg aaatcagatttagtgccgcgtggctcgggccatggaacgggctccacgggaagtggtagctcagg tacggcctcgtcggaagataataacatggccgttattaaagaatttatgcgttttaaagttcgtatggaa ggttctatgaatggtcatgaatttgaaattgaaggtgaaggtgaaggtcgtccatatgaaggtactca

	aactgctaaattaaaagttactaaaggtggtccattaccatttgcttgggatattttatctccacaatttat gtatggttctaaagcttatgttaaacatccagctgatattccagactacaagaaactgtcttttccagaa ggttttaaatgggaacgtgttatgaattttgaagatggtggtttagttactgttactcaagattcttctttac aagatggtactctgatttacaaagtcaagatgcgtggtactaattttccaccagatggtccagttatgc aaaaaaaaactatgggttgggaagcttctactgaacgtttatatccacgtgatggtgttttaaaaggtg aaattcatcaagctttaaagctgaaagacggtggccattacctggttgaatttaagacgatctatatgg ctaagaaaccagttcagctgccaggttactattacgttgatactaagttagatatcacttctcataacga agattatactattgttgaacaatatgaacgttctgaaggccgtcatcatttattcttatatggaatggatg agttgtataagggacacgggggcaccaccaccaccaccatcatcaccatcactga
Nucleotide Sequence of FnIII9-4G-10+Thrombin digest site+tdTomato +His10	atgggatcttgtaatcaagaacaagtcagtccccttggcttagattctccgactggaattgacttctca gacattacggccaattccttcacagtgcactggatcgcaccccgcgcaaccattactggataccgta ttcgtcatcaccctgaacacttttcaggacgtccccgcgaggaccgcgtaccacattcgcgcaaca gtatcactcttactaatttgacccctggtactgagtatgtagtttccatcgtcgctctgaacgggcgcga ggaatccccaccgttaattggtcaacaatctaccgtttcaggaggaggaggagatgttccccgtgat ttagaagttgtagcagctactccgacatctttactgatttcttgggacgcaccagctgtcacagttcgct attaccgcatcacatacggtgaaaccggtgggaactcgcctgttcaggaatttactgtgccaggtag taagtcgaccgcaacaatctccggcttaaagccgggcgtggattatacaattactgtctatgcagtta ccggccgcggcgattccccggcgtcgtcaaagccgatcagtatcaattatcgcaccggtggtgga gatcatccgccgaaatcagatttagtgccgcgtggctcgggccatggaacgggctccacgggaag tggtagctcaggtacggcctcgtcggaagataataacatggccgttattaaagaatttatgcgttttaa agttcgtatggaaggttctatgaatggtcatgaatttgaaattgaaggtgaaggtgaaggtcgtccata tgaaggtactcaaactgctaaattaaaagttactaaaggtggtccattaccatttgcttgggatattttat ctccacaatttatgtatggttctaaagcttatgttaaacatccagctgatattccagactacaagaaact gtcttttccagaaggttttaaatgggaacgtgttatgaattttgaagatggtggtttagttactgttactca agattcttctttacaagatggtactctgatttacaaagtcaagatgcgtggtactaattttccaccagatg gtccagttatgcaaaaaaaaactatgggttgggaagcttctactgaacgtttatatccacgtgatggtg ttttaaaaggtgaaattcatcaagctttaaagctgaaagacggtggccattacctggttgaatttaaga cgatctatatggctaagaaaccagttcagctgccaggttactattacgttgatactaagttagatatcac ttctcataacgaagattatactattgttgaacaatatgaacgttctgaaggccgtcatcatttattcttatat ggaatggatgagttgtataagggacacgggggcaccaccaccaccaccatcatcaccatcactg a
Translate Protein Sequence FnIII9*10	GLDSPTGIDFSDITANSFTVHWIAPRATITGYRIRHHPEHFSGRP REDRVPHSRNSITLTNLTPGTEYVVSIVALNGREESPPLIGQQST VSDVPRDLEVVAATPTSLLISWDAPAVTVRYYRITYGETGGNS PVQEFTVPGSKSTATISGLKPGVDYTITVYAVTGRGDSPASSKP ISINYRT
Translate Protein Sequence FnIII9-4G-10	GLDSPTGIDFSDITANSFTVHWIAPRATITGYRIRHHPEHFSGRP REDRVPHSRNSITLTNLTPGTEYVVSIVALNGREESPPLIGQQST VSGGGGDVPRDLEVVAATPTSLLISWDAPAVTVRYYRITYGET GGNSPVQEFTVPGSKSTATISGLKPGVDYTITVYAVTGRGDSP ASSKPISINYRT

Figure 7. List of nucleotide and protein sequences for FnIII9*10 and FnIII9-4G-10 engineered fragments.

The original expression constructs were susceptible to metabolic stress and often resulted in DNA mutations eventually affecting the expression rate/sum or peptide constructs. These mutations can influence 3D structure causing increased aggregates or expression of the engineered protein into inclusion bodies. The problems of this original expression system resulted in difficulty in purification and eventually ineffective protein. Decisions were made for designing the vector which include creating a better regulating unit lacO to be induced with IPTG and this control reduces the metabolic stress on the bacterial cell allowing for more regulation of expression and maximized cell growth and control resulting in maximal protein expression.

The cloning techniques used for design are outlined in Bryksin *et al.* for insertion of RBS as well as similar techniques used for insertion of other design features[151]. Translation efficiency is described in this work as well and is applied here where it is important to the overall design for maximum expression and optimized production.

The expression system for these recombinant Fn fragments was optimized from prior work and high throughput production was the goal. Other design features were included for application with cellular assays and other basic biological observations of the fragment influences on cell behavior and fate. For ease of immobilization onto surfaces and incorporation into natural and synthetic hydrogel biomaterials both fragments were produced with an N-terminal cysteine residue to allow Michael type addition modifications and a factor XIIIa substrate sequence, consisting of residues 1–8 of the protein alpha2 plasmin inhibitor ($\alpha_2PI_{1\text{-}8}$, NQEQVSPL)[152] to allow enzymatic conjugation[141].

3.2.2 Optimize Expression

The fusion-reporter design of the bacterial expression vector allows for protein production to be monitored in real time via the presence of tdTomato fusion protein. Optimization of growth conditions were explored by varying conditions such as media composition, growth temperature, induction concentration, and growth timing.

Plasmid constructs were transformed into MDS™42 LowMut ΔrecA chemically competent bacterial cells from Scarab Genomics. After transformation, a colony was expanded and then frozen down with 7% DMSO as a bacterial stock.

A 100mm LB/Agar plate with 50µg/mL Kanamycin was streaked with bacterial frozen stock of desired protein vector. Colonies were grown on LB/Agar plate overnight in incubator at 37°C. Colonies were picked for starter culture by adding 5mL of media (TB, 2xYT, SOB, or Korz) with 5uL of stock antibiotic Kanamycin (50µg/mL) in a 10mL tube. Each starter culture was grown overnight at 37°C with shaking. Cultures were then diluted to OD_{600} approximately 0.4 and grown to OD_{600} 0.8 at 37°C with shaking. Cultures were transferred to a 96 well plate with different starter cultures (in triplicate) and to have different induction (via IPTG) concentrations added. IPTG concentration range included 0.25mM, 0.5mM, 1mM, and 1.5mM. Beginning at 24 hours, expression was monitored on BioTek Synergy H4 Microplate Reader with shaking at temperatures 22.7°C and 25°C. Expression levels were monitored via tdTomato expression fluorescence tracking at excitation 554nm, emission 581nm.

Individual clones were picked and used for subsequent expansion and increased protein yields. 1L of 2xYT media is prepared and autoclaved (Liquid Cycle for 30 min at 121°C) for sterility. 2.5mL of 2xYT media was distributed across four 10mL sterile culture tubes.

Antibiotic (Kanamycin) was added at 50µg/mL from stock. 100uL bacterial stock previously frozen at -80°C with 7% DMSO added to each tube. Cell density of stock was unknown so optical density was monitored. Incubated starter culture at 37°C for ~3 hours then added this starter culture to 250mL of 2xYT media in 1L flaks. Closely monitored OD_{600} (blank with 2xYT media) for ~ 2 hours until OD_{600} was roughly 0.8-1.2 then induced cultures with 1.5mM IPTG and incubated overnight (~16 hours) with shaking in incubator at 37°C. Tdtomato was visibly apparent after overnight expression for maximal protein production and bacterial culture appears "pink-ish" in color (Figure 8). Cells are pelleted via centrifugation at 4000 x g for 10 minutes at 4°C. The supernatant was discarded and "pink" cell pellet was then resuspended in protease inhibitor in 45mL of 1x PBS[141]. Cells were then lysed by addition of 10mg/mL lysozyme (in 25mM Tris-HCl pH 8.0). Cells were then sonicated on and off for 20 seconds each for a total of 1 min and 20 seconds on. Triton X-100 at 1% and 10U/mL of DNAse was added to each sample. Samples were shaken for 30 minutes in the cold room and then frozen overnight (minimum) at -20°C and then thawed. At this point the release of subcellular components should have occurred through mechanical disruption forces, high frequency sound waves, and freeze/thaw cycling. Proteins are consistently stored on ice to avoid protein denaturation and aggregation. Samples were then spun down (12,000 x g at 4°C for 15 minutes) to remove cell debris and isolate soluble proteins in supernatant. Soluble protein supernatant (pink if lysis was effective) can then be filtered through a 0.22 µm pore filter.

Figure 8. Purified FnIII9'10+tdTomato+His10. Purification of protein can be tracked through observation of pink color from tdTomato fluorescent protein which is downstream from the FnIII9'10 protein and upstream from the His10 tag protein.

3.2.3 Detailed Purification Process

Recombinant FnIII9-10-tdtomato-His_{10} proteins were purified on a HisTrap FF nickel column (ÄKTA Start, GE Healthcare) via affinity chromatography using Unicorn 1.0 Method Editor. Up to three 5mL prepacked columns were daisy chained together to maximize protein binding for each culture. Binding buffer (20mM sodium phosphate, 0.5M sodium chloride, 25mM imidazole, pH 7.4) and elution buffer (20mM sodium phosphate, 0.5M sodium chloride, 0.5M imidazole, pH 7.4) was used for washing and elution steps based on affinity release on a nickel column. Protein was monitored at this step by observation of fluorescent protein, tdTomato, as the protein bound to the column and then subsequently eluted. At each step the peptide was tracked as it went into the collected fractions based on the fractions that contained a pink color. Peptide was buffer dialyzed

(just buffer exchange for second run so that the peptide doesn't run through the column due to high imidazole concentration) in 1x PBS overnight at 4°C using a 10kDa snake-skin tubing. The fusion protein, tdTomato, and 10-His affinity tag were removed from FnIII9-10 fragments by utilizing the thrombin cleavage site and bovine thrombin (Sigma-Aldrich, 20U/mg of protein, room temp 1 hr or overnight at 4°C) and was often done in combination with the previously mentioned dialysis step to separate the fragment and the tdtomato fusion protein (See Appendix Figure A1). A Benzamidine FF column (GE Healthcare, Life Sciences) bound the free bovine thrombin and the His tag allows collection of C-terminal tdtomato in the HisTrap FF column again and the Fn fragments (FnIII9*10 or FnIII9-4G-10) were released. Gel Filtration was completed on size exclusion column (GE Healthcare, HiLoad 16/60 Superdex 200 prep grade) to separate protein dimer and monomer (break disulfide bonds of dimer with immobilized TCEP disulfide reducing gel). Isolated protein of molecular weight ~20kDa is likely the desired FnIII9-10 fragment. Protein presence in each fraction was validated using SDS-PAGE.

3.2.4 SDS-PAGE

Fractions collected were analyzed via SDS-PAGE and nanodroped (Thermo Fisher NanoDrop), to determine protein presence and concentration. MicroBCA assay (Thermo Fisher Scientific) was also used to verify concentration. Purified, denatured/reduced proteins and Precision Plus Protein All Blue Prestained Protein Standard (1610373) were separated with a 10% SDS gel through SDS-PAGE and stained using SimplyBlue SafeStain (Invitrogen).

3.2.5 ELISA

In a competitive ELISA assay experiment, 96 well plates were coated with purified proteins at the specified concentrations diluted in 1x PBS overnight at 4°C. Washes with PBST (0.1% Tween-20 in PBS) removed unbound protein and then well plates were blocked with MPBS (2% wt/vol nonfat dry milk in PBS) for 30 minutes at room temperature on an orbital shaker. Bound proteins were then detected using a primary antibody. One plate was coated with the phage isolated H5 antibody (100ng/mL), which is known to contain a myc-tag, and a control plate was incubated with the primary antibody HFN 7.1 (1:2000, Thermo Fischer, MA5-12314), a monoclonal mouse antibody to the integrin-binding domain of Fn. The plates were then coated with an anti-myc biotin (1:2000, Sigma Aldrich, B7554) or anti-mouse biotin (1:2000, abcam, ab97044) respectively. These steps were followed by HRP conjugated extravidin (1:1000, Sigma Aldrich, E2886). One-step Ultra TMB (3,3',5,5'-tetramethylbenzidine) ELISA substrate was used to complete the assay (Thermo Fischer, 34028). Absorbance readings were read at 450nm on a BioTek Synergy H4 microplate reader and blank wells were subtracted so that relative protein concentration could be determined.

3.2.6 Dot Blot

Purified proteins were spotted in duplicate (5µL each dot) at indicated concentrations onto a nitrocellulose membrane and given time to dry. The dot blots were then blocked with MTBS (5% wt/vol nonfat dry milk in 1xTBS) at room temperature for one hour then incubated with H5 or HFN 7.1 (1:6000) overnight at 4°C on a 3D rocker. The H5 dot blot was then incubated with an anti-myc mouse monoclonal antibody (1:6000, Thermo Fischer, R950-25). Both dot blots were then incubated with a LI-COR goat anti-

mouse IR dye 800CW (1:15000, LI-COR, 926-32210). Imaging of the dot blots was completed with a LI-COR scanner.

3.2.7 Western Blot

Purified, denatured/reduced proteins and Precision Plus Protein All Blue Prestained Protein Standard (1610373) were separated with a 10% SDS gel through SDS-PAGE and transferred to a nitrocellulose membrane where the blot was then cut to allow for separate staining. The western blots were then blocked with MTBS (5% wt/vol nonfat dry milk in 1xTBS) at room temperature for one hour then incubated with H5 or HFN 7.1 (1:6000) overnight at 4°C on a 3D rocker. The H5 blot was then incubated with an anti-myc mouse monoclonal antibody (1:6000, Thermo Fischer, R950-25). Both blots were then incubated with a LI-COR goat anti-mouse IR dye 800CW (1:15000, LI-COR, 926-32210). Imaging of the blots was completed with a LI-COR scanner.

3.2.8 Attachment assay

Cell attachment assays were performed as previously described[153]. Briefly, surfaces were coated with 2μM Fn fragments (FnIII9*10 and FnIII9-4G-10 have similar coating efficiencies) or 10μg/mL full length WT Fn and blocked with 1% hd-BSA[92,154]. CHO.K1 express only α5β1 integrins and CHO.B2 cells express only αvβ3 integrins. Cells were seeded at 20,000 cells/well and were allowed to attach for approximately 20 minutes at 37°C in 10%-serum F12-K media then washed to remove unbound cells, fixed with 5% glutaraldehyde, and stained. A 0.1% crystal violet solution was used to stain the cells. After drying the stain was solubilized with 10% acetic acid and absorbance was quantified on the BioTek H4 Microplate Reader at 570nm. Linear regression was performed on the

standard curve to determine reliability of the assay. Attachment values were normalized to cell attachment levels hd-BSA (0% attachment). Data from the triplicate experiment was normalized to the cells remaining in the highest cell density wells from the standard curve and presented as average +/- standard error. Normalized remaining cell percentage is presented on the y-axis.

3.3 Results

3.3.1 Optimized Expression

During protein expression optimization the fusion protein fluorescent tdTomato was monitored as a sign that protein was produced. The downstream location of the tdTomato indicated that if tdTomato folded properly and reveals a fluorescent protein then we could assume that the upstream FnIII9-10 fragment had been produced as well (Figure 9).

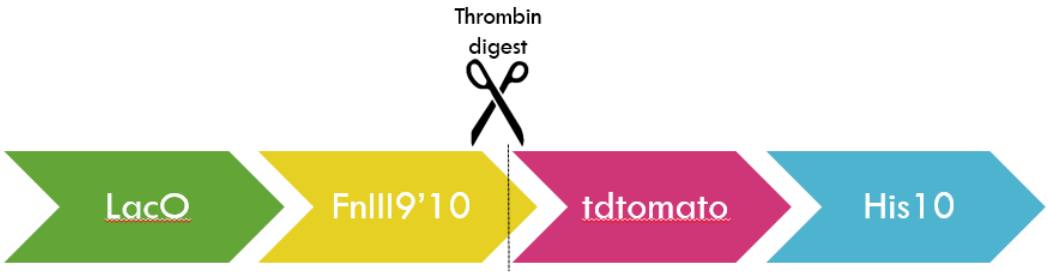

Figure 9. Basic outline of FnIII9-10 expression profile. This schematic highlights the important features from protein expression designed for these engineered Fn fragments. The lacO is associated with IPTG inducible control. FnIII9'10 represents the Fn fragment that is desired. The thrombin digest site allows for cleavage of the tag proteins for complete purification. tdTomato is the fluorescent protein associated with the expression system to track production and allows for ease in optimization and purification tracking. The His10 represents the 10 consecutive Histidine residues used to tag the protein for affinity chromatography in a nickel column.

Here we observed the expression of tdTomato over 24 hours after induction under variable conditions (media variations, and IPTG concentration) (Figure 10). This

experiment was performed at different expression temperatures as well, in order for us to get a sense of which conditions would be best for maximal protein production and convenient, efficient, cost effective optimized process. From this process we chose good condition candidates in order to scale up. The chosen conditions were 2xYT media, at 30°C for overnight expression after 1.5µM IPTG induction. These conditions were chosen because their efficiency but also with consideration to ease of use, access, cost and experimental timing. This protein expression optimization scheme is capable of generating ~20 mg/L of protein within the culture prior to purification.

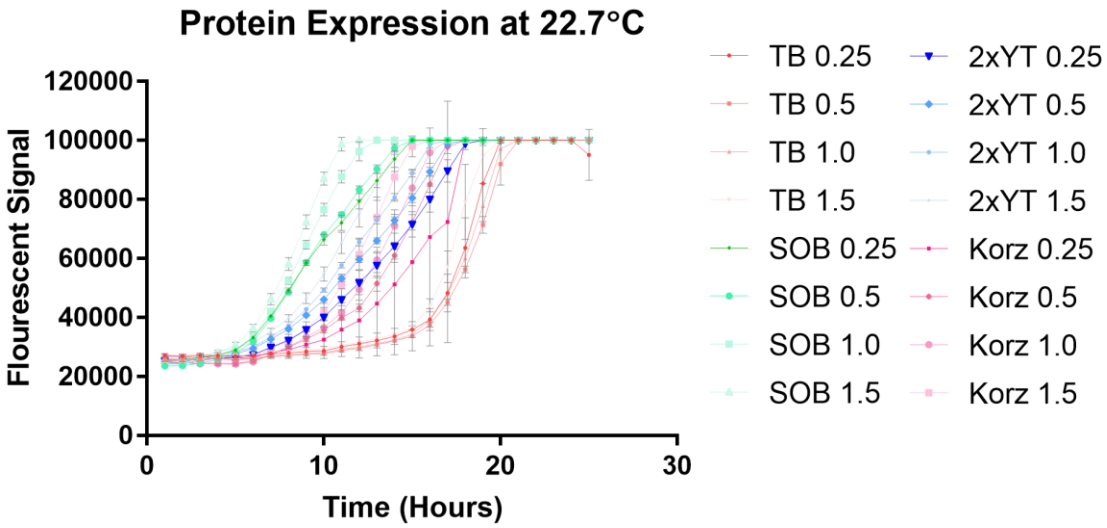

Figure 10. Fluorescent protein tracked for optimization of purification. Conditions of growth were eventually chosen based on results from these optimization results, convenient times, and inexpensive reagents.

3.3.2 Purity Identification

The purity of FnIII9-10 protein fragments was analyzed by SDS-PAGE as mentioned in previous works[30,92]. Analysis of proteins at varying stages of the purification

process is important to understand if your product is pure or if there is major loss of protein at other steps of the process.

Molecular weight of ~20kDa is seen in SDS-PAGE results (Figure 11). Observation of the changing concentration as fractions are run through the column. The thrombin digest is visible on SDS-PAGE as well.

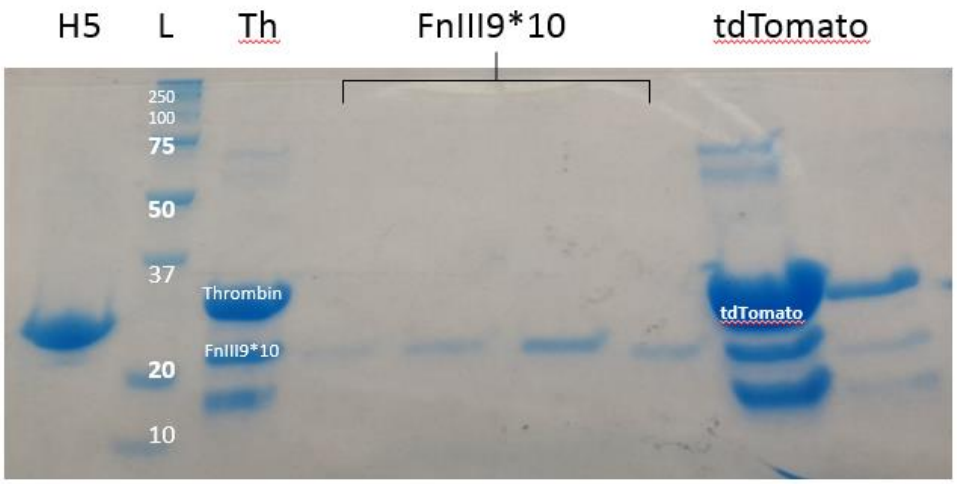

Figure 11. SDS-PAGE analysis to observe purification of FnIII9*10 fragment. Lane 1 shows the H5 scFv phage-based antibody fragment (MW ~28kDa). Lane 2 is the Bio-Rad Precision Plus Protein All Blue Standard. Lane 3 indicates the thrombin digest and identifies the individual halves digested by thrombin and the presence of thrombin (Thrombin MW ~36kDa and FnIII9*10 MW ~20kDa). Lane 4-7 show purified FnIII9*10 after thrombin digest (MW~20kDa) and a second run through the column which washes out purified protein. Lane 8-9 show that proteins that were bound to column after thrombin digest which includes tdTomato+His10 (tdTomato+His10 MW ~32kPa).

Size Exclusion Chromatography (SEC) is used to separate based on size, larger proteins will elute first and smaller proteins will elute later. A calibration kit is run to compare elution time with approximate protein size. Gel filtration validates size after calibration which indicated dimer and monomer configurations (Figure 12). It is

determined with the analysis of the gel filtration column run that there is typically 1.1:1 (12:11) ratio of dimer to monomer concentrations respectively. These dimeric units are not visible on a denaturing SDS-PAGE gel due to reducing agent added therefore this is the best way for different size proteins to be identified.

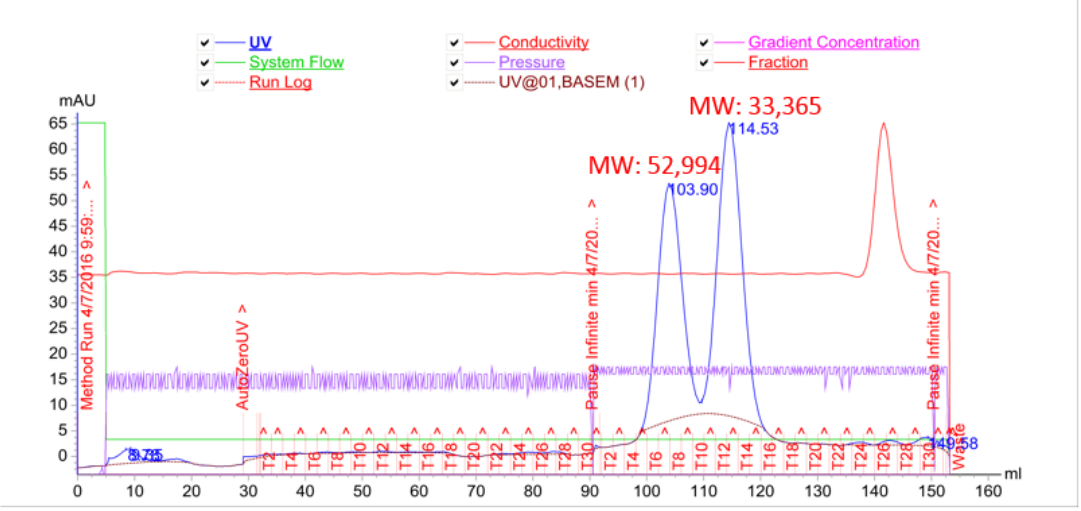

Figure 12. SEC of purified FnIII9-4G-10 fragment dimer and monomer. Monomer unit can either be isolated based on fraction or further reduction of di-sulfide bond can be used to reduce dimer to monomeric form.

The dimer product can be treated with Immobilized TCEP Disulfide Reducing Gel (Fischer Scientific) to reduce di-sulfides that link monomer units together to form the dimer. This reduced product monomer is then known to have a free-cysteine and this thiol (-SH2) can be used as a bifunctional linker to solid supports such as the glass surface of a coverslip or tissue culture plastic[155]. AKTA start was used for purification and this validates purity by verifying size of desired proteins and their unique purity through

collection of desired fractions (reference Appendix Figure A2 to AKTA profile). The yield of purified protein was estimated to be 10mg from a 1L culture.

3.3.3 Quality Control Check

The recombinant proteins have been optimized in both design and in use. Quality analysis was completed to verify purity and activity via SDS-PAGE, gel filtration, ELISA, Western Blot, and Crystal Violet Adhesion Assay studies.

A phage based antibody probe called "H5" was isolated to selectively identify FnIII9-4G-10 over FnIII9*10. This antibody was then used to verify activity and purity of the recombinant protein fragments. Previously purified Fn fragments had shown a selectivity of H5 binding to the FnIII9-4G-10 fragment was approximately an order of magnitude greater compared to FnIII9*10.

The results of this ELISA or protein coated well plates and detection with previously isolated antibody fragment scFv, "H5", as well as a commercially available antibody HFN7.1, an antibody targeting FnIII9-10, binding to full-length Fn and Fn fragments can be seen in Figure 13.

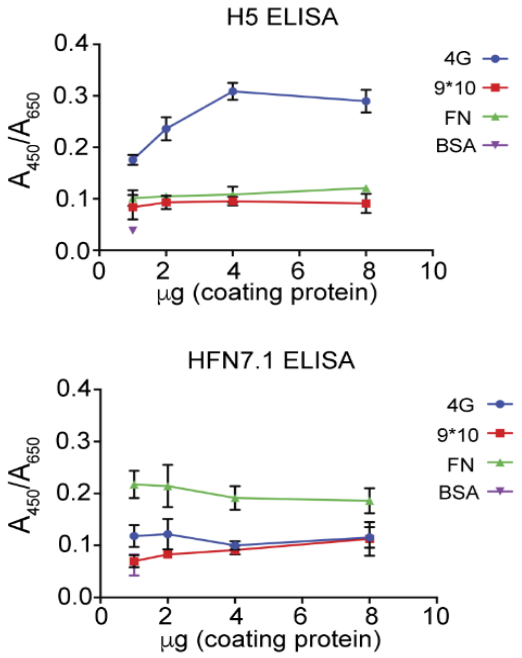

Figure 13. ELISA of H5 or HFN7.1 on various Fn substrates. H5 is the scFv phage-based antibody fragment found to target FnIII9-4G-10 over FnIII9*10. HFN7.1 is a commercially available antibody used to target FnIII9-10 region. H5 bound FnIII9-4G-10 to a significantly greater degree than FnIII9*10 at all concentrations ($p < 0.0001$), whereas HFN7.1 only bound FnIII9-4G-10 to a significantly greater degree than FnIII9*10 at 1 μM ($p < 0.05$) and was not significant at higher concentrations (Two-way ANOVA with Tukey's post-test, N = 3)

Antibody scFv H5 bound FnIII9-4G-10 to a significantly greater degree than FnIII9*10 at all concentrations ($p < 0.0001$), whereas HFN7.1 only bound FnIII9-4G-10 to a significantly greater degree than FnIII9*10 at 1 μM ($p < 0.05$) and was not significant at higher concentrations (Two-way ANOVA with Tukey's post-test, N = 3). The Fn

fragments were also visualized on nitrocellulose dot blots of H5 or HFN7.1 binding to full-length Fn and engineered FnIII9-10 fragments (Figure 14).

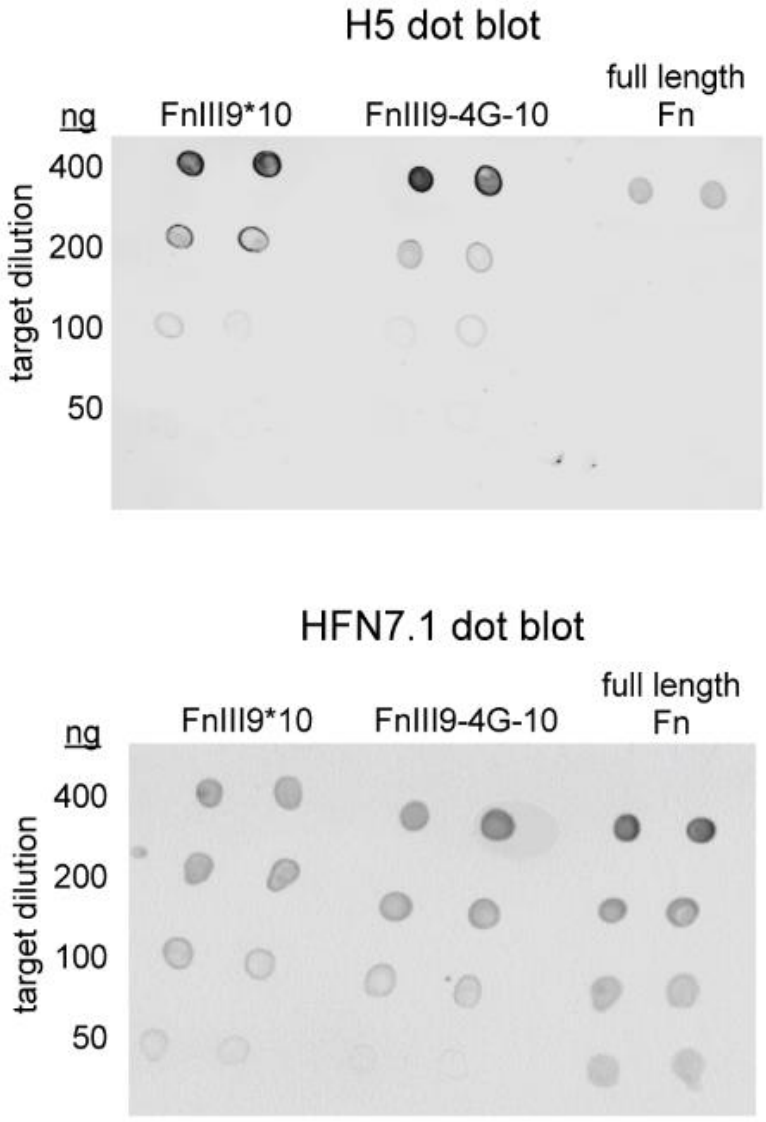

Figure 14. Nitrocellulose dot blots of H5 or HFN7.1 binding to full-length Fn and Fn fragments.

In Figure 15 denaturing Western blots of H5 or HFN7.1 binding to full-length Fn and Fn fragments. The increased affinity of H5 to FnIII9-4G-10 versus FnIII9*10 is

observed in ELISA, but not in dot blot or traditional denaturing Western blots, suggesting that the epitope bound by H5 is likely not solely just a linear peptide sequence but instead a more complex 3D structure.

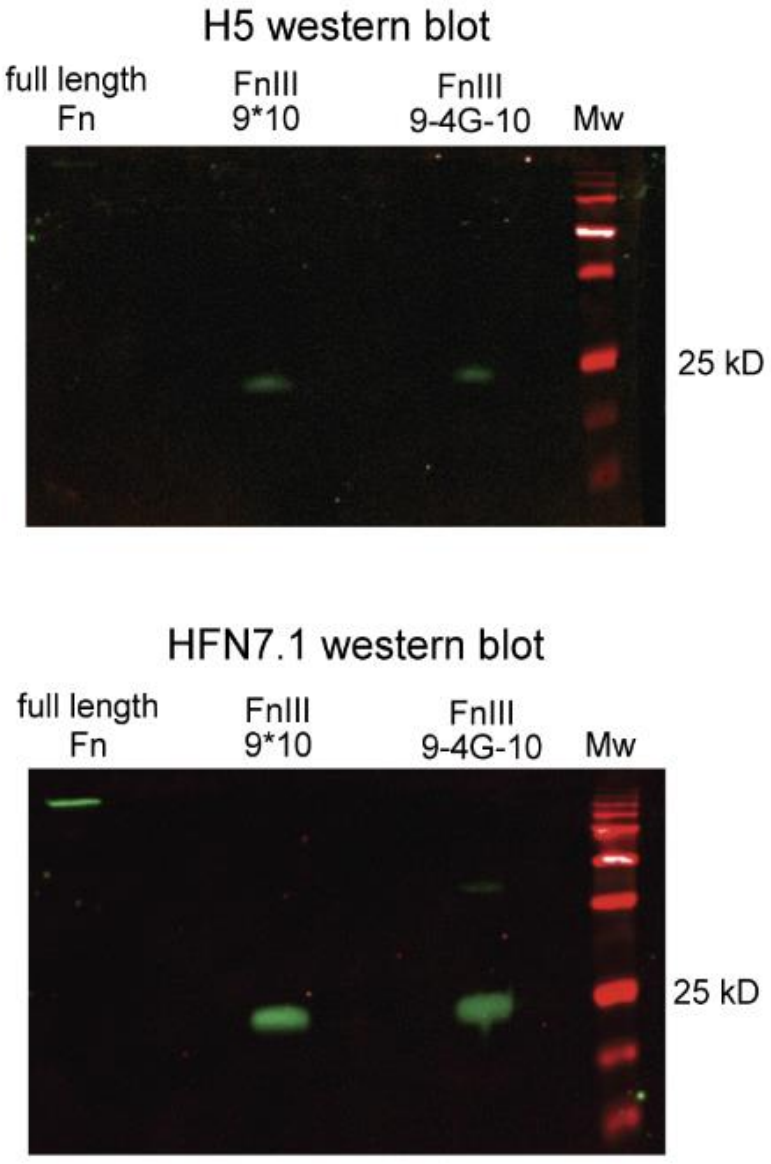

Figure 15. Denaturing Western blots of H5 (E) or HFN7.1 (F) binding to full-length Fn and Fn fragments.

Finally, experiments to observe cell activity are measured using an attachment assay and CHO cells that are designed to express specific integrins. CHO.K1 cells are designed for α5β1 expression and CHO.B2 cells are designed for αvβ3 expression. Using these cells and an attachment assay it is determined that CHO.K1 cells preferentially bind FNIII9*10 and CHO.B2 cells do not preferentially bind either fragment or full-length Fn which aids in the conclusions that FnIII9*10 will favor engagement with α5β1 integrins and FnIII9-4G-10 will favor engagement with αvβ3 integrins. Seen in Figure 16 I observe this trend to be true.

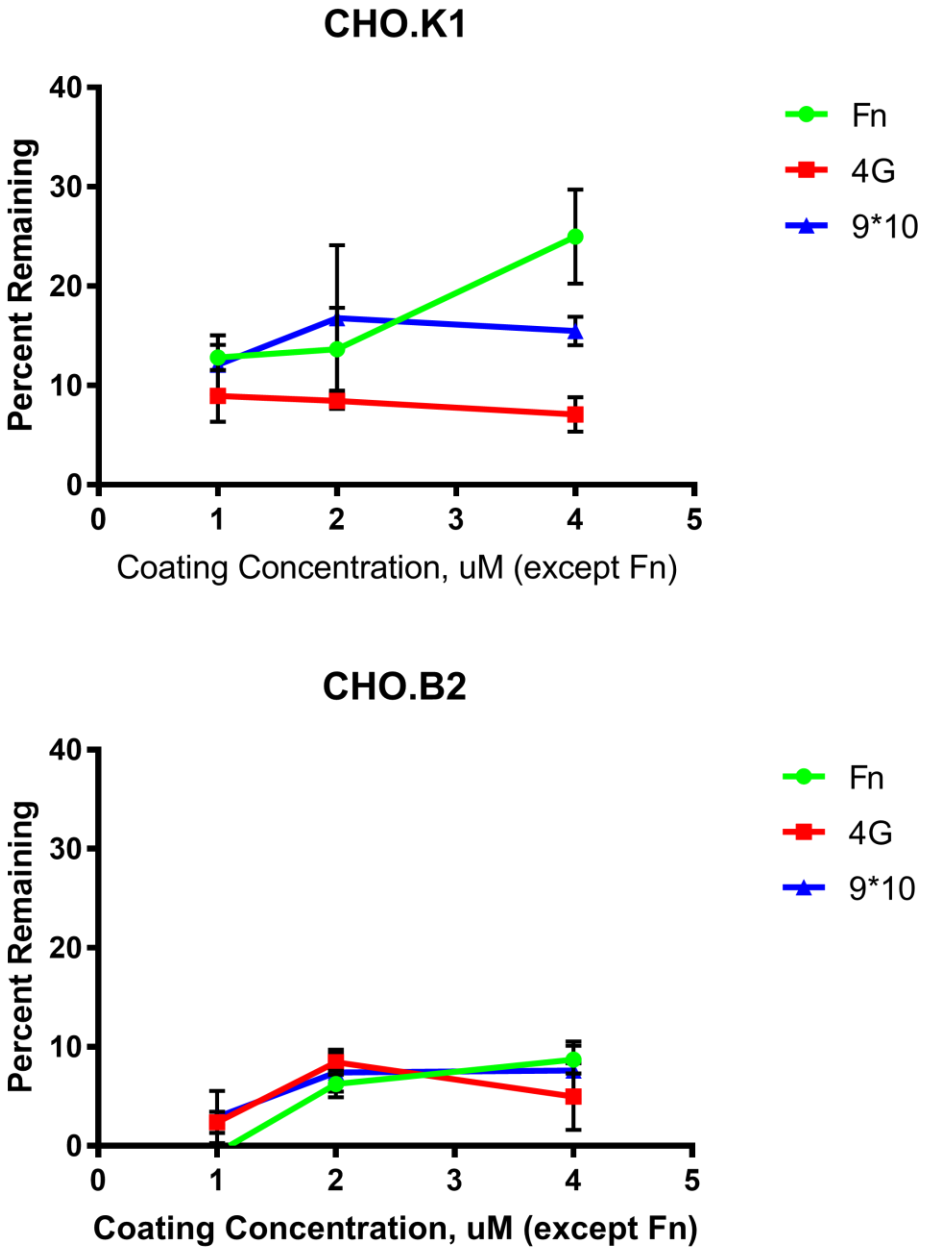

Figure 16. Crystal Violet analysis of cell attachment for CHO.K1 and CHO.B2 cells on various coating substrates. CHO.K1 cells express α5β1 integrins so their preference for FnIII9*10 verifies the hypothesized integrin "switch" behavior. CHO.B2 cells express αvβ3 and since it is hypothesized that both FnIII9*10 and FnIII9-4G-10 can bind to this integrin the similarity in cell binding is appropriate.

3.4 Discussion

Since these engineered recombinant FnIII9-10 fragments were previously designed but the protein production process was inefficient, it was determined that the system should be re-engineered in order to optimize protein expression and simplify the purification process. The vector construct design is justified for incorporation of key design elements including the controllable induction via a lac operon, thrombin cleavage site, tdTomato fluorescent protein, and 10x His tag. The method was optimized and well characterized and the route to purification was easily traced via the fluorescent protein. A system to observe the protein during expression and purification was put in place. Quality assurance methods were developed to determine activity levels of the proteins and to make sure that based on these assays the proteins appear to have the correct conformations. Analysis of the quality of these proteins is important for every batch as mutations can occur easily which influence cell response. Recombinant FnIII9-10 fragments effects on normal human lung cells are further explored in subsequent chapters so the quality of the peptides that will coat the surfaces is important in order to observe key differences in cell response.

The optimized expression design seemed effective. The design features provide valuable control of expression reducing the mutations that previously caused DNA mutations that dysregulated the system. Using many sequential His-tags increased the affinity of the desired protein to bind to the nickel column during purification. The tdTomato was valuable to track expression and purification of the protein from the cell lysate. Additionally the thrombin cleavage site allowed for successful clean cleavage between the FnIII9-10 fragment and the tdTomato + His tag. These features were successfully implemented and were tracked via visual observation and SDS-PAGE analysis. The plasmid backbone pBR322 had these additional engineered features that

allowed for successful regulation. To maintain low rate of DNA mutation it is also important to monitor freeze-thaw cycles of stocks and maintaining early generations of the clone. Frozen stocks of early generations can be made in mass quantity and aliquoted to small volumes to prevent excessive freeze-thaw.

The use of these FnIII9-10 fragments can be of particular interest since the presence of force or mutational distanced type III repeats could result in preferential engagement of certain integrins over others. It has been seen that ECM protein conformations have been shown to affect integrin binding to the same protein. Different integrin binding could potentially lead to differential downstream cellular responses and ultimately could influence cell differentiation and phenotype characteristics.

These fragments are essential for the continuation of the work in Markowski *et al.* and Cao *et al.* and so the maintenance of these fragments for the remaining work discussed in this dissertation and for future projects is imperative[29,43]. It is known that small forces can regulate the distance between the RGD and synergy site. Alternatively these force mediated conditions can be mimicked by increasing linker chain length through point mutations between the two repeats which ultimately reduces α5β1 integrin binding (our Fn fragments, FnIII9-10)[78]. Previous work suggests that α5β1 integrin binding can be mediated mechanically by force stretching into this intermediate lengthened state or beyond. The influence of these alterations can have significant influence on cell fate. Further exploration into the effects of the engineered integrin mediated-Fn IBD on cell fate will be discussed in subsequent sections of this dissertation.

CHAPTER 4. PROBING CELL BEHAVIOR IN RESPONSE TO RECOMBINANT FNIII9-10 FRAGMENTS

4.1 Introduction

4.1.1 CCL-210

CCD19Lu (ATCC® CCL210™) are primary human normal lung fibroblasts. These cells are used in this work to probe events that may trigger these normal cells to being to manifest characteristics closer to myofibroblasts or at least mimic phenotypes that may be present in fibrosis. CCL210s are known to express α5β1 and αvβ3 integrins, and we hypothesize they will respond to biochemical and physical cues through differential integrin engagement. Others such as Wang *et al.* have used CCD19Lu (ATCC® CCL-210™) to explore potential therapeutic options for lung fibrosis. Understanding the responses of these cells to their environment can direct our understanding of the diseased tissue *in vivo* and how these lung fibroblasts can help us to understand the relationship between cell-matrix interactions and their role as drivers in fibrotic disease.

4.1.2 Focal Adhesions

A focal adhesion refers to the contact between a cell and the extracellular matrix through interactions between transmembrane proteins referred to as integrins and intracellular ligands. The intercellular multiprotein focal adhesion complexes that are connected the actin cytoskeleton upon these contacts modulate mechanical force sensing and transmit regulatory signals that are transmitted between the environment and the cell and can regulate cell motility and other phenotypes contributing to functional diversity

within cell populations and tissues. These physical connections to the ECM can provide sensory responses, which inform the cell about the architecture and composition of the ECM and ultimately can affect cellular behavior. The ECM provides both biochemical cues (through protein orientation) and mechanical stimuli (through varying matrix stiffness). These components among other such as present growth factors and cytokines and triggering event like inflammation or injury can provide information to the cell about how it should behave. Lung fibroblasts can respond to their environment based on changes in matrix composition, rigidity, and matrix protein conformation. The cell's stability is in flux as the cell migrates and FAs are associating and dissociating as the leading edge of the cell builds new contacts and the trailing edge contacts are broken[28]. In wound healing focal adhesion maturation transduces cell signals from the environment to trigger the healing events and cell signals associated with this phenomena. Fibroblasts respond to wounds in three discrete phenotypic ways: recruitment, differentiation, and resolution. After injury activation and recruitment of fibroblasts to the site of injury is initiated[156]. Fibroblastic proliferation is triggered based on the recruited fibroblasts engaged with inflammatory cytokines[157]. Evidence also indicates that matrix stiffness stimulates fibroblast proliferation as well[5]. After the provisional matrix tissue is deposited the local fibroblasts undergo transition to differentiated myofibroblasts or "activated" fibroblasts. The cells now known as myofibroblasts will continue to synthesize and assemble matrix proteins and with apply contractile forces triggering the expression of α-SMA into contractile filaments furthering their force influence[158].

4.1.3 Integrins αvβ3 and α5β1

Integrins are heterodimeric transmembrane receptors that link the cell's cytoskeleton and the ECM[142]. Published works have indicated that integrin affinity can result from conformational changes in the ECM[159,160].Fn matrix assembly is matrix assembly into Fn fibrils evidenced by the fact that cells which lack αv and α5 integrin subunits fail to assemble fibrils even though their matrix protein secretion is unaffected[144]. Although it is known that many integrins can bind to Fn the integrin α5β1 is the major regulator of this relationship and the integrin that cells primarily use to engage and assemble Fn molecules into the ECM[145,146]. Well-studied integrins are αvβ3 and α5β1 integrins are both known to engage RGD within FnIII10; however, it has been shown that α5β1 is a synergy dependent integrin meaning that it is responsive to Fn's IBD when RGD (FnIII10) and the synergy site, PHSRN, (FnIII9) are coordinated in a spatial conformation that allows access to both sites[22,92,161]. Recent evidence indicates that the fibroblast integrins αvβ3 and α5β1 can work together to improve rigidity sensing on an Fn-based substrate[148]. This improved mechanosensing has implications in cell migration and invasion present in known fibrotic pathologies. It is hypothesized that the spatial relationship between RGD and PHSRN may result in differential integrin engagement and mediation of different signaling events associated with specific integrin engagement. This integrin "switch" has been characterized with endothelial cells and HFFs but it is of interest to look at lung fibroblasts due to their role in pulmonary fibrosis. If confirmed, the integrin "switch" could be a potential target for therapeutic options[162].

4.1.4 Downstream signaling

The physical attachment site between cells and the ECM are integrin-based adhesions. Adhesions of associated molecules are clustered at the site of integrin and

cytoskeletal forces. In this thesis, we refer to these molecular clusters as focal adhesions (FAs). On the cytoplasmic tails of integrins the associated proteins serve as scaffolds which include cytoskeletal binding and other adaptor proteins (kinases and phosphatases)[120]. Propagation of biochemical signals are triggered based on the macromolecular complexes associated with these FAs. It is known that FAs are mechano-sensitive and can grow and change composition in response to mechanical force[118,119]. Based on these conclusions it is known that specific proteins are recruited to FAs and trigger specific downstream responses in a force-dependent manner[120,163164]. Scaffolding molecules like paxillin, a nascent complex, will form at the leading edge of FAs. Activation of downstream signaling molecules such as focal adhesion kinase (FAK) and Src in response to increased mechanical tension can occur as ECM ligation occurs and FAs assemble and turnover[124]. Interestingly, when exogenous force is applied to integrins similar signaling pathways are stimulated by internally generated forces. Work by Choquet *et al.* demonstrated that adhesion reinforcement and cytoskeletal linkage is localized and strengthened in response to cells sensing the restraining force that is applied by Fn-coated beads[165]. The rearrangement of the cytoskeleton results in stiffening of the cell at the cell-ECM interface[125]. The receptor-ligand reaction landscape and potential for cryptic binding site exposure may be altered by single molecule force and could modulate the output and dynamics f downstream signaling pathways. This is demonstrated through the cytoskeleton associated protein interin[126,127]. The complexity of FA architecture, composition, and interactions make resolving mechano-signaling a challenge.

4.1.5 MRTF and actin relationship

Through examination of MRTF nuclear localization gene expression myofibroblast differentiation and potential for wound healing activity can be monitored. Since nuclear localization of MRTF indicates a myofibroblast phenotype observation of this effect on variable substrates may indicate how myofibroblastic the cells appear to be. It is known that enhanced polymerization of F-actin precedes nuclear localization of the cytoplasmic G-actin bound transcription factor MRTF. In the nucleus MRTF complexes with serum response factor and continues to drive α-SMA expression indicative of myofibroblast differentiation[166,167]. In response to stress, MRTFs are essential regulators of the smooth muscle contractile phenotype so monitoring their behavior can provide important indications of the relationship between MRTF and cytoskeletal dynamics. The relationship known that cytoskeletal actin polymerization signals the MRTF cofactor and induces nuclear transcription of SRF which then modulates the expression of genes which can further have regulatory and structural impacts that further link the cytoskeleton dynamics with genome activity (Actin-MRTF-SRF)[168]. Fibrotic disease could be treated through inhibition of the myofibroblast differentiation and wound healing regulatory pathways since their dysregulated activation is what leads to the disorder.

4.1.6 Phenotypes of myofibroblasts

Myofibroblasts are activated fibroblast cells physiologically found in wound and pathologically associated as the effector cell of fibrosis. These cells once activated can be distinguished by known phenotypes: differential integrin engagement, phosphorylation of FA associated proteins (FAK and Src), paxillin formation, MRTF nuclear localization, increased adhesion, increased cell contractility, increased cell proliferation and metabolism. Other indicators of activated fibroblasts include increased matrix synthesis

and generally increased anabolism, and resistance to apoptosis but these have not been explored in this work. Metabolic reprogramming is associated with myofibroblast differentiation and increased proliferation is a known phenotype of myofibroblasts as well. It is known that α-SMA expression should increase as cells differentiate towards a myofibroblast phenotype.

It is believed that as cell phenotype changes due to the sensitivity of lung fibroblasts to Fn IBD a feedback loop is created due to increased cell contractility and additional matrix deposition which then further destabilizes the proteins in the matrix. The recombinant Fn fragment variants allow a controlled system which can probe the integrin relationship with outputs on cell phenotype. Once the phenotypic effects on lung fibroblasts are characterized potential therapeutics can be tested to observe their influence on cell behavior (furthering myofibroblast differentiation or re-initiating proper wound healing and resolution).

4.2 Materials and Methods

4.2.1 Cell Culture

CCL-210 cells, normal human lung fibroblasts, were obtained from ATCC and maintained in DMEM media supplemented with 10% FBS and 1% Penicillin Streptomycin (PenStrep). For experiments analyzing the role of FnIII9-10 fragments on directing cell behavior, cells were plated on 0.1-8μM Fn-fragment coated glass coverslips, TC plastic, or Matrigen HTS hydrogel plates for 15 minutes - 48 hours depending on the experiment. Surfaces were then blocked with 1% hd-BSA and were sometimes cultured for experiments in serum-free, low serum (0.2-2% FBS), or full serum (10% FBS) DMEM.

4.2.2 Immunofluorescent Staining (αv and α5 Integrin)

For experiments analyzing the role of FnIII9-10 fragments on integrin engagement, glass coverslip surfaces were coated with 4μM overnight at 4°C. Surfaces were then blocked with 1% hd-BSA and were then cultured (6,000 cells/cm^2 at 37°C) for the experiment in full serum (10% FBS) DMEM for 15 - 60 minutes. Samples were fixed with acetone:methanol 1:1 mixture at -20°C for 5 minutes. Cells were permeabilized with 0.1% Triton X-100 and then blocked with 5% NGS for 1 hour. Cells were then incubated with 1:500 of AB1928 (Millipore) anti-α5 rabbit antibody and 1:200 AB16821 anti-αv mouse antibody. After primary stain overnight at 4°C the secondary stain of anti-mouse 546 (Invitrogen) and anti-rabbit 488 (Invitrogen) as well as Phalloidin (Alexa Fluor 488 Phalloidin, Invitrogen, 1:2000) was used for immunofluorescent imaging. Cell were incubated for 1 hour in secondary antibodies then 1 minute Hoescht (Thermo Fischer Scientific) nuclear stain and mounting to slides with ProLong Gold Antifade Mountant (Thermo Fischer Scientific). Ratiometric images were generated using an in-house MATLAB algorithm. Images were thresholded using Otsu's method, and masked based on where both α5 and αv signals passed the threshold. Fluorescence intensity of α5 staining was then divided by staining intensity of αv[29].

4.2.3 Immunofluorescent Staining (Paxillin)

Plate was coated with protein (Fn, FnIII9*10, FnIII9-4G-10) overnight at 4°C and blocked for 1 hour with 1% hdBSA. Cells were seeded at a density of about 6,000 cell/cm^2 in 10% FBS (full-serum) DMEM conditions. Cells were given 1-25 hours to attach and spread in response to the biochemical presentation of the proteins. Controls were all treated

appropriately before fixation (1% BSA and no primary). Cells are fixed with 4% PFA for 10 mins for each time point and permeabilized in 0.2% Triton X-100 for 5 minutes. Coverslips are washed 3x with 1xPBS and blocked with 5% NGS for 1 hour at room temperature. Cells are then stained with primary antibody (Anti-Paxillin Rabbit, clone Y113, EMD Millipore, 1:200) overnight at 4°C. Cells are then washed three times with 1xPBS and stained in secondary antibody (Alexa Fluor 546 goat anti-Mouse, Invitrogen, 1:2000 and Alexa Fluor 488 Phalloidin, Invitrogen, 1:2000) at room temp for 1 hour. Cells were incubated with 1:1000 Hoechst (thermos Fischer Scientific) nucelar stain for 1 min, wash 3 x with PBS and once with DIH_2O. Samples were mounted using ProLong Gold Antifade Mountant (Thermo Fischer Scientific) and later sealed using clear nail polish. Images were acquired with PerkinElmer UltraVIEW VoX using Spinning Disk detector Hamamatsu FLASH 4 sCMOS version 2 and a 60x Oil objective on a Nikon Ti-E with Perfect Focus 3.

4.2.4 Magnetic Bead Pull-down Assay

Approximately $3x10^6$ CCL-210 cells are plated on several 100 mm TC plastic petri dishes. Magnetic Dynabeads, (Dynabeads M-280 Tosylactivated, Invitrogen), are coated with Fn, FnIII9*10, and FnIII9-4G-10 (50μg). After preparation of the beads the bead suspension was added to the cell plates and they are allowed to incubate for ~40 minutes. Magnet is applied to provide 10-16pN of magnetic force to activate the cell focal adhesions which are conjugated to the Fn/Fn fragment coated magnetic beads for variable time (0-30 minutes). Cells are collected and lysed with 2x laemmli buffer and collections from the beads (the force-induced focal adhesion proteins) were analyzed to verify concentration using a Pierce 660nm Protein Assay Reagent with 50mM Ionic Detergent Compatible

Reagent (IDCR) and then SDS-PAGE and Western blots were performed . After transfer to nitrocellulose membrane and blocking with 5% milk primary antibodies (pY397-FAK (1:1,000, rabbit, 44-624G; Invitrogen), c-Src (1:1,000, rabbit, 32G6; Cell Signaling Technology), FAK (1:1000, rabbit, ab40794; Abcam), and pY416-SFK (1:1,000, rabbit, 2101; or 1:1,000, rabbit, D49G4; Cell Signaling Technology) were incubated overnight at 4°C. Next, secondary antibody (Goat anti-Rabbit IgG secondary antibody, HPR conjugated, 31460, ThermoFisher) was incubated for 1 hour. Stained proteins were observed using a Bio-Rad ChemiDoc imaging system based on size (Src/p-Src MW~56kDa and FAK/p-FAK MW~110kDa).

4.2.5 Size and Shape Analysis of Cell Body

Plate was coated with protein (Fn, FnIII9*10, FnIII9-4G-10) overnight at 4°C and blocked for 1 hour with 1% hdBSA. Cells were seeded at a density of about 5,000 cell/cm^2 in 10% FBS (full-serum) DMEM conditions. Cells were given 1-25 hours to attach and spread in response to the biochemical presentation of the proteins. Controls were all treated appropriately before fixation (1% BSA and no primary). Cells are fixed with 4% PFA for 10 mins for each time point and permeabilized in 0.2% Triton X-100 for 5 minutes. Coverslips are washed 3x with 1xPBS and blocked with 5% NGS for 1 hour at room temperature. Cells are then washed three times with 1xPBS and stained in Alexa Fluor 488 phalloidin, Invitrogen, 1:2000 at room temp for 1 hour. Cells were incubated with 1:1000 Hoechst (Thermo Fischer Scientific) nuclear stain for 1 min, wash 3 x with PBS and once with DIH_2O. Samples were mounted using ProLong Gold Antifade Mountant (Thermo Fischer Scientific) and later sealed using nail polish. Images were acquired with PerkinElmer UltraVIEW VoX using Spinning Disk detector Hamamatsu FLASH 4

sCMOS version 2 and a 60x Oil objective on a Nikon Ti-E with Perfect Focus 3. Cell area was measured with an intensity-based auto-detection algorithm within the PerkinElmer Volocity software that allows for specific identification of cell borders and pixel number.

4.2.6 Crystal Violet Attachment Assay

Cell attachment assays were performed as previously described[153]. Briefly, surfaces were coated with 2μM Fn fragments (FnIII9*10 and FnIII9-4G-10 have similar coating efficiencies) or 10μg/mL full length WT Fn and blocked with 1% hd-BSA[92,154]. CCL-210's were analyzed for their adhesion on carious surfaces. Cells were seeded at 15,000-30,000 cells/well and were allowed to attach for approximately 20 minutes at 37°C in 10%-serum DMEM then washed to remove unbound cells, fixed with 5% glutaraldehyde, and stained. A 0.1% crystal violet solution was used to stain the cells. After drying the stain was solubilized with 10% acetic acid and absorbance was quantified on the BioTek H4 Microplate Reader at 570nm. Linear regression was performed on the standard curve to determine reliability of the assay. Attachment values were normalized to cell attachment levels hd-BSA (0% attachment). Data from the triplicate experiment was normalized to the cells remaining in the highest cell density wells from the standard curve and presented as average +/- standard error. Normalized remaining cell percentage is presented on the y-axis.

4.2.7 CyQuant Assay

CCL-210's are serum-starved for 2 days in serum-free (no FBS) DMEM. Proteins (Fn, FnIII9*10, FnIII9-4G-10, were used to coat a 96-well plate at varying concentrations overnight at 4°C. The wells were then washed 3x with 1xPBS, blocked with 1% hdBSA

for 1 hour at room temperature, washed again 3x with 1xPBS. Cells were then trypsinized and plated into 96-well plate at 10,000-20,000 cells/well (100,000-200,000 cell/mL) in 10% Fn-depleted DMEM. Growth was monitored at variable time points (16-24 hours). Detection Reagent 2x is prepared with PBS, CyQuant Direct nucleic acid stain and CyQuant Direct background suppressor I (Thermo Fischer). Equal volume of 2x Detection Reagent was added to wells and incubated at 37°C for 1 hour. Flourescence is read on BioTek micro plate reader bottom up at excitation/emission 508nm and 527nm respectively.

4.2.8 MTT Assay

Cells were serum-starved for 2 days in DMEM without phenol red. Proteins (Fn, FnIII9*10, FnIII9-4G-10, were used to coat a 96-well plate at varying concentrations overnight at 4°C. The wells were then washed 3x with 1xPBS, blocked with 1% hdBSA for 1 hour at room temperature, washed again 3x with 1xPBS. Cells were then trypsinized and plated into 96-well plate at 20,000 cells/well (200,000 cell/mL). Media conditions were described as low serum (0.2% FBS) media and full serum (10% FBS). Most wells are plated with cells in low serum except for a control. All samples are run in triplicate. Control wells for TGF-β (Recombinant Human TGF-β1, Fisher Scientific, 5 ng/mL, addition at initial cell plating) and LatB (Latruculin B, Sigma-Aldrich, 2 µM, 30 minutes prior to assay) were prepared as well. Cells were incubated for 16-48 hours at 37°C. After incubation the media was removed and fresh media was added. Next, 10 µl of 12 mM (5 mg/mL) of the MTT dye (MTT Cell Proliferation Assay, Thermo Fischer Scientific) is added to the wells. The MTT dye is photosensitive so it is protected from the light. Plate is then incubated for 3 hours at 37°C and purple soluble formazan is visible with tabletop

microscope 10x (See Appendix). Next, 85µL of medium was removed from each well and 50µL of DMSO was added to dissolve the formazan and mixed thoroughly. The plate was then incubated for 10 minutes at 37°C, samples are mixed again, and cells are read on BioTek micro plate reader at excitation/emission 540nm and 570nm respectively.

4.2.9 Immunofluorescent Staining (MRTF)

Plate was coated with protein (Fn, FnIII9*10, FnIII9-4G-10) overnight at 4°C and blocked for 1 hour with 1% hdBSA. Cells were seeded at a density of about 5,000 cell/cm^2 in 10% FBS (full-serum) DMEM conditions. Cells were given 1.5-4 hours to attach and spread in response to the biochemical presentation of the proteins. Controls (LatB (Latrunculin B, Sigma-Aldrich, 2 µM, 30 minutes prior to assay) and Cytochalasin D (Sigma-Aldrich, 40 minutes prior to fixation)) were all treated appropriately before fixation (1% BSA and no primary). Cells are fixed with 4% PFA for 10 mins for each time point and permeabilized in 0.2% Triton X-100 for 5 minutes. Coverslips are washed 3x with 1xPBS and blocked with 5% NGS for 1 hour at room temperature. Cells are then stained with primary antibody (Anti-MKL1 antibody (anti-MRTF-A), Rabbit, 1:500, Sigma Aldrich) overnight at 4°C. Cells are then washed three times with 1xPBS and stained in secondary antibody (Alexa Fluor 546 goat anti-Rabbit, Invitrogen, 1:2000 and Alexa Fluor 488 phalloidin, Invitrogen, 1:2000) at room temp for 1 hour. Cells were incubated with 1:1000 Hoechst (Thermo Fischer Scientific) nuclear stain for 1 min, wash 3 x with PBS and once with DIH_2O. Samples were mounted using ProLong Gold Antifade Mountant (Thermo Fischer Scientific) and later sealed using nail polish. Images were acquired with PerkinElmer UltraVIEW VoX using Spinning Disk detector Hamamatsu FLASH 4 sCMOS version 2 and a 60x Oil objective on a Nikon Ti-E with Perfect Focus 3. Single

cells or multicellular aggregates are segmented based on actin and nuclear signaling, and MRTF signal in each compartment is background corrected (using intensities from the no primary control). Ratios of background corrected MRTF signal from the whole cells and from the nuclear compartment are used to estimate the nuclear fraction of MRTF.

4.3 Results

4.3.1 Integrin staining (α5 and αv)

This experiment seeks to characterize the integrin expression of CCL-210, normal human lung fibroblasts, on different FnIII9-10 fragments at varying time points (30 and 45 minutes). It is hypothesized that cells will begin to lay down their own Fn matrix around 4 hours after attachment so there is validity in observing the initial attachments (~30-45 minutes) and the integrins associated with the focal adhesions associated at that time (applied force 1-30 minutes). Previous work completed in Cao *et al.* on integrin staining of αv and α5 provides insight into the specific integrins that are engaged on these same engineered Fn fragments utlized in this work[29]. Immunofluorescence staining of integrins on human foreskin fibroblasts cultured on these Fn fragments confirms that this molecular modification results in a switch in the integrin binding profile from α5β1 and αvβ3 to predominantly αvβ3 at the cellular level (Figure 17), supporting earlier reports of FnIII9*10 fragment's ability to engage α5β1 integrins preferentially[92].

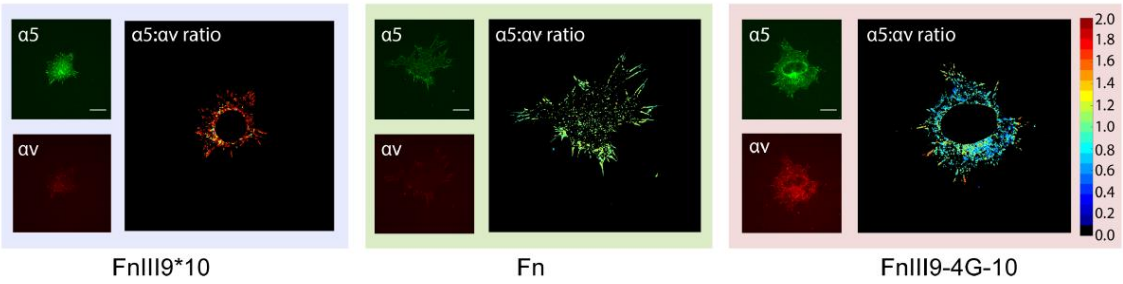

Figure 17. HFFs immunostained for integrins α5 and αv. Fibroblasts cultured on FnIII9*10 and FnIII9-4G-10 fragments and immunostained for integrins α5 and αv demonstrate the fragments' capability of skewing cellular binding toward specific integrins. Scale bar is 20 μm.

Comparison of this effect on the normal human lung fibroblasts was explored to determine if the same trend was apparent, but here the trends are similar but not as stark (Figure 18). The ratio of α5 to αv integrin engagement is less significant; however, the trend of preferred engagement of α5β1 on FnIII9*10 substrate and αvβ3 on FNIII9-4G-10 is possibly there.

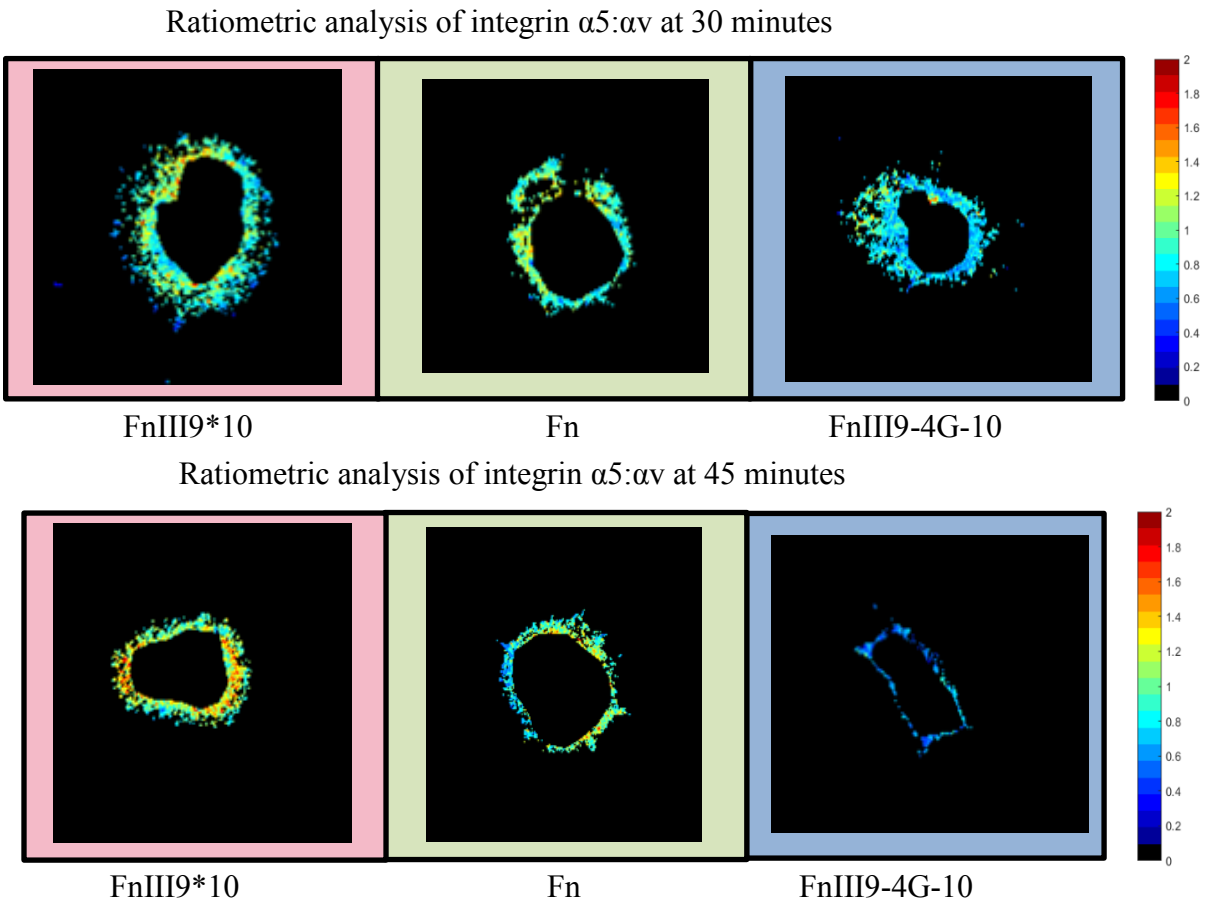

Figure 18. Ratiometric analysis of α5:αv using in-house MATLAB script. Slight differences are apparent visually for interpretation of greater α5 engagement on FnIII9*10 and full-length Fn.

By observing the quantitative differences in Figure 19 it can be examined if there are significant differences between the α5:αV ratio of CCL-210s on substrate FnIII9-4G-10 and FnIII9*10 (*$p<0.05$ at both 30 and 45 minutes) as well as between FnIII9-4G-10 and full-length Fn (*$p<0.05$ at 30 minutes, ***$p<0.0005$ at 45 minutes). However, the mean values of each condition appear to sit within the deviation calculated at each value. This can make our determination of the true significance of these differences unclear

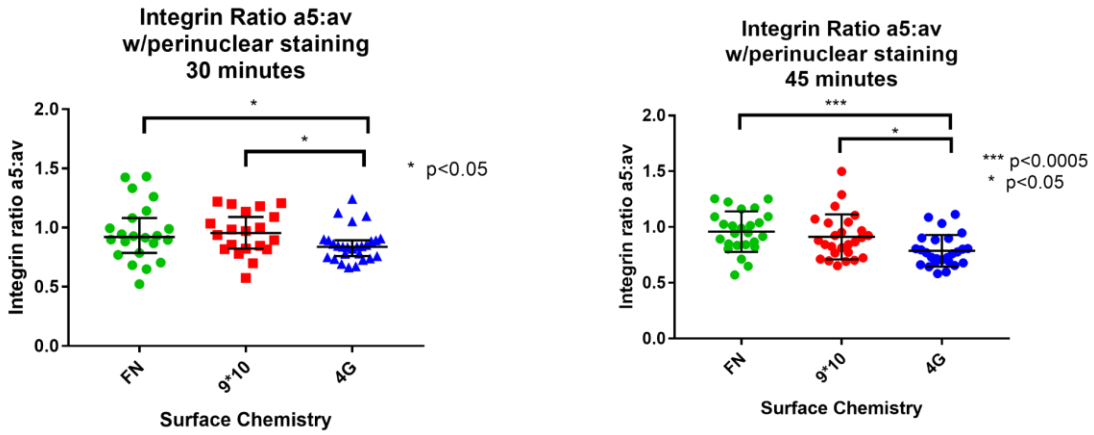

Figure 19. Quantitation of integrin staining intensity on Fn fragments and full length Fn. Human lung fibroblasts were seeded onto fragments (FnIII9*10 or FnIII9-4G-10) or full-length Fn in serum free media, fixed at 30 or 45 minutes, and stained for α5 and αv as described in Methods and materials. Ratiometric images of each cell were generated by thresholding individual channels and dividing α5 by αv. Median α5:αv values were calculated for each image and compared using one-way ANOVA with Tukey's post-test, N = 10 cells for each condition. *p < 0.05 and ****p<0.0005.

Overall, these results indicate that there may be an increased presence of α5 to αv integrin within CCL-210's focal adhesions on FnIII9*10 in comparison to the FnIII9-4G-10 fragment; however the effect does seem to be dampened when compared to other cell results such as HFFs (Figure 17). This could result from CCL-210's having a different integrin profile which may contain more αv containing integrins muddling the signal ratio. Since previous works suggested that the spatio-temporal relationship of RGD and PHSRN sites serve as an on/off switch for α5β1 binding to Fn such that destabilization between these sites may turn off the "switch" for α5 integrin binding we can compare these findings to our work. Although this theory seemed supported by our results, it appears that the "switch" behavior is less dramatic with CCL-210 human lung fibroblasts. This could be indicated in their expression of other αv integrins besides only αvβ3 (such as αvβ5). A relative dominance of these integrin switch behaviors may be dampened by the fact that

both Fn fragments will engage αvβ3 integrins. It appears that the mutation between the RGD and synergy sites is sufficient to drive fibroblasts to predominantly attach through αv and not α5.

4.3.2 Paxillin-containing Focal Adhesions

Paxillin was interrogated to characterize the size, position and number of focal adhesions present between CCL-210's and the recombinant Fn fragment matrix using immunofluorescence at variable time points (1, 3, 7, 25 hours). In this experiment we can compare FnIII9-4G-10 and FnIII9*10 by observing the morphology, length, and location of paxillin-containing focal adhesions and their formation over time via staining of the paxillin molecule. The results apparent in Figures 20-23 indicate that the focal adhesions seen on full-length Fn are both distal, extended, distinct, and have a clear polarized morphology as early as 1 hour after plating. The cells on Fn appear to be in a migratory lamellipodia as the focal adhesions are attaching to the leading edge and absent from the tailing edge. Whereas in Fn the adhesions are clear at early time points (as early as 1 hour) there are differences in the fragment-associated focal adhesions in a temporal-dependent manner. On Fn9*10 there are significantly less prominent focal adhesions formed at earlier time points (1 and 3 hours); however, after 7 hours when it is believed that the cells have begun to lay down their own matrix consisting of self-assembled Fn there are indications of more distinct distal focal adhesions. On FnIII9-4G-10 we see prominent focal adhesion indicated in paxillin staining on early time points including 1 and 3 hours and we see this trend continue as it aligns with the results seen on FnIII9*10 at 7 and 25 hours as cells have begun to lay down their own Fn matrix and the focal adhesions formed at these later time points probably indicate the adhesion to the newly assemble Fn. In both FnIII9-4G-10 and

FnIII9*10 we do not see the same migratory pattern indicated by paxillin staining a leading and lagging end as was seen on full-length Fn.

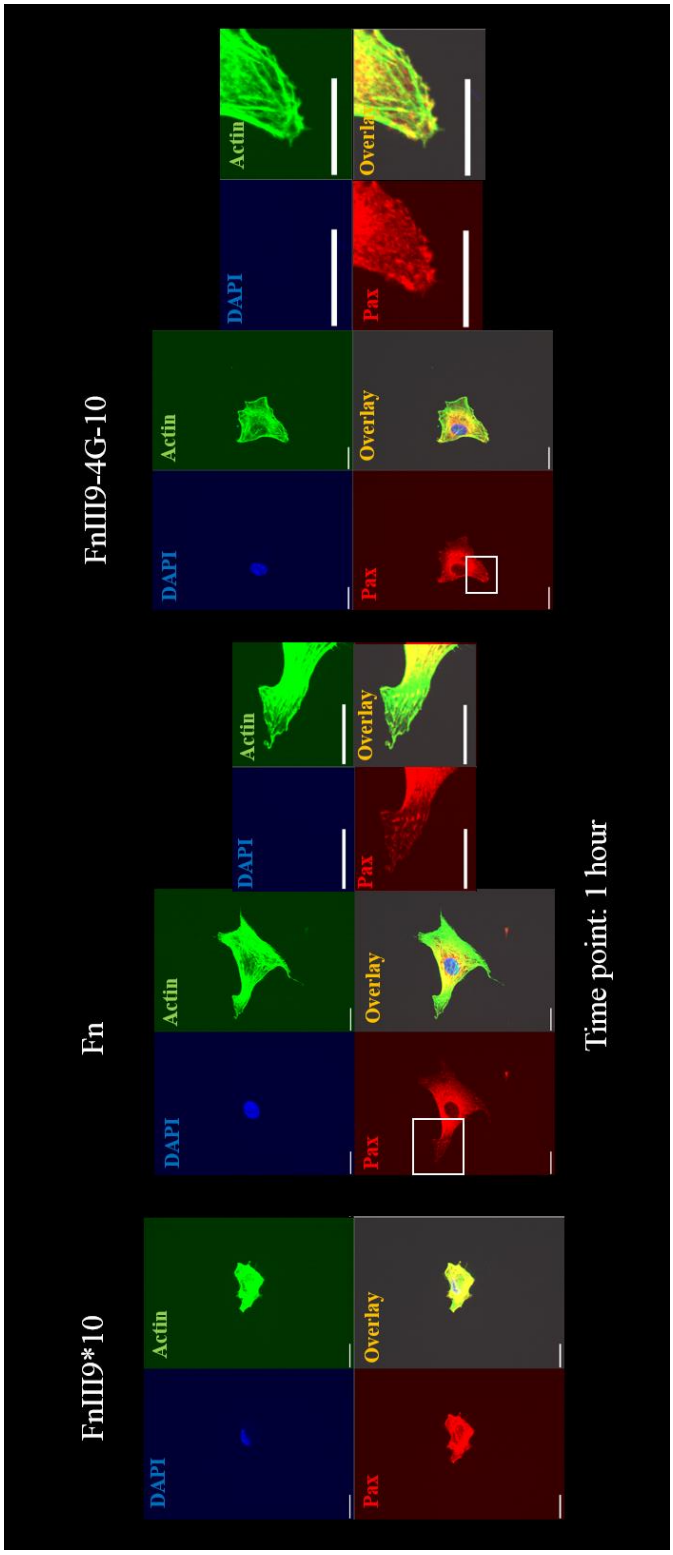

Figure 20. Paxillin immunostaining of FAs at 1 hour on FnIII9*10, FnIII9-4G-10, and full-length Fn. CCL-210 cells cultured on FnIII9*10 and FnIII9-4G-10 fragments and immunostained for DAPI, Paxillin, and Actin demonstrate the fragments' capability of skewing focal adhesion formation. Scale bar is 20 µm.

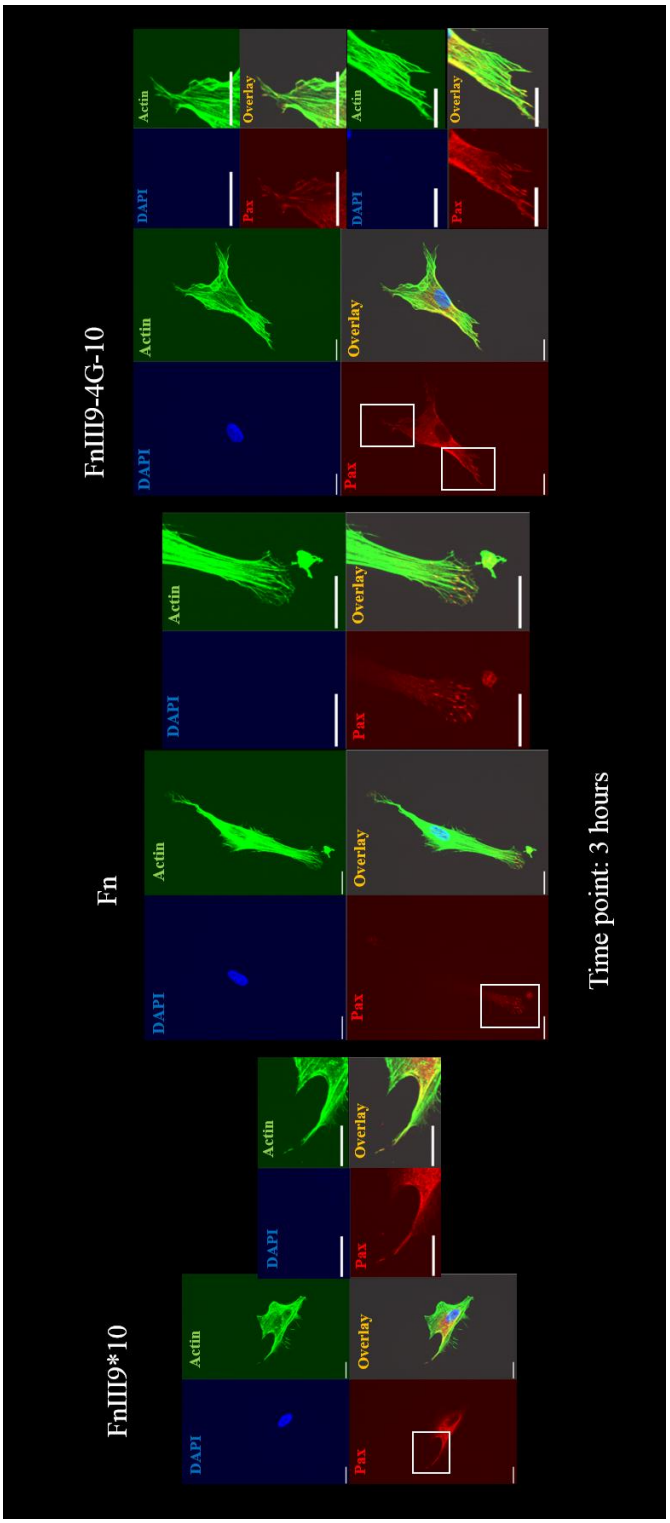

Figure 21. Paxillin immunostaining of FAs at 3 hours on FnIII9*10, FnIII9-4G-10, and full-length Fn. CCL-210 cells cultured on FnIII9*10 and FnIII9-4G-10 fragments and immunostained for DAPI, Paxillin, and Actin demonstrate the fragments' capability of skewing focal adhesion formation. Scale bar is 20 μm.

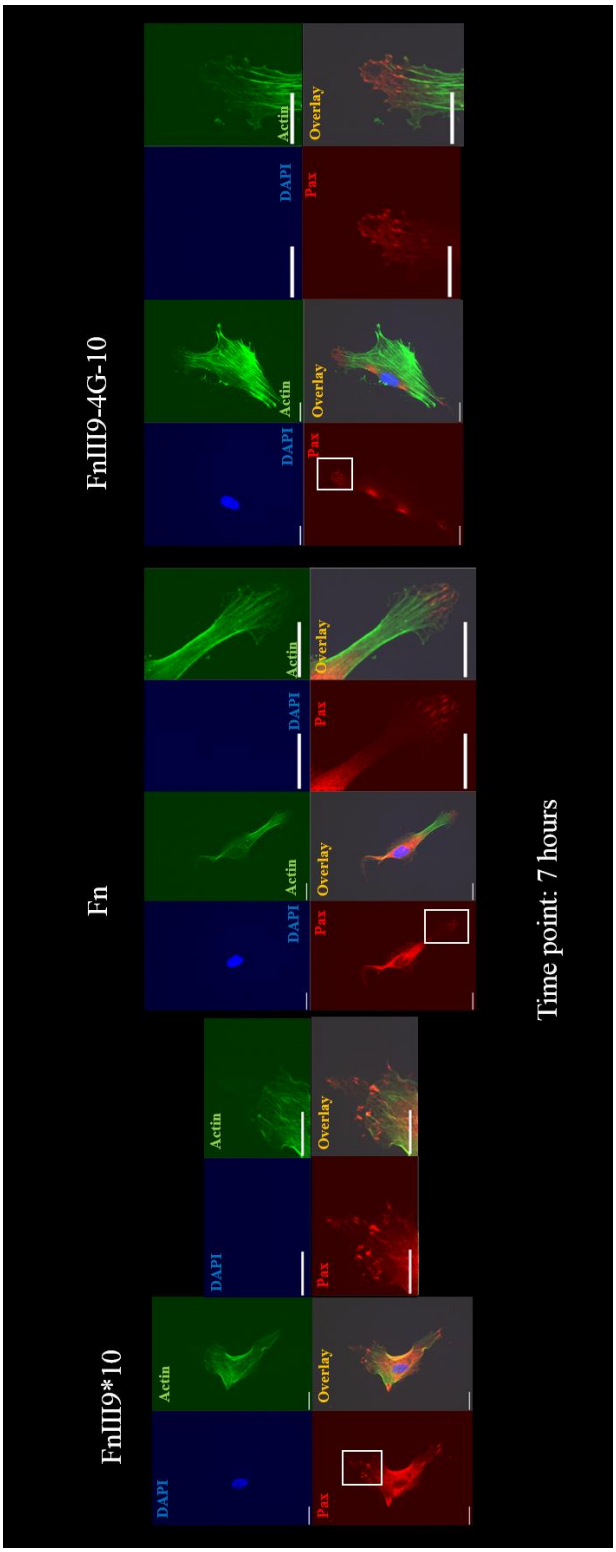

Figure 22. Paxillin immunostaining of FAs at 7 hours on FnIII9*10, FnIII9-4G-10, and full-length Fn. CCL-210 cells cultured on FnIII9*10 and FnIII9-4G-10 fragments and immunostained for DAPI, Paxillin, and Actin demonstrate the fragments' capability of skewing focal adhesion formation. Scale bar is 20 µm.

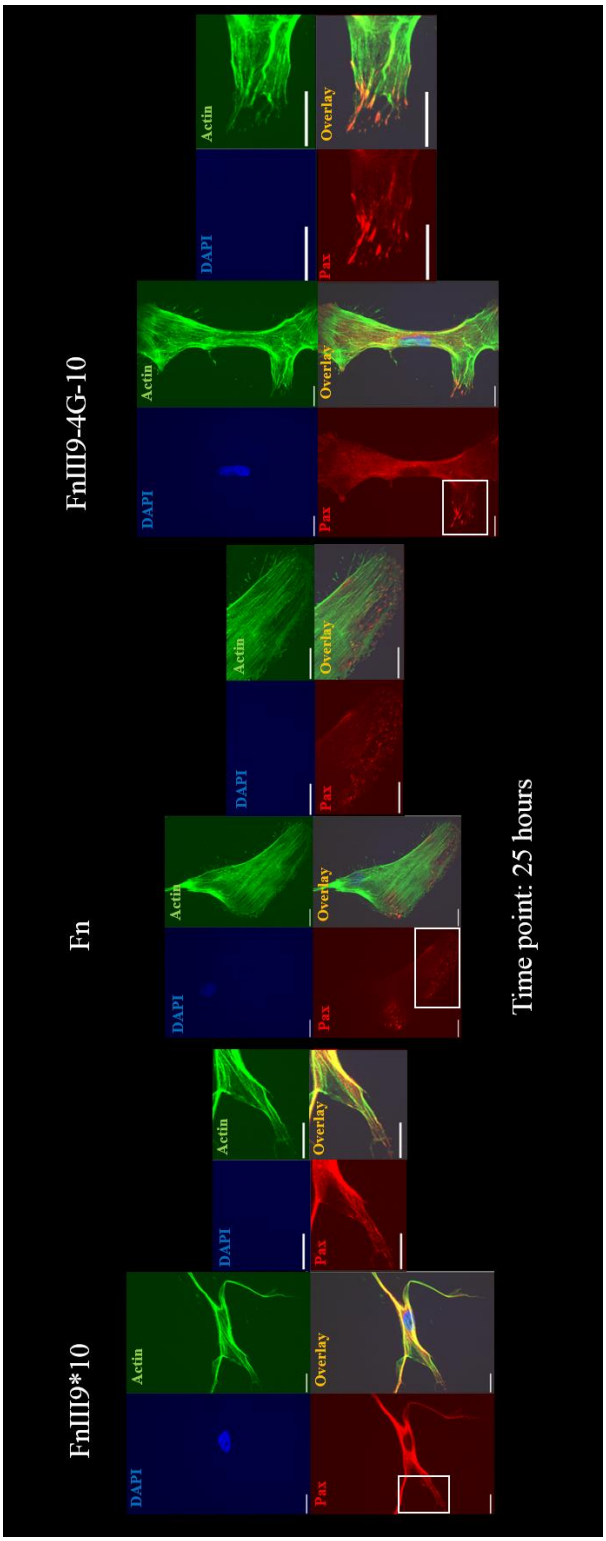

Figure 23. Paxillin immunostaining of FAs at 25 hours on FnIII9*10, FnIII9-4G-10, and full-length Fn. CCL-210 cells cultured on FnIII9*10 and FnIII9-4G-10 fragments and immunostained for DAPI, Paxillin, and Actin demonstrate the fragments' capability of skewing focal adhesion formation. Scale bar is 20 μm.

4.3.3 Force-mediated Focal Adhesion Complex Associated Proteins

To understand whether FnIII9-4G-10 and FnIII9*10 affect mechano-transduction, a magnetic bead pull-down assay was used. Pre-coated magnetic beads with FnIII9-4G-10 or FnIII9*10 fragment (or full-length Fn) were incubated with CCL-210 cells then magnetic force (10-16pN) was applied to active cell focal adhesion conjugated with magnetic beads through the active magnetic force pulling out the magnetic beads. Our results showed that force induced phosphorylation of FAK significantly increases in FnIII9-4G-10 but not in FnIII9*10 group. Interestingly, force activated phosphorylated Src was not detected to change in any significant amount with FnIII9*10 nor the FnIII9-4G-10 group (Figure 24, Figure 25). Based on previous work completed in Fiore *et al.* the pFAK expression levels at 5 minutes seem consistent for FnIII9-4G-10; however, the lack of pSrc increase seems to counter previous results found when cells engaged with full-length Fn.

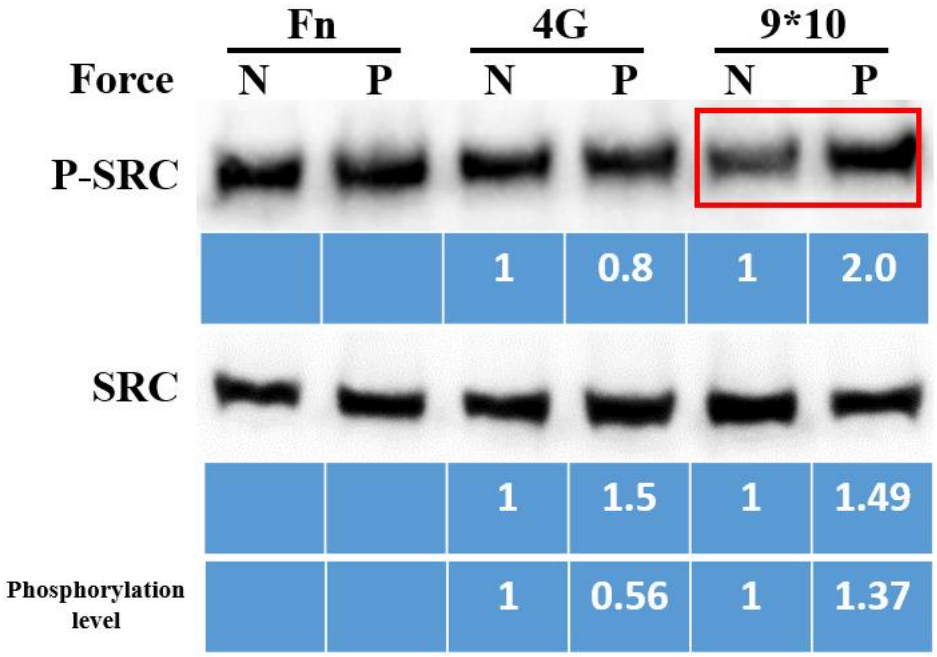

Figure 24. Magnetic bead analysis of phosphorylation of Src with 5 mins force application. CCL-210s are cultures and given time to adhere with magnetic bead coated with Fn variants. Force is not applied (N) or applied (P) for 5 minutes and increase in p-Src on FnIII9*10 were observed.

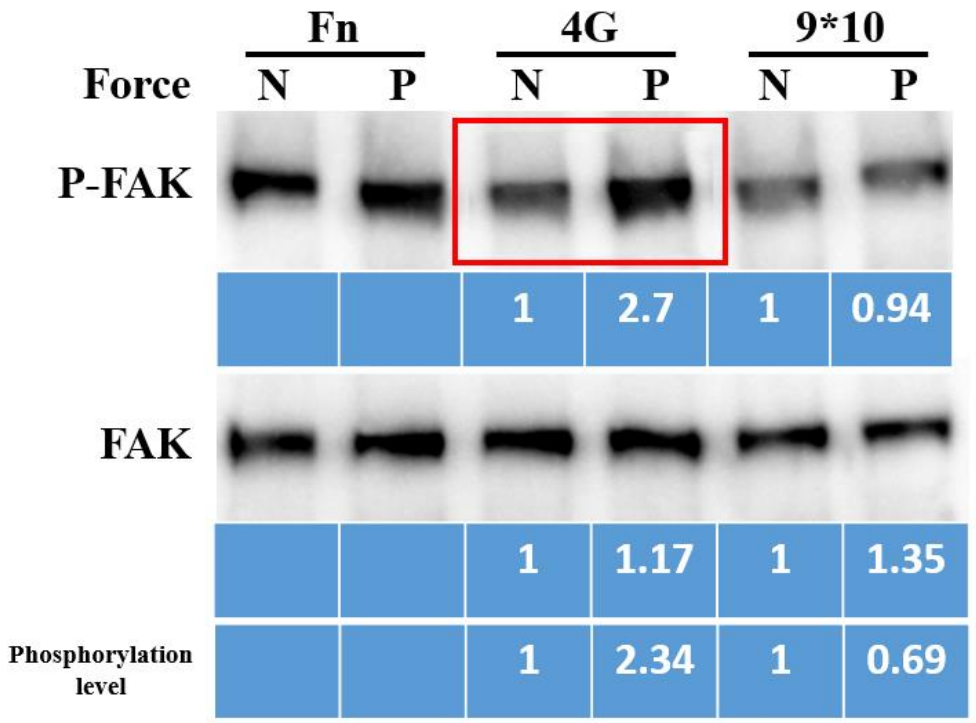

Figure 25. Magnetic bead analysis of phosphorylation of FAK with 5 mins force application. CCL-210s are cultured and given time to adhere with magnetic bead coated with Fn variants. Force is not applied (N) or applied (P) for 5 minutes and increase in p-FAK on FnIII9-4G-10 were observed.

To confirm how magnetic force applied over time affected the phosphorylation of FAK and Src based on presentation with FnIII9-4G-10 or FnIII9*10, we measured p-FAK and p-Src at 1, 5, 10 and 30 minutes. These results showed phosphorylation of FAK raised at 1 min and sustained for 30 mins when presented with FnIII9-4G-10. However, on FnIII9-4G-10 we do not see influence on Src phosphorylation levels through 30 minutes of applied force. For the cells exposed to magnetic beads coated with FnIII9*10 the phosphorylation at Src appeared to happen earlier than the phosphorylation of FAK. Increasing levels of phosphorylation of Src was detected at 5 mins and came back to basal line at 10 mins. However, FAK phosphorylation increased at 10 to 30 mins after forced applied concluding

that the results on FnIII9*10 appear much less consistent and may not be reliable (Figure 26 and Figure 27).

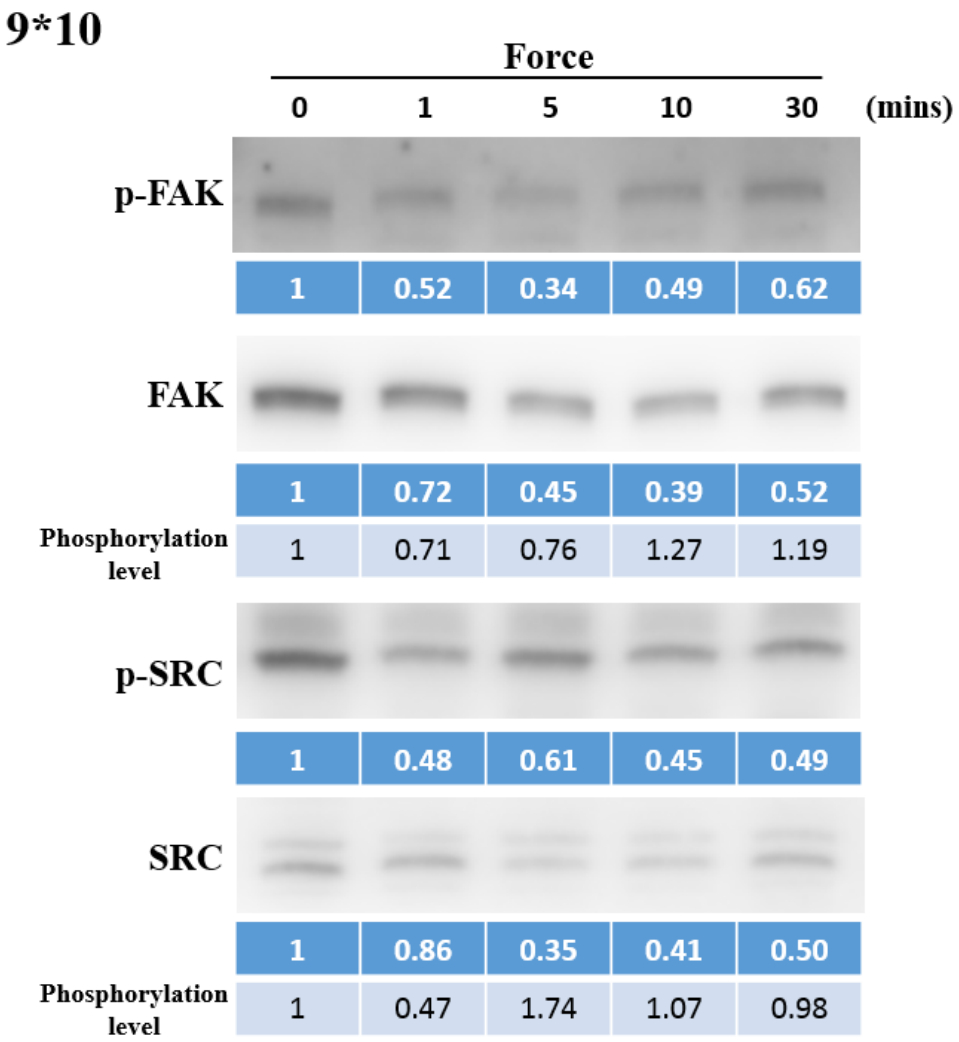

Figure 26. Magnetic bead analysis of magnetic FnIII9*10 coated beads from 0-30 minutes. CCL-210s are cultured and given time to associate with magnetic bead coated with FnIII9*10. Force is applied for 0-30 minutes and changes in phosphorylation of FAK and Src over this time are observed.

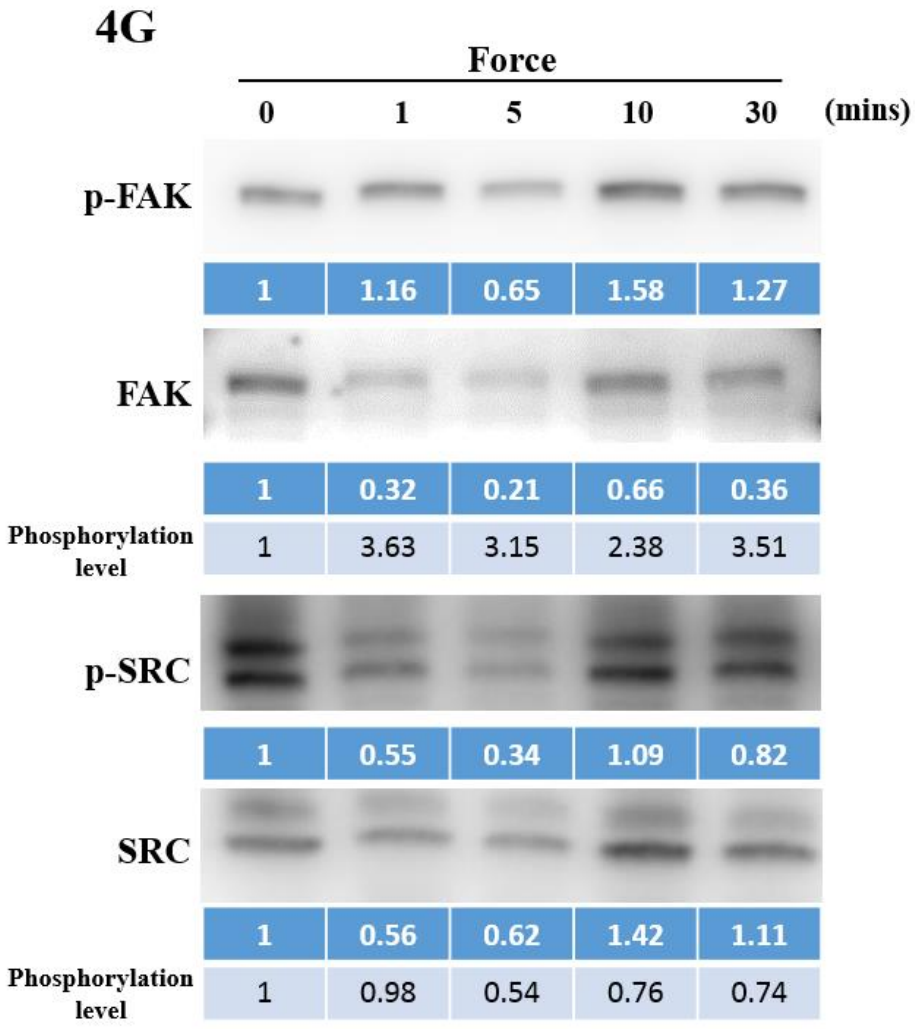

Figure 27. Magnetic bead analysis of magnetic FnIII9-4G-10 coated beads from 0-30 minutes. CCL-210s are cultured and given time to associate with magnetic bead coated with FnIII9-4G-10. Force is applied for 0-30 minutes and changes in phosphorylation of FAK and Src over this time are observed.

Band intensity of the western blots was analyzed to visually compare the influence of each fragments force-mediated focal adhesion complex associated proteins (FAK and Src). The values were normalized to the no-force control. Normalized quantitative values

above 1.5 indicate a reliable increase in phosphorylation, indicated on FnIII9-4G-10 coated beads over time of applied force (Figure 28).

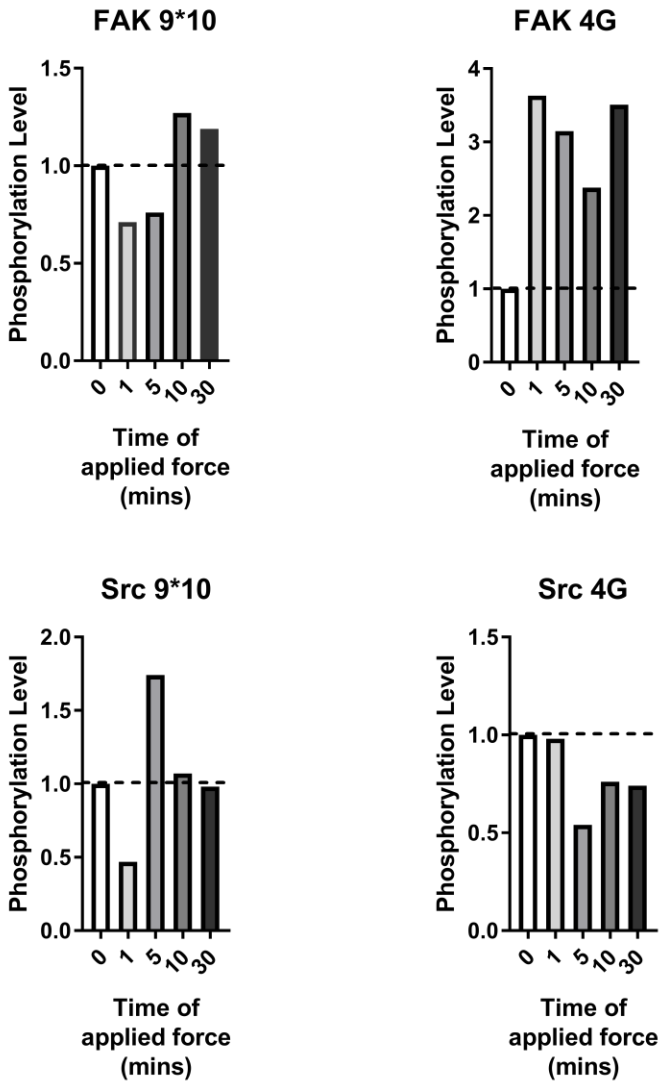

Figure 28. Quantitation of normalized intensities for magnetic bead analysis FnIII9-4G-10 and FnIII9*10 for 0-30 minutes of applied force. Values are normalized to no-force control for FAK and Src phosphorylation levels. Fold increase >1.5 indicated significant regulation of adaptor proteins. Consistent results seen with FnIII9-4G-10 coated beads influence on FAK phosphorylation levels.

4.3.4 Size and Shape for Cell Contractility

Cell contractility has been shown to scale with cellular spread area and polarity[169]. Therefore, observation of cell contractility was determined in this experiment through comparison of cell size (surface area and perimeter) and shape (polarity vs circularity). In this experiment both shorter (30, 45, 60, 90, 120, 240 mins) and longer (1, 3, 7, 25 hour) time points are analyzed (Figure 29-34). The data show different trends in the shorter and longer time points indicating that the CCL-210s may kinetically engage the different substrates differentially. In the earlier time points it appears that cells on all substrates (full-length Fn, FnIII9*10, and FnIII9-4G-10) appear to be roughly similar in size; however, there is indication that FnIII9*10 seems to be initially (after ~ 1 hour) more polar with FnIII9-4G-10 become more polar around the 4 hour mark.

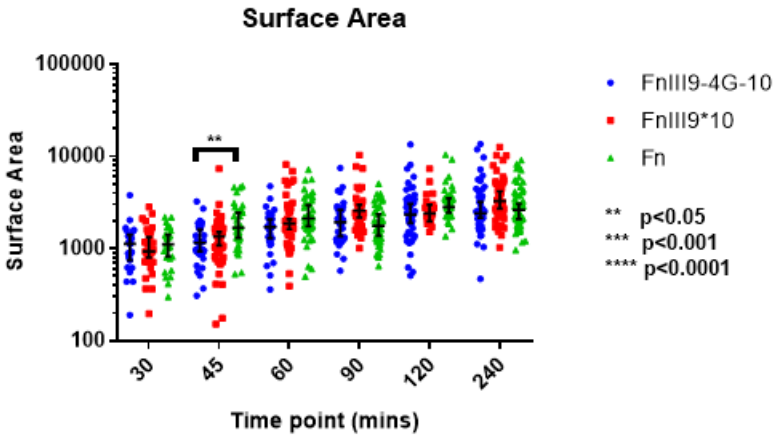

Figure 29. Surface area analysis at time point range (30-240 mins). CCL-210 cells are cultured on FnIII9*10 and FnIII9-4G-10 fragments (and full-length Fn) and immunostained for Hoescht nuclear stain and Actin. Volocity software is used to determine surface area of individual cells. Mean values of the surface area of actin is calculated for each image and compared using multiple t-test for each coating substrate, N = 30 cells for each condition. **p < 0.05.

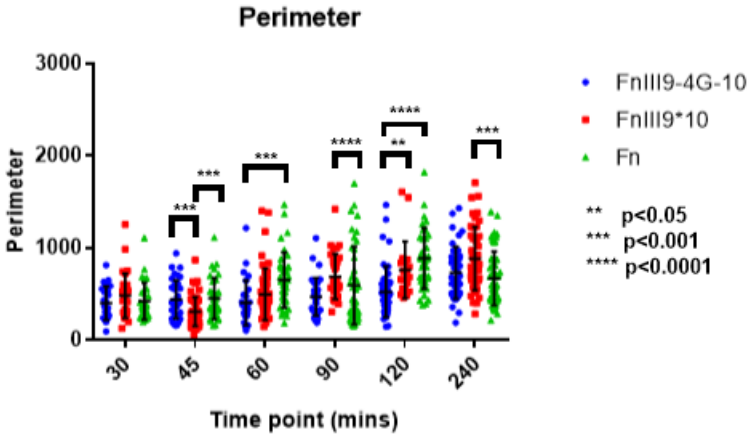

Figure 30. Cell perimeter analysis at time point range (30-240 mins). CCL-210 cells are cultured on FnIII9*10 and FnIII9-4G-10 fragments (and full-length Fn) and immunostained for Hoescht nuclear stain and Actin. Volocity software is used to determine the perimeter of individual cells. Mean values of the perimeter of actin is calculated for each image and compared using multiple t-test for each coating substrate, N = 30 cells for each condition. **p < 0.05, *** p<0.001, ****p<0.0001.

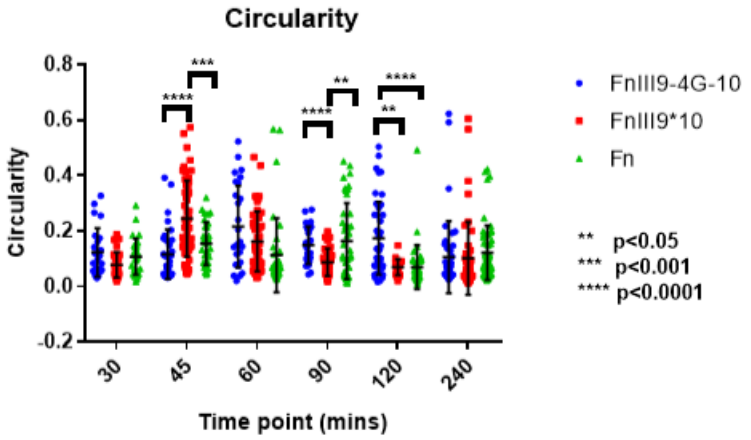

Figure 31. Circularity analysis at time point range (30-240 mins). CCL-210 cells are cultured on FnIII9*10 and FnIII9-4G-10 fragments (and full-length Fn) and immunostained for Hoescht nuclear stain and Actin. Volocity software is used to determine circularity of individual cells (circularity= 4π (area/perimeter^2)). Mean values of the surface area of actin is calculated for each image and compared using multiple t-test for each coating substrate, N = 30 cells for each condition. **p < 0.05, ***p<0.001, ****p<0.0001.

The trend of FnIII9-4G-10 becoming even more polar over time is enhanced at the 7 hour time point and all cells seem to reach the same general shape and size profile by 25 hours.

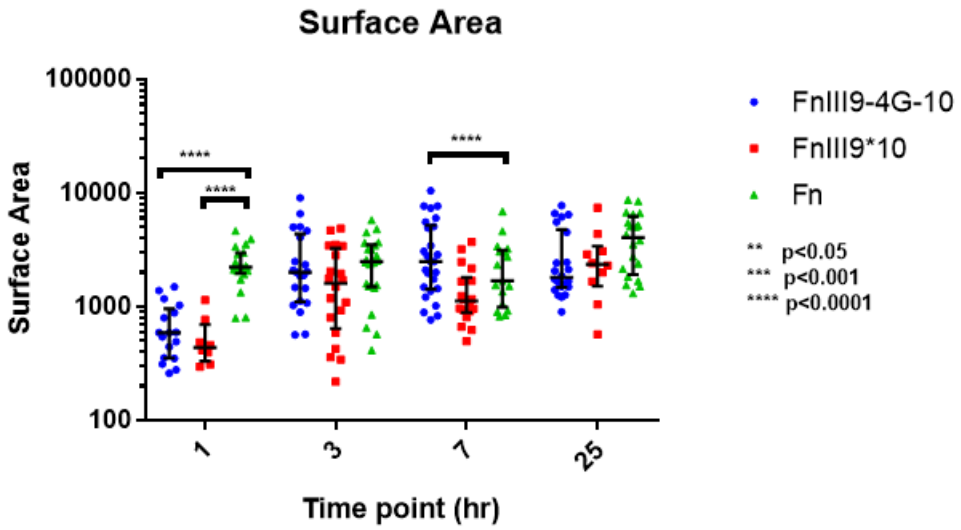

Figure 32. Surface area analysis at time point range (1-25 hours). CCL-210 cells are cultured on FnIII9*10 and FnIII9-4G-10 fragments (and full-length Fn) and immunostained for Hoescht nuclear stain and Actin. Volocity software is used to determine surface area of individual cells. Mean values of the surface area of actin is calculated for each image and compared using multiple t-test for each coating substrate, at least N = 15 cells for each condition. ****p < 0.0001.

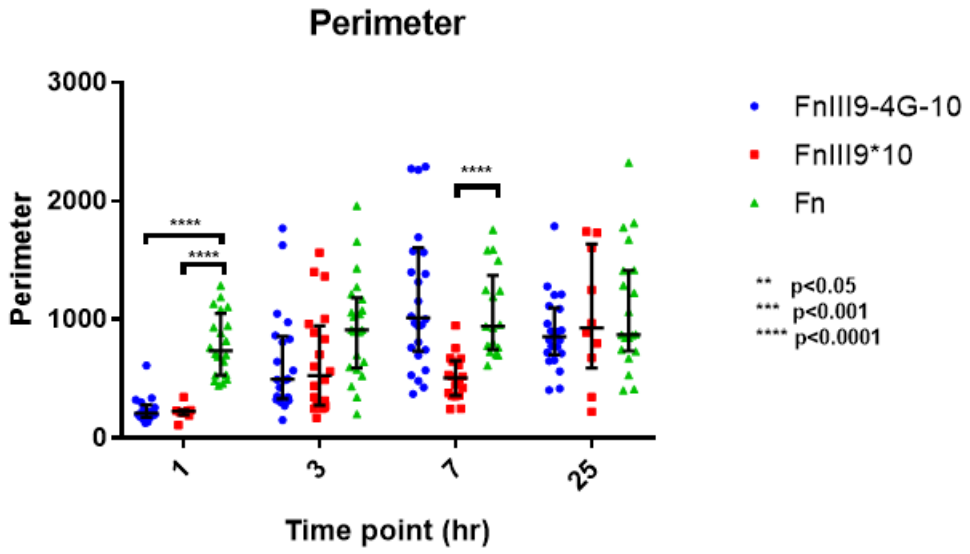

Figure 33. Cell perimeter analysis at time point range (1-25 hours). CCL-210 cells are cultured on FnIII9*10 and FnIII9-4G-10 fragments (and full-length Fn) and immunostained for Hoescht nuclear stain and Actin. Volocity software is used to determine the perimeter of individual cells. Mean values of the perimeter of actin is calculated for each image and compared using multiple t-test for each coating substrate, at least N = 15 cells for each condition. ****p<0.0001.

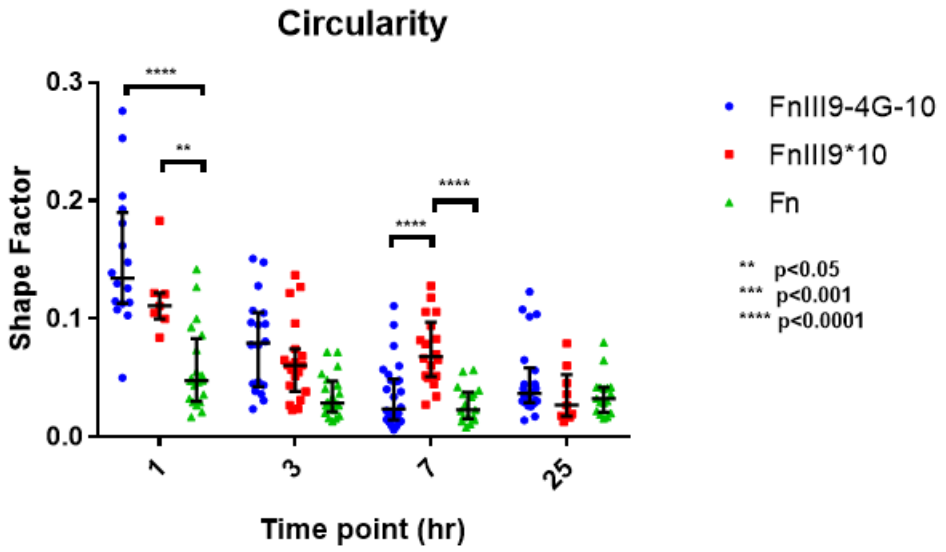

Figure 34. Circularity analysis at time point range (1-25 hours). CCL-210 cells are cultured on FnIII9*10 and FnIII9-4G-10 fragments (and full-length Fn) and immunostained for Hoescht nuclear stain and Actin. Volocity software is used to determine circularity of individual cells (circularity=4π(area/perimeter^2)). Mean values of the surface area of actin is calculated for each image and compared using multiple t-test for each coating substrate, at least N = 15 cells for each condition. **p < 0.05, ****p<0.0001.

4.3.5 Cell Adhesion Assay

To characterize how human lung fibroblasts attach to different FnIII9-10 variants, CCL-210 human lung fibroblasts were analysed via a crystal violet attachment assay. The results of this assay demonstrate that although full-length Fn has the greatest ability for cell adhesion, likely due to the complex nature of the molecule and the related influences of other cell-binding components, the engineered Fn fragments appear to have differences in cell attachment as well. These results indicate that FnIII9*10 shows more cell adhesion than cells plated on FnIII9-4G-10. Seen in Figure 35 we observe this trend to be true. The results shown are presented as percent attachment compared to attachment on high density

cells on Fn. Overall, these results indicate that stabilization of the RGD and synergy sites in FnIII9*10 variant facilitate cell attachment over FnIII9-4G-10.

Since adhesion is related to integrin engagement the ability of FnIII9*10 to bind both αvβ3 and α5β1 this is the suggested interpretation of the data. However, increased elevated, activated adhesion signaling is a key phenotypic indicator of fibrotic cells. Adhesion could be an indicator for cell persistence as well.

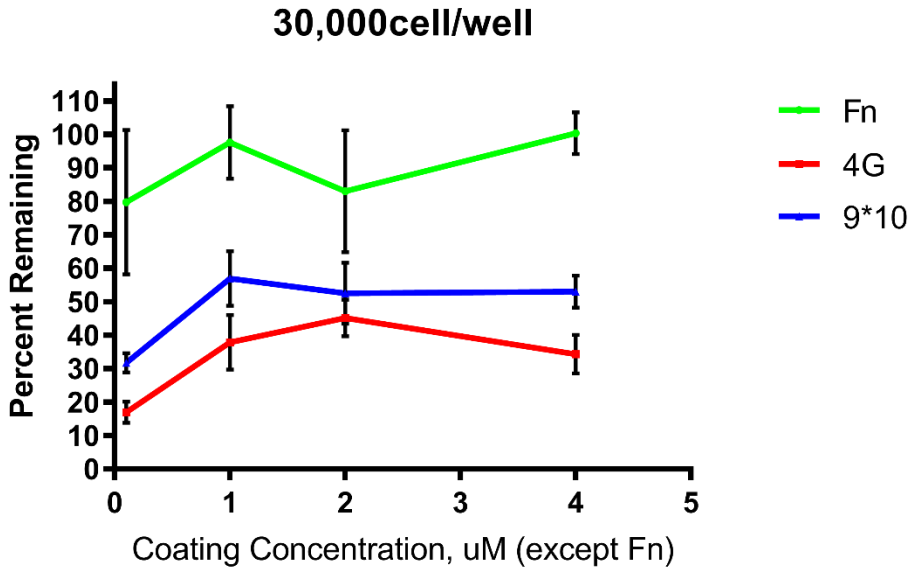

Figure 35. Crystal Violet Attachment Assay of CCL-210s on full-length Fn and FnIII9-10 variants. CCL-210 cells are cultured on FnIII9*10 and FnIII9-4G-10 fragments (and full-length Fn) and stained using crystal violet dye. Attachment is determined based on cell percentage remaining after washing (determined based on high density cells on Fn).

4.3.6 CyQuant Proliferation Assay

The CyQuant Direct Cell Proliferation Assay is a cell-permeable nucleic acid dye which allows detection of DNA content and membrane integrity. Many additional factors can influence metabolic activity (such as media conditions, confluence, and passage

number) therefore studying proliferation is an important observation, unique from metabolism. Myofibroblasts are thought to have a higher replication rate than quiescent fibroblasts therefore analyzing cell proliferation can indicate myofibroblast differentiation. The results presented in Figure 36 indicate that there are difference in proliferation rate between FnIII9*10 and FnIII9-4G-10. The difference on the substrates is significant at **$p < 0.05$ comparing both fragments at 8μM concentrations. This trend remains similar as the concentration decreases. Although full-length Fn and FnIII9-4G-10 do not appear to have stark differences in proliferation there is a significant increase in FnIII9*10 over Fn of **$p < 0.05$.

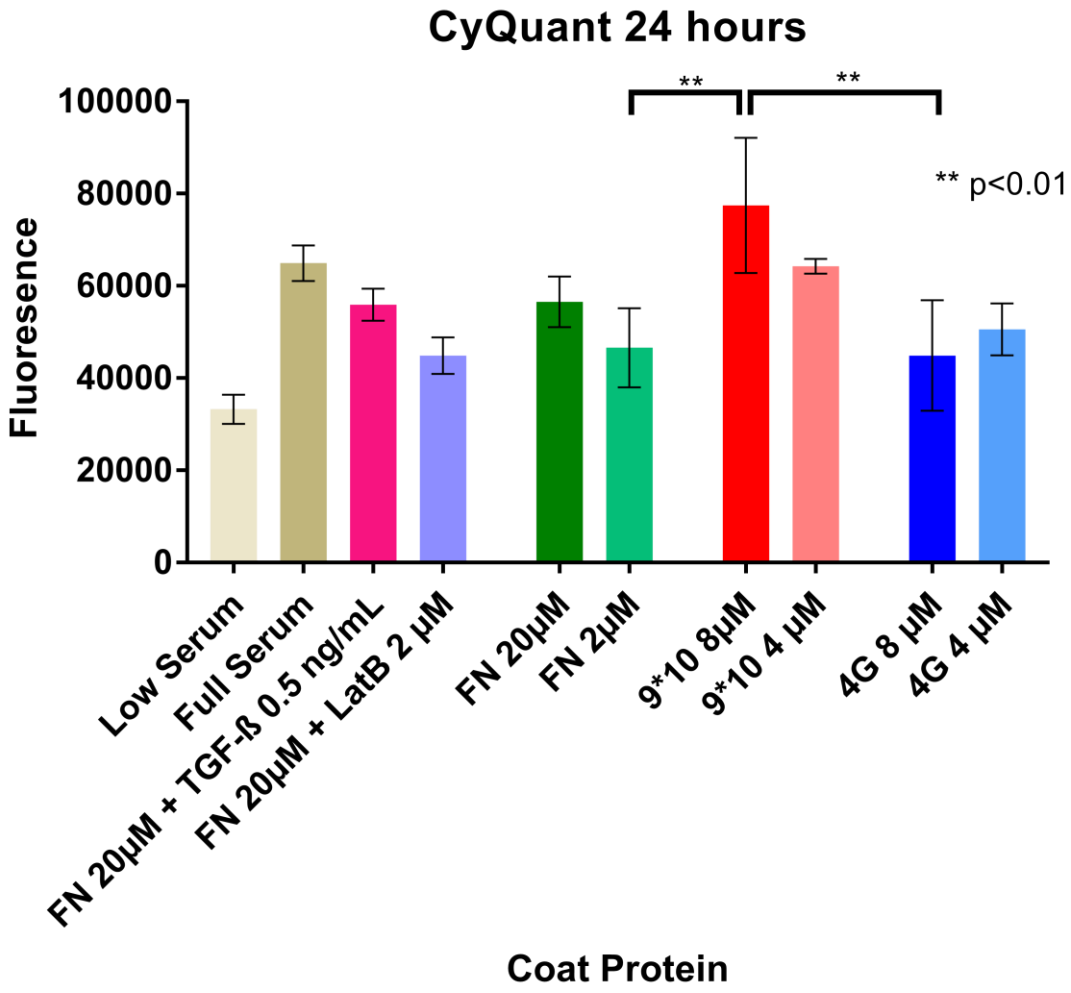

Figure 36. CyQuant analysis of cell proliferation at 24 hours on Fn and Fn variants. CCL-210 cells are cultured on FnIII9*10 and FnIII9-4G-10 fragments (and full-length Fn) and CyQuant assay is performed. Fluorescent signal is used to determine relative cell proliferation. Mean values of each condition is calculated for each image and compared using ordinary One-way ANOVA, N = 3 cells for each condition. **p < 0.01.

4.3.7 MTT Metabolism Assay

To look at cell metabolic activity the MTT assay was used to compare CCL-210s on full-length Fn, FnIII9*10, and FnIII9-4G-10. When cells are plated on each recombinant fragment in decreasing concentration we see a decrease in cell activity indicating that the

presentation of the integrin binding domain to the cell's integrins provides signals that trigger metabolic response within the cell in a controllable fashion. When comparing the Fn fragment to one another we do not see a significant difference in metabolic activity level; however, at coating concentrations ≤ 2µM there seems to be a trend that indicated that FnIII9-4G-10 has increased embolic activity.

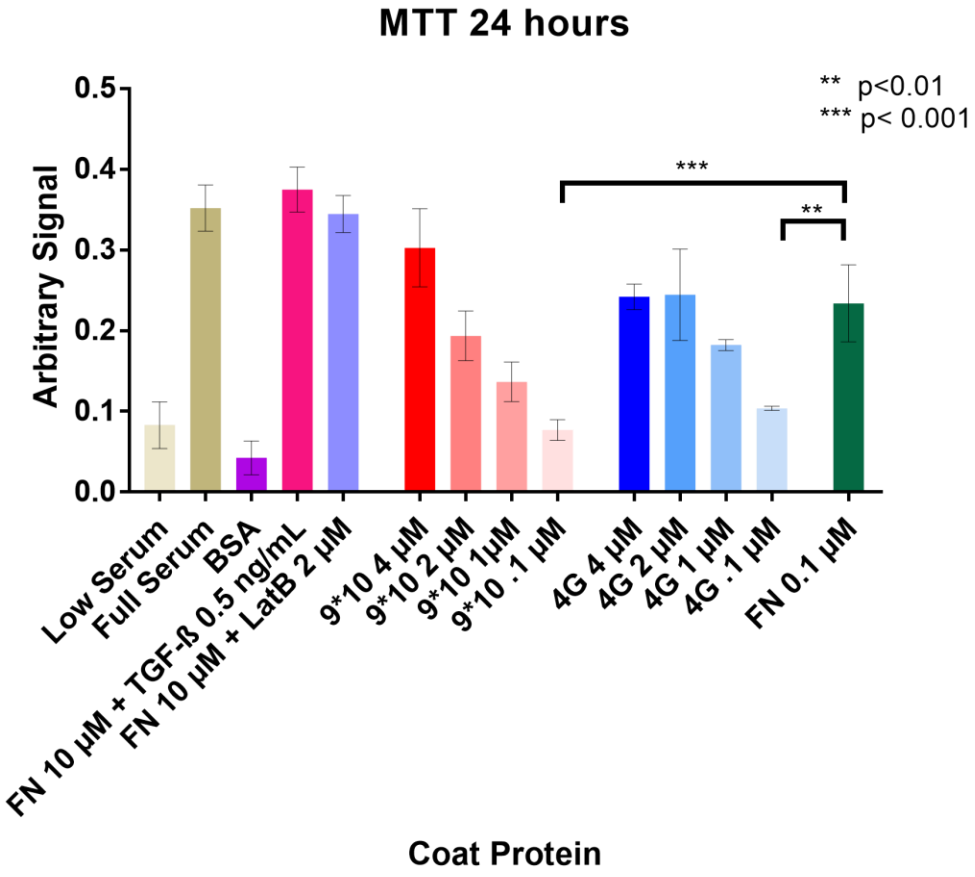

Figure 37. MTT analysis of cell metabolism at 24 hours on Fn and Fn variants. CCL-210 cells are cultured on FnIII9*10 and FnIII9-4G-10 fragments (and full-length Fn) and MTT assay is performed. Absorbance signal is used to determine relative cell metabolism. Mean values of each condition is calculated for each image and compared using ordinary One-way ANOVA, N = 3 cells for each condition. **p < 0.01, **p<0.001.

The significant differences noted in this experiment are highlighted as ** $p < 0.001$ Fn having a higher metabolic rate over FnIII9*10 when comparing direct molar ratios of the proteins. Fn's higher metabolic rate over FnIII9-4G-10 is less significant at ** $p < 0.05$ when comparing molar ratios (0.1μM). Controls were utilized to look at low or full serum effects such as: low serum conditions do not proved as much exogenous Fn for cells to assemble and therefore there is a lessened effect on cell proliferation, BSA control is used to block binding of any other proteins to the surface and provides a weak cell binding protein for minimal cell adherence, TGFβ is believed to trigger myofibroblast phenotype so this was used as a positive control.

4.3.8 Nuclear Localization of MRTF

In order to quantify MRTF nuclear localization, MRTF immunofluorescence was compartmentalized between the nuclear Hoescht signal and the 'cellular' phalloidin signal. We can observe that on full-length Fn there is the most nuclear localization of MRTF. This is to be expected due to the complex structure of Fn providing many additional signals to the cell which may cause MRTF to localize to the nucleus. Controls CD (Cytochalasin D) and LatB (Latrunculin B) both toxins which affect actin polymerization respond accordingly, CD pushes MRTF to the nucleus and LatB pulls MRTF out of the nucleus. These results have great significance ****$p < 0.0001$ when compared to FnIII9-4G-10. When comparing the Fn fragments (FnIII9*10 and FnIII9-4G-10) there is a significant different in nuclear localization of *$p < 0.05$ in favor of FnIII9*10 (Figure 38). This is not the originally hypothesized result. Initially it was hypothesized that FnIII9-4G-10 which is believed to disengage the α5β1 integrin would be more myofibroblastic because it would

drive actin assembly and free MRTF fir nuclear translocation through its G-actin binding RPEL domains.

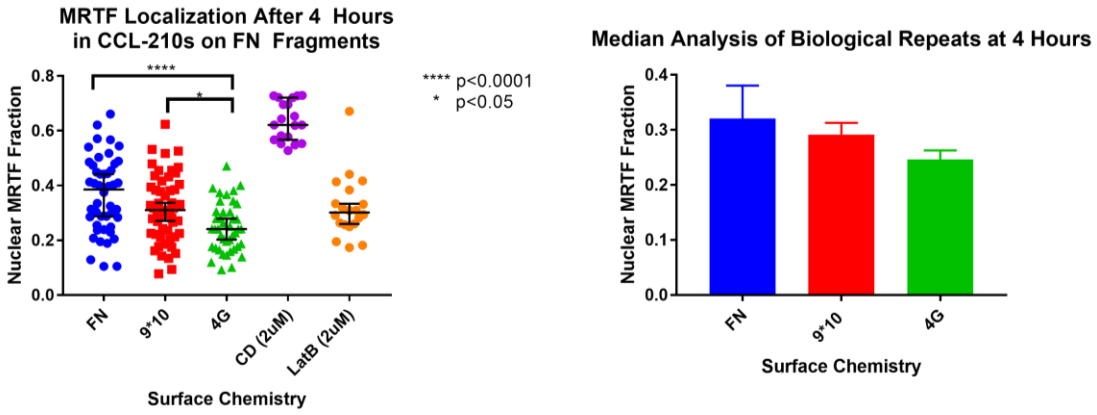

Figure 38. MRTF nuclear localization analysis. CCL-210 cells are cultured on FnIII9*10 and FnIII9-4G-10 fragments (and full-length Fn) and immunostained for Hoescht nuclear stain, Actin, and MRTF-A. Single cells or multicellular aggregates are segmented based on actin and nuclear signaling, and MRTF signal in each compartment is background corrected (using intensities from the no primary control). Ratios of background corrected MRTF signal from the whole cells and from the nuclear compartment are used to estimate the nuclear fraction of MRTF. Single cell analysis is visible on the left with controls Cytochalasin D and Latrunculin B. Multicellular aggregates are depicted on the right to represent biological repeats. Mean MRTF nuclear localization values were calculated for each image and compared using ordinary one-way ANOVA with Tukey's post-test, N = 40 cells for each condition. *p < 0.05 and ****p<0.0001.

4.4 Discussion

4.4.1 Differential Integrin Engagement through Recombinant Fibronectin IBD Effects on Downstream Signaling and Mechano-transduction

Recombinant Fn IBD variants were engineered to mimic the biochemistry of normal and fibrotic Fn. We are interested in using these variants to interpret their promotion of various myofibroblast phenotypes like differential integrin engagement, differential focal adhesion composition, cellular morphology, proliferation, metabolism, and mechanical

signaling (MRTF). Differences in integrin engagement (mimicking the "integrin-switch" behavior described in Cao *et al.*) in normal lung fibroblasts was observed with FnIII9*10 and FnIII9-4G-10 though not to the same degree as human dermal fibroblasts[29]. Immunofluorescent staining of CCL-210's (normal human lung fibroblasts) integrin α5 and αv should have characterized this integrin-switch behavior as well; however, the differences are not distinguishable. The slight reduction in α5 staining of cells on FnIII9-4G-10 is not distinct enough to make conclusions that the integrin switch behavior is occurring. Although the trends mimic those seen with human dermal fibroblasts and HFFs it is unclear if these cells disengage α5 integrins when the RGD and "synergy" site are interrupted. Myofibroblast differentiation has been shown to be controlled by multiple αv integrins such as αvβ5 and αvβ3 which may muddle the signal observed when comparing the ratio since only the influence of αv was observed and not the β3 heterodimer[170,171]. This could influence the effect of the ratio when attempting to compare the ratio of α5 to αv. To clarify the effects that play into integrin engagement future studies could observe α5β1 vs αvβ3 with antibodies used to target the heterodimer pair.

Paxillin was stained to observe length, concentration, and location of focal adhesions. It is observed that focal adhesions formed at early time points (1 and 3 hours) are visibly different on various Fn fragments. On full-length Fn there is indication of migratory cells as we can observe the leading and tailing edge of the cell indicated by the association and dissociation of focal adhesions respectively visible with paxillin immunofluorescent staining. At these early time points the cells on FnIII9-4G-10 seem to be concentrated, distinct, distal, and well-developed where as we do not see this effect on cells plated on FnIII9*10 until later time points (7 and 25 hours).

Also of interest was the resulting downstream signals that were associated with these focal adhesions. In the magnetic bead pull down assay a comparison of the engineered Fn fragments was utilized to observe differences in the mechano-transduction pathway. Our previous studies using the recombinant Fn IBD fragments have shown that FnIII9-4G-10 has an increased affinity for αvβ3 integrin and FnIII9*10 more specific binds to α5β1 integrin. Typically, mechano-transduction through integrin engagement triggers p-FAK prior to pSrc; however, our results from cells engagement with FnIII9*10 contrast this philosophy.

In mechano-transduction, FAK Y397 will auto-phosphorylate after the activation of integrin and subsequently will provide a binding site for the SH2 domain of Src, leading to Src activation. Our results showed FnIII9-4G-10 involved mechano-transduction increases the phosphorylation of FAK significantly after mechanical stimulation and consistent with results on full-length Fn. Conversely, cells engaged with FnIII9*10 do not appear to have consistent demonstrable influence on FAK or Src phosphorylation levels. . To further tease out conclusions we can make about the cell interaction with FnIII9*10 there are few options to be explored. It is hypothesized that pSrc is upstream of pFAK, pSrc is signaled earlier than pFAK, or they are using different pathways then cells engaged on FnIII9-4G-10[172]. Experimentation using Src or FAK inhibitors could be utilized to answer these questions.

Previous studies showed the Src signaling pathway is directly downstream of receptor tyrosine kinase (RTK). To trigger the Src pathway (without phosphorylation of FAK) could occur due to growth receptors and cadherin engagement. It would be useful to explore the relationship that FnIII9*10 engineered fragment may have in engaging with other receptors

such as receptor tyrosine kinase or growth factor receptors. Ideally, further immunoprecipitation studies could be completed to determine whether FnIII9*10 can bind growth factor receptors and activate them through force to determine if this is what is at play with the downstream signaling effects. Additionally, Roca-Cusachs *et al.* explores the unique roles of α5β1 and αvβ3 integrins which could be implicated within these magnetic bead assays[173]. This work explores the relationship of α5β1 as an integrin responsible for adhesion strength and αvβ3 as an integrin related to mechano-transduction. These roles fit well with the results of the magnetic bead assay. CCL-210s exposed to FnIII9*10 potentially favorably engage the synergy dependent α5β1 integrin indicated in their increased adhesion (crystal violet adhesion assay). Since this integrin is likely the primary influencer for cells on FnIII9*10 we do not see consistent mechanosensitive responses based on length of time of applied force. However, CCL-210s exposed to FnIII9-4G-10 which likely disengage their α5β1 integrin engagement and preferentially favor αvβ3 (the believed mechanosensitive integrin) appears consistent with the influence of applied force on downstream mechano-related signaling proteins (significant increase of FAK phosphorylation).

There is evidence linking focal adhesion formation with FAK phosphorylation and the assembly of the cytoskeleton. We explored this directly using MRTF nuclear localization (a known indicator of myofibroblast differentiation). Interestingly, we do not see a correlation between FAK phosphorylation and MRTF nuclear transport across the different Fn fragments. These results could indicated some differential early cellular adhesion kinetics that are implicated elsewhere in this work. It appears that there may be some initial kinetics that occur early on in the cell that are triggered based on integrin engagement and

some of these transduced signals may be influenced further down the cells lifetime. Previous work indicated MRTF engagement associated with adaptor protein or integrins, we can interpret that based on results from magnetic bead pull down and the differences apparent in downstream signaling there could be other factors affecting nuclear localization. The Fn molecule has many complex cues that provide cells many more opportunities to bind as well as triggering signals that continue to dictate cell phenotype besides sole engagement of varying integrins. The results from paxillin immunostaining can be used to compare how FnIII9-4G-10 and FnIII9*10 can affect lung fibroblast focal adhesion complex formation. The cell signaling events that occur within these focal adhesions such as paxillin expression and comparison on various substrates is compared with the results found through the magnetic bead pull down assay which indicates which signaling events are triggered by force application on the various ligands. FnIII9*10 appears to engage a preference for α5β1 integrins but the focal adhesions visible with paxillin staining and the complexes associated with adhesions and force are less clear and more inconsistent. FnIII9*10 does appear to trigger MRTF nuclear localization, which appears to be contradictory to the original hypothesis that this conformation of Fn's IBD would not drive myofibroblast differentiation. It is unclear if FnIII9-4G-10 preferentially engages αvβ3 integrin because the ratio of α5 to αv is not what has previously been seen in epithelial cells and HFFs which may be due to increased presence of other αv subunit-containing integrins presented on CCL-210s. FnIII9-4G-10 has clear focal adhesion formation and has a consistent effect on FAK phosphorylation; however, there is significantly less MRTF nuclear localization indicating a less myofibroblastic phenotype. Some of these effects are counter hypothesis because we expected that FnIII9-4G-10 is

mimicking the extended conformation (disengagement of synergy effect of RGD and PHSRN) and we would anticipate that adhesion events associated with this spatially disjointed conformation would direct cells down a myofibroblast differentiation pathway. Factors at play may be other cell receptors that may bind to the variant fragments or the disengagement of α5β1 integrins has more impact on cell adhesion therefore less cellular persistence overall.

4.4.2 Myofibroblast Phenotype Characterization Due to Conformational Bias of Recombinant Fibronectin IBD

Myofibroblast phenotypes like proliferation, metabolism, cell contractility, and adhesion which are promoted by α5:αv engagement due to the hypothesized conformational bias of recombinant fibronectin integrin binding domain are explored here. Indications of slight differences in integrin engagement and observation of differences in adhesion proteins (FAK and Src) may influence further effects to phenotype. Our original hypothesis was that through biochemically mediated spatial decoupling of Fn's IBD (RGD and PHSRN) there would be a shift towards myofibroblast differentiation. Evaluation of myofibroblastic characteristics such as cell contractility is analyzed in this work. It has been implicated that cells that appear larger and more polar are more contractile. Here I draw conclusions that a shift between a kinetic and steady-state effect of the recombinant Fn fragments is indicated.

Cell surface area is measured for indication of cell contractility (increased spreading due to cytoskeletal formation and the cell forces linked to this). Appearance of polarity (less circular as the cell forces are increased) is used to draw a hypothesis about

the cellular responses of CCL-210s on the various fragments. Typically size and shape are correlated and it is expected that myofibroblast-like cells would be more polar. We have also shown in previous work with Fiore *et al.* that cell area and cell stiffness are directly correlated[169]. Size-wise at shorter time points (up until ~4 hours) cells on full-length Fn, FnIII9*10, and FnIII9-4G-10 are similar in size; however, cells on FnIII9*10 are more polar and, although this was not anticipated, it could be an indication that the cells have an initial response to the integrins they engage with but the effects that occur may influence longer term cell response differently. These results indicate that initially cells on FnIII9*10 appear more contractile; however, as time passes and the cells begin to assemble their own matrix there appears to be a shift in the trend that may effect of some of the initial signals associated with early integrin engagement leading to downstream signaling and longer-term phenotype. Another explanation for the shift is that CCL-210 cells are slower to engage FnIII9-4G-10 because FnIII9*10 allows engagement of both α5β1 and αvβ3 whereas FnIII9-4G-10 is on expected to engage αvβ3 integrins.

Cell adhesion can also be a useful indicator of cell phenotype. A cell's adhesion based on the variable recombinant fibronectin fragments or full-length Fn is compared to better understand the structure and stability that the Fn variants provide and the influence this has on various cell activities. Our adhesion results indicated that FnIII9*10 induces greater cell adhesion than CCL-210s on FnIII9-4G-10. This could be a result of the integrin engagement on FnIII9*10 being increased since it also allows for engagement of α5β1 in addition to the αvβ3 integrin that is engaged on FnIII9-4G-10 as well. Again the adhesion effect observed here may be related to the association of α5β1 integrin with an adhesion

strength role. A more adhesive phenotype may indicate cell behavior linked to resistant to apoptosis.

To observe some of the long term responses (up to 24 hours) other lung myofibroblast phenotypic characteristics were analyzed such as proliferation and metabolism. Proliferation is integral for the wound healing process and is increased in fibrotic tissues. It is also important to recognize that analysis of DNA synthesis within a cell may provide alternative results to those found using a metabolic assay. This is an interesting result because it may indicate that there are differences in integrin engagement and the effects of cell proliferation or metabolism individually and not as a combined effect. It may be that proliferation is more closely controlled by integrin engagement and overall metabolism is influenced more by underlying stiffness. It is also important to remember that metabolism can be regulated by many influencing factor not just those responsible for cell proliferation which may result in the differences between these responses.

The MTT assay was used to make assumptions about the rate of metabolism in response to different ECM peptides mimicking spatial decoupling of Fn's integrin binding domain. It is shown that recombinant Fn fragments that mimic the "strained" Fn conformation, FnIII9-4G-10, show an increase in cell metabolism in comparison to the "relaxed" conformation, FnIII9*10 at 24 hours. We see a shift in metabolism as concentration of Fn or recombinant Fn fragments decreases in concentration. Another observation is the trends that seem reasonable for the control samples (positive control is Fn with TGF-β, negative control with BSA). Proliferation observed with the CyQuant DNA synthesis Assay showed a differing influence affecting cell proliferation. In this assay FnIII9*10 was shown to have more influence on cell proliferation.

Although this CyQuant assay indicates as converse trend to what appears in the metabolism MTT assay this could be due what dictates metabolism and proliferation. It is known that myofibroblasts have higher rates of proliferation so this contradicts the original hypothesis that FnIII9-4G-10 fragments loss of α5β1 engagement would increase rates of proliferation. The higher metabolic activity on Fn is likely influenced by the many other binding sites available in the presence of full-length Fn. This difference in metabolic activity between FnIII9*10 and FnIII9-4G-10 is noteworthy because it may be one of the downstream phenotypes affected by earlier cell signaling events associated with the differential integrin engagement. This could indicate that cells on FnIII9-4G-10 are more "synthetic" and therefore potentially more myofibroblastic.

The original hypothesis was that FnIII9-4G-10 would be myofibroblast inducer and that the FnIII9*10 would inhibit the myo-like differentiation; however this is not what is seen. Myofibroblasts would be more proliferative, contractile, synthetic, increased metabolism. Further studies to determine which integrins control the different phenotypes could be explored. One integrin may not control all different phenotypes since we looked at controlling biochemistry but only at a uniform stiffness. It is likely that mechanical and biochemical cues can interact and further work should be done on soft *vs* stiff substrates to determine what mimics the disease state *vs* native tissue. Comparing the combinatorial contributions of rigidity and the biochemical peptide presentation may provide an experimental system that more closely mimics nature. As the Fn molecule experiences force and the typical integrin binding RGD and "synergy" sites are displaced a conformational bias can influence cell phenotype. Looking at many facets of cell behavior we can begin to understand and profile the ways that cells respond to their ECM as they

are stimulated with biochemical and mechanical cues. The differences observed may indicate that there is a kinetic influence and that over time the cell's own matrix assembly may dissolve these differences; however, the long term effects on cell phenotype seem to be present. There is indication that the field needs further exploration of the influence of the specific integrins (including both α and β subunit) engaged and their effects on cell behavior for the CCL-210 cells. The conformational bias of recombinant fibronectin IBD may not have the impact originally hypothesized, and it may be need to be compared with underlying stiffness to further appreciate the biochemical influence.

CHAPTER 5. DISCUSSION AND FUTURE DIRECTIONS

This thesis work began by asking if conformation changes to the IBD of Fn lead to differential integrin engagement and whether this shift in integrin engagement changes the phenotype profile that normal human lung cells will present. The original hypothesis included presumptions that when fibroblasts were disengaged with α5β1 integrins through the spatial separation of the RGD and synergy site that cells would become more myofibroblastic in phenotype, but the results we see are much more complex. When comparing the cellular behaviors associated with exposure to recombinant engineered peptides that mimic the RGD and PHSRN sites in stabilized (FnIII9*10) and spatially divided (FnIII9-4G-10) conformations to full-length Fn we can determine that other components of the Fn molecule must play a role in myofibroblast transition. The initial hypothesis was derived through our understanding of previous work indicated in Brown *et al.* that these recombinant fragments are able to guide epithelial transition[30] and through work in Cao *et al.* where these fragments are used to visualize the "integrin-switch" with human foreskin fibroblasts (HFFs)[29]. However, the results presented through this thesis work indicate the complex nature of the effect that these recombinant proteins have on lung fibroblast phenotypes and our limited understanding of normal human lung fibroblasts. This work will inform further research to understand the role of integrins in cell phenotype for fibroblasts and the integrin profiles for lung fibroblasts as well as further examination of what drives fibroblast towards a myofibroblast phenotype as well as guide our definition of the myofibroblast phenotype.

Through the redesigning efforts of engineered recombinant FnIII9-10 fragments, we are able to explore the relationship of these specific Fn domains with the biochemical response to normal human lung cells and aid in the ability to examine the direct effect that the differential integrin engagement has on various cell phenotypes of interest in fibrotic tissues. Accompanying the redesign of these proteins came a streamlined high throughput process for protein expression and purification for ease of isolation of the desired peptides. These recombinant fragments utilize the integrin binding domain of Fn to explore the relationship with shifts in integrin binding profiles of cells on surfaces that have altered spatiotemporal effects. We have been able to further characterize the differences we see in integrin engagement when these different conformations of FnIII9-10 are presented and then further characterize some of the signaling events associated with these engagement events. Characterizing the shift of normal human lung fibroblasts as they become myofibroblasts based on mechanical stimuli in combination with biochemical molecule stimulation is key to understanding the events which ultimately trigger the uncontrolled constitutive activity of fibroblasts and how this ultimately leads to fibrosis.

With the field's continuing knowledge of the biological importance of integrin engagement in controlling cellular fate, we took a similar approach to specifically assess the contribution of Fn's IBD on lung fibroblast phenotype. We found that there appears to be an initial integrin engagement which may slightly trigger α5>αv preference on FnIII9*10 engineered Fn fragment over what is seen on FnIII9-4G-10. It appears as if the engagement of αv integrin is similar for both cell lines but much more so on HFFs than what we see on CCL-210s. These lung fibroblasts seem to have this preference in integrin α5 on the FnIII9*10 however the difference is dampened from what has been shown in

other data we have represented in Cao *et al.* and there are many things that can explain this phenomena[29]. It could be conceived that these normal human lung fibroblasts have a different integrin profile or that other integrins such as αvβ5 and α3β1 may be engaged which may influence our staining ratios. Future studies looking at the integrins should consider doing FACS analysis to determine the integrin dimer pairs that are present on CCL-210s.

When looking at general focal adhesion staining using an anti-paxillin antibody it is observed that on FnIII9-4G-10 there appears to be more clustered focal adhesions, greater length, more distinct and distal formations. This trend is apparent at shorter time points but the effect lessens as time passes and cells on FnIII9*10 have time to create and assemble adhesions. Another effect influencing longer time point cell adhesion is that fibroblasts will begin to lay down and assemble their own matrix proteins further muddling the signals seen based on the initial integrin engagement. The magnetic bead pull down assay that shows activation of different intracellular pathways appears to differ and maintain with up to 30 minutes of applied force. Cells plated in a dish are given time to associate with magnetic beads coated with the various ligands and when a magnet is applied, force is transduced and the effect on mechano-transduction influence on cells can then be interpreted. Initial studies on adhesion reinforcement revealed that cells are able to sense and respond to the restraining force (through matrix stiffening) applied to Fn-coated beads through strengthening and localization of cytoskeletal linkages[165]. The structural importance of adhesion strengthening and mechano-transduction is demonstrated based on force related FA proteins and its recruitment or activation at the site of exogenous force application[174]. Although the FnIII9*10 beads associated adherent proteins FAK and Src

and their phosphorylation are unclear and inconsistent we are able to determine that under the influence of FnIII9-4G-10 beads and force increased phosphorylation of FAK is observed. This effect could mean that there are other factors at play. Previous studies showed that the Src signaling pathway is directly downstream of the receptor tyrosine kinase (RTK) including some growth factors receptors and integrin-tensin relationship after force activation[172]. Most of the current literature shows that Fn binds to growth factors but does not directly bind to growth factor receptors. Since our system used serum-free media there should be no growth factor present. Further immuno-precipitation experimentation need to be completed to determine if growth factor receptors are found directly bound and if they are activated with the addition of force. It is hypothesized that maybe cadherin or cell-cell junctions are playing a role affecting the different focal adhesion proteins which are controlling different downstream effects of mechano-transduction. This work can also be compared to work looking at the role of α5β1 as an adhesion strength based integrin and αvβ3 as the integrin playing a key role in mechano-transduction.

In this work, lung fibroblasts are examined for their MRTF nuclear localization as this is a marker of myofibroblast transition and the results are unexpected. Although cells are only tracked at 90 minutes and 4 hours the trend that cells on FnIII9*10 have more nuclear localization of MRTF than when cells are on FnIII9-4G-10 is obvious and significant. Observation of cell shape and size to compare cell contractility is explored. Results indicate that at shorter time points cells on FnIII9*10 are larger and more circular but at longer time points (after ~2-3 hours) cells are larger and more circular on FnIII9-4G-10. This could imply that cells at earlier time points which have not yet had time to fully

recognize and respond to their surface coatings may not be as pronounced and at longer time points that influence of the conformational differences of Fn are recognized and differences in size and shape are realized. When looking at proliferation we see that cells on FnIII9*10 are more proliferative then on FnIII9-4G-10. Metabolic rate is observed through an MTT assay and it is seen that FnIII9-4G-10 induces greater metabolic engagement. Since both proliferation and metabolic rate are examined at longer time points (~24 hours) it is useful to consider that it is possible that different integrin engagement has influence on proliferation or metabolism. Since metabolism is measuring cell activity the converse effect between proliferation is not shocking; however further exploration into what metabolic activities if not the activities that influence proliferation are being regulated. The hypothesis that cells have longer term downstream effects based on initial integrin engagement could be what is seen through this work.

Through our advanced understanding of these relationships between matrix and fibroblasts we could propose that the effects between them could be as a result of much more than simply integrin engagement. It could be concluded that integrin engagement alone is not the determining factor that drives fibroblast to myofibroblast transition. We know that there is significant influence based on matrix rigidity and further exploration of the combined effects of biochemical cues via integrins and underlying substrate stiffness should be examined to see if these combined effects could better mimic the matrix environment[40,42,166]. Exploring the engineered fragments as a potential for mimicking specific cell behavior can be useful for continuing to probe therapeutic targets.

Further investigation into our H5 antibody that we have shown can preferentially bind FnIII9-4G-10 over FnIII9*10 can be further examined as a target. This phage-based

antibody can be optimized via directed evolution to increase affinity and used as a diagnostic tool and a therapeutic. Using the engineered fragments to test H5 as a potential therapeutic option could lay preliminary work with *in vitro* experiments.

Others in the field have previously explored the influence of Fn's integrin binding domain on directing epithelial cell behavior; however, these approaches have not looked at lung fibroblasts specifically. Additionally it is important to better understand the role that Fn's IBD has on lung fibroblasts in order to determine if therapeutic options which target "strained" imitators of Fn IBD are a viable option both *in vitro* and *in vivo*. Other groups such as Huang *et al.* have explored mechanical stiffness as a director of cell behavior towards a myo-like phenotype and towards myo-like cell behavior[166]. Although these conclusions were useful we should continue to explore the complete relationship between both the mechanical stimuli and presentation of binding interactions. Our approach remains unique in that we determined that Fn IBD alone does not appear to direct lung fibroblasts in this way without mechanical stiffness associated and that there appear to be differences in short-term and long-term effects.

In the future, this work could be expanded upon in many ways to further understand lung fibroblasts and their transition to myofibroblasts during wound healing as well as the feed-forward loop that leads to lung fibrosis. This work sought to target this transition and how integrin engagement plays a role in this transition as a strategy to expand the field. However, to further explore the desired outcome, of increased understanding of fibronectin's role in fibrosis and improved therapeutic options, there are other strategies that would need to be utilized. It is important to further understand the other components of the complex Fn molecule that are affected under protein unfolding that help potentiate

the myofibroblast lineage. The H5 phage-based antibody fragment would need to be characterized as a therapeutic inhibitor and more *in vitro* data would need to be considered before moving forward *in vivo*. Furthermore, investigation of mechanical stiffness via verifying hydrogel rigidity, should be done to further connect the myofibroblast transition via cues through mechanical stimuli and biochemical cues.

The characteristics of the normal human lung fibroblasts that are observed after they encounter recombinant Fn IBD could indicate what the fibrotic ECM may look like and how cells respond to it. Characteristics like differential integrin engagement and the downstream effects that result from these differences were initially explored. The preliminary effects of the cell's engagement with the recombinant Fn fragments can affect some of the phenotypic characteristics like phenotype, cell contractility, as well as other mechano-transduction effects. Based on conclusions from chapter 3 and chapter 4 we could further investigate the combined effects of underlying substrate stiffness in combination with some of the phenotypes we observed. Determination of the expression of α-SMA, a known myofibroblast associated protein, could be analyzed in combination with stiffness. We could look at migration of cells on the Fn fragments or use a scratch assay to further understand the effects of the ECM on wound healing. Observing migration factors like speed or distance via DIC to do live cell imaging could be performed to examine the migratory patterns of cells on full-length Fn, FnIII9-4G-10, and FnIII9*10. It could be expected that those cells which are more myo-like will be more invasive therefore will have increased migratory patterns providing information on cell behavior based on integrin binding specificity dominating attachment to the surface and the effect of this engagement over time. The myofibroblast characteristic of resistance to

apoptosis could be studied to better understand how the cells interpretation of integrin binding will affect the ability of a cell to become resistant to apoptosis and therefore remain persistent.

Detailed information regarding fibroblast to myofibroblast transition based on ECM signals has yet to be obtained. Additional experiments could be done to elucidate and characterize cell behaviors by observing myofibroblast markers such as α-SMA, MyoD, and Myf-5 and considering underlying stiffness (soft 2kPa and stiff 18kPa) as a component that can contribute to myofibroblast differentiation in combination to the biochemical cues that are presented. Alternative methods could be used to further characterize cell contractility such as contractility AFM to observe the relative elastic modulus of cells on variable surface presentations in combination with surface stiffness. Another useful tool for looking at overall cell contractility would use traction force microscopy to analyze the traction force applied by cells on their surface that are utilized in the Curtis lab and portrayed in the work of Dumbauld *et al.*[122] An ongoing collaboration with Khalid Salaita is focused on observing individual adhesion events using a FRET-like probe which would signal when the cell is pulling on the ECM which mimics similar studies done in Salaita *et al.*[175-177] Further understanding these specific force results in combination with clarifying some of the work completed with the magnetic bead pull-down assay which indicates adhesion proteins associated with force-induced mechano-transduction will be useful to further understand the cell signaling pathways associated with initial integrin engagement and the downstream effects on cell behavior. Imitating work by Huang *et al.*to utilize real time PCR to observe shifts of integrins or other interesting focal adhesion associated proteins on soft vs stiff underlying

substrate to further characterize matrix stiffness-induced myofibroblast differentiation in combination with the biochemical cues associated with the microenvironment during these changes[166].

An effective treatment for idiopathic pulmonary fibrosis is still elusive and the previously discovered antibody fragment, scFv H5, from Cao *et al.* could be explored as a potential therapeutic (Cao *et al.* to be submitted)[83 29]. It has been demonstrated that H5 can be used as a probe for fibrotic tissue *in vivo* so it could be have an application in targeting the fibrotic region. Recent reports suggests that αv integrins on myofibroblasts are implicated in fibrogenesis in a broad range of fibrotic diseases, and that pharmacological blockade of αv integrins ameliorates liver and lung fibrosis. The *in vivo* data our lab has generated regarding H5 staining of bleomycin-treated lungs are particularly interesting in the context of idiopathic pulmonary fibrosis (IPF). The lungs of IPF patients are mechanically and biochemically heterogeneous, with areas of soft, normal lung tissue and stiffer regions of mature fibrosis. The H5 antibody developed may be used to delineate regions of high ECM strain, perhaps indicative of active ongoing fibrosis. Further characterizing these events and better understanding how scFv H5 targets FnIII9-4G-10 could assist in treatments for IPF as well as lead to a deeper understanding of cellular fate in regards to environmental biochemical and mechanical stimuli.

It would be useful to further explore if scFv H5 could be used to inhibit fibrotic mimicking cellular responses. Another useful tool would be to obtain a crystal structure of FnIII9-4G-10 in combination with scFv H5 to better understand the relationship of how this antibody fragment binds to the ECM mimic (FnIII9-4G-10) and how this complex may mimic the occurrence on a larger scale. We also aim to drive the shift from

the engagement of integrin αvβ3 to α5β1 by using H5 to block αvβ3 engagement. Another goal will be to use the H5 antibody to bring human lung fibroblasts back to normal adhesion phenotypes.

One application of the H5 scFv could be to probe pathologic ECMs, specifically tumor stroma and fibrotic ECMs which contain highly contractile myofibroblasts. Recent reports suggests that αv integrins on myofibroblasts are implicated in fibrogenesis in a broad range of fibrotic diseases, and that pharmacological blockade of αv integrins improves liver and lung fibrosis[178].

The ability of the H5 antibody to extract structural information from the ECM was also demonstrated in a model of retinal angiogenesis, the process by which new blood vessels form by endothelial sprouting[179]. In mouse tissue sections, regions of high H5:Fn ratio were found at the extensions of endothelial tip cells, suggesting that Fn is unfolded in these regions. Fn is known to be a mediator of retinal angiogenesis, wherein astrocytes deposit fibronectin prior to differentiation of angioblasts to endothelial cells[180]. Our results build on this foundation by suggesting that forces from endothelial tip cells unfold Fn, presenting an αvβ3 binding character within the provisional matrix that may influence the formation of new blood vessels, a result further supported by the work of Segura *et al.* using engineered Fn fragments of the integrin binding domain in reparative angiogenesis[29,141].

Understanding how tissue rigidity changes as a consequence of fibrosis and the influence this has on cell behavior is an essential component of determining therapeutically targetable mechanisms underlying the physical and biochemical microenvironment's involvement in progression of fibrotic disease. Long term goals of discovering novel

molecular pathways for therapeutic intervention in IPF is essential and adding to the knowledge of the mechanisms that are linked to the pathophysiology of IPF are ideal targets to enable further studies to discover and test novel therapeutics. Before these studies are performed, it would be advised that further characterization of integrins in lung fibroblasts be analyzed. In contrast to the study outlined in this dissertation, it may be beneficial to look at the complex Fn molecule as a whole or within a 3D matrix to better understand the microenvironment seen by a cell. Work done by Smith *et al.* seems to convey that the experiments done on full Fn fibers provide a new level of insight to cell-integrin relationships and cell behavior. Even though the conclusions of this work are that looking solely at the IBD of Fn as a biochemical promoter of individual integrin engagement and subsequent cell differentiation is not plausible; if considerations of mechanical stimuli through substrate stiffness were additionally explored then this work could still have significant benefit on mimicking the microenvironment of lung fibrosis and would allow for a platform to better understand cell behavior and potential therapeutics.

It is valuable to acknowledge the challenge of the simplicity of these peptides as a way to antagonize preferential integrin engagement and directing phenotype of fibroblasts to myofibroblasts as a necessary difficulty for the future progress in the field of bio-mimetics of the matrix environment. It is realized that it is essential to combine substrate stiffness to imitate the changing lung micro-environment during the wound healing processes.

The overarching summary of this work is that Fn IBD alone may trigger differences in integrin engagement but this phenomena alone does not seem to be responsible solely

for myofibroblast transition in human lung cells. Although understanding how to direct myofibroblast transition is valuable to understanding how this relationship become dysregulated it is also useful for us to continue to explore systems that can mimic the environment to be able to best understand the factors that influence differentiation and dysregulation. Being able to have a platform for testing therapeutic options for IPF by observing their effect on cell behavior based on the local matrix is key for moving the field forward and creating an option for patients.

APPENDIX. ADDITIONAL INFORMATION

A.1 Thrombin Cleavage Site

The thrombin digest site is used for cleavage of the fluorescent protein tdTomato and His10 tag proteins after the first round of purification. This design feature was used to allow for protein expression visualization and for removal the affinity tag. After bovine thrombin is used to proteolytically digest the Fn fragments can be isolated further through another run through affinity chromatography which will entrap the tdTomato+His10 and allow for washing out of the purified protein. Figure A1 outlines the specific design of the thrombin cleavage site.

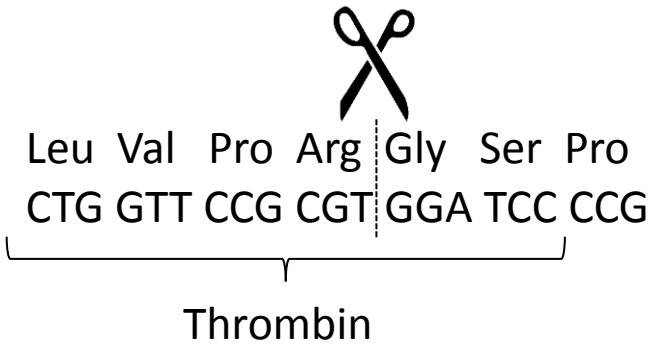

Figure A1. Thrombin digest site between FnIII9-10 and tdTomato+His10.

A.2 AKTA start Elution Profile

The AKTA Start program was run using Unicorn 1.0 software to track the wash and elution steps during chromatography with a GE Healthcare Life Sciences FPLC AKTA start. Figure A2 shows the elution profile during gel filtration using a size exclusion

chromatography column. Visualized on the elution profile is the separation of FnIII9-4G-10 from the tdTomato+His10 portions of the engineered protein after thrombin cleavage. It can be determined which fractions collected will contain each portion of the protein for further analysis. This technique is utilized to further purify the protein and verify its purity based on size.

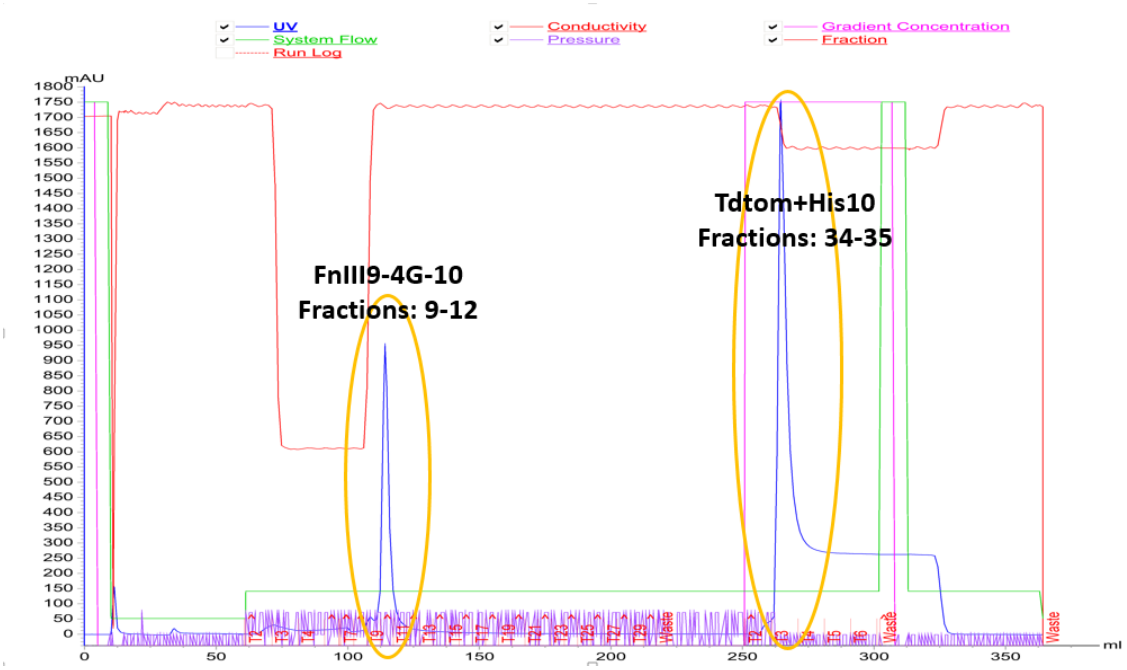

Figure A2. SEC AKTA profile of sample run after thrombin digest.

A3. Formazen staining of cells during MTT Assay

Visualized via microscope are the CCL-210 cells stained during the MTT assay. MTT is a yellow tetrazole which is reduced to purple formazan in living cells. Cells seen after 2 hours on substrates show differences in adhesion and proliferation based on coating substrate (Figure A3). After 24 hours the cell density is higher indicating proliferation has occurred and CCL-210 cells continue to have differences based on substrate coating

conditions however the trend is less visible by eye and is computed using a plate reader to verify absorption levels of the dye (Figure A4).

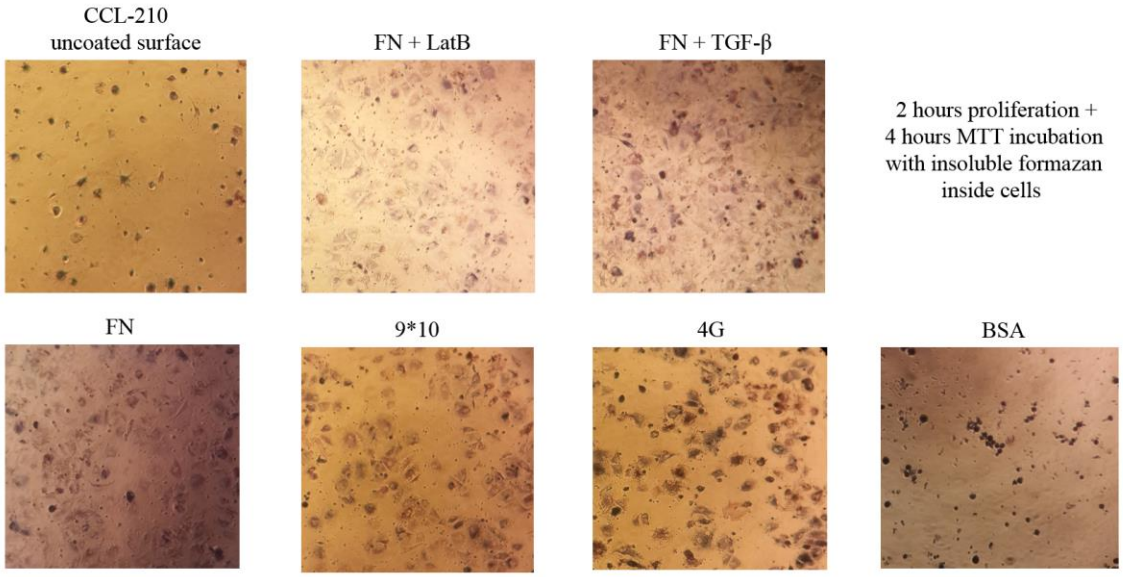

Figure A3. Formazen cell dye used in MTT assay visible under microscope after 2 hours of cell growth.

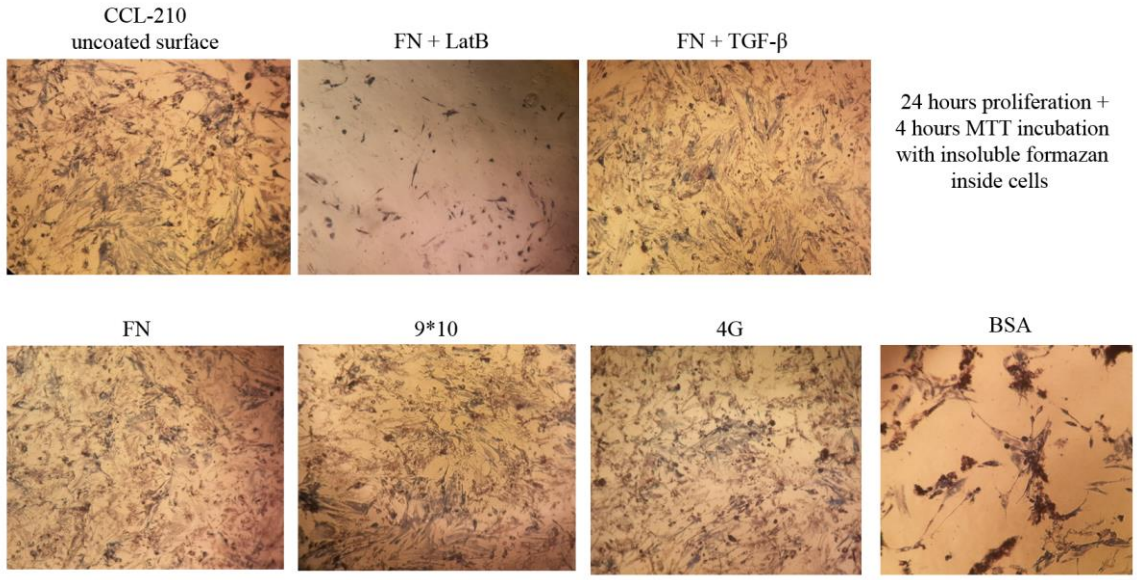

Figure A4. Formazen cell dye used in MTT assay visible under microscope after 24 hours of cell growth.

REFERENCES

1 *What Is Idiopathic Pulmonary Fibrosis?*, <https://www.nhlbi.nih.gov/health/health-topics/topics/idiopathic-pulmonary-fibrosis> (

2 Bachman, H., Nicosia, J., Dysart, M. & Barker, T. H. Utilizing Fibronectin Integrin-Binding Specificity to Control Cellular Responses. *Adv Wound Care (New Rochelle)* **4**, 501-511, doi:10.1089/wound.2014.0621 (2015).

3 Hubbard, B., Buczek-Thomas, J. A., Nugent, M. A. & Smith, M. L. Fibronectin Fiber Extension Decreases Cell Spreading and Migration. *J Cell Physiol* **231**, 1728-1736, doi:10.1002/jcp.25271 (2016).

4 Gao, M., Craig, D., Vogel, V. & Schulten, K. Identifying unfolding intermediates of FN-III(10) by steered molecular dynamics. *J Mol Biol* **323**, 939-950 (2002).

5 Liu, S. *et al.* Expression of integrin beta1 by fibroblasts is required for tissue repair in vivo. *J Cell Sci* **123**, 3674-3682, doi:10.1242/jcs.070672 (2010).

6 Lin, G. L. *et al.* Activation of beta 1 but not beta 3 integrin increases cell traction forces. *FEBS letters* **587**, 763-769, doi:10.1016/j.febslet.2013.01.068 (2013).

7 Bitterman, P. B. & Henke, C. A. Fibroproliferative disorders. *Chest* **99**, 81s-84s (1991).

8 Ghosh, A. K., Quaggin, S. E. & Vaughan, D. E. Molecular basis of organ fibrosis: potential therapeutic approaches. *Exp Biol Med (Maywood)* **238**, 461-481, doi:10.1177/1535370213489441 (2013).

9 Wolters, P. J., Collard, H. R. & Jones, K. D. Pathogenesis of idiopathic pulmonary fibrosis. *Annual review of pathology* **9**, 157-179, doi:10.1146/annurev-pathol-012513-104706 (2014).

10 King, T. E., Jr., Pardo, A. & Selman, M. Idiopathic pulmonary fibrosis. *Lancet* **378**, 1949-1961, doi:10.1016/s0140-6736(11)60052-4 (2011).

11 Gunther, A. *et al.* Unravelling the progressive pathophysiology of idiopathic pulmonary fibrosis. *European respiratory review : an official journal of the European Respiratory Society* **21**, 152-160, doi:10.1183/09059180.00001012 (2012).

12 Balestrini, J. L., Chaudhry, S., Sarrazy, V., Koehler, A. & Hinz, B. The mechanical memory of lung myofibroblasts. *Integrative Biology* **4**, 410-421, doi:10.1039/C2IB00149G (2012).

13 Liu, B. A. *et al.* SH2 Domains Recognize Contextual Peptide Sequence Information to Determine Selectivity. *Molecular & Cellular Proteomics* **9**, 2391-2404, doi:10.1074/mcp.M110.001586 (2010).

14 Tschumperlin, D. J. Fibroblasts and the Ground They Walk On. *Physiology* **28**, 380-390, doi:10.1152/physiol.00024.2013 (2013).

15 Tomasek, J. J., Gabbiani, G., Hinz, B., Chaponnier, C. & Brown, R. A. Myofibroblasts and mechano-regulation of connective tissue remodelling. *Nat Rev Mol Cell Biol* **3**, 349-363, doi:10.1038/nrm809 (2002).

16 Du, J. *et al.* Integrin activation and internalization on soft ECM as a mechanism of induction of stem cell differentiation by ECM elasticity. *Proceedings of the National Academy of Sciences of the United States of America* **108**, 9466-9471, doi:10.1073/pnas.1106467108 (2011).

17 Darby, I. A., Laverdet, B., Bonté, F. & Desmoulière, A. Fibroblasts and myofibroblasts in wound healing. *Clinical, Cosmetic and Investigational Dermatology* **7**, 301-311, doi:10.2147/CCID.S50046 (2014).

18 Baum, J. & Duffy, H. S. Fibroblasts and Myofibroblasts: What are we talking about? *Journal of cardiovascular pharmacology* **57**, 376-379, doi:10.1097/FJC.0b013e3182116e39 (2011).

19 Krammer, A., Craig, D., Thomas, W. E., Schulten, K. & Vogel, V. A structural model for force regulated integrin binding to fibronectin's RGD-synergy site. *Matrix Biology* **21**, 139-147, doi:http://dx.doi.org/10.1016/S0945-053X(01)00197-4 (2002).

20 Mould, A. P. *et al.* Defining the topology of integrin alpha5beta1-fibronectin interactions using inhibitory anti-alpha5 and anti-beta1 monoclonal antibodies. Evidence that the synergy sequence of fibronectin is recognized by the amino-terminal repeats of the alpha5 subunit. *J Biol Chem* **272**, 17283-17292 (1997).

21 Mardon, H. J. & Grant, K. E. The role of the ninth and tenth type III domains of human fibronectin in cell adhesion. *FEBS Lett* **340**, 197-201 (1994).

22 Aota, S., Nomizu, M. & Yamada, K. M. The short amino acid sequence Pro-His-Ser-Arg-Asn in human fibronectin enhances cell-adhesive function. *J Biol Chem* **269**, 24756-24761 (1994).

23 Garcia, A. J., Schwarzbauer, J. E. & Boettiger, D. Distinct activation states of alpha5beta1 integrin show differential binding to RGD and synergy domains of fibronectin. *Biochemistry* **41**, 9063-9069 (2002).

24 Richeldi, L. *et al.* Efficacy and Safety of Nintedanib in Idiopathic Pulmonary Fibrosis. *New England Journal of Medicine* **370**, 2071-2082, doi:10.1056/NEJMoa1402584 (2014).

25 Raghu, G. *et al.* An official ATS/ERS/JRS/ALAT statement: idiopathic pulmonary fibrosis: evidence-based guidelines for diagnosis and management. *Am J Respir Crit Care Med* **183**, 788-824, doi:10.1164/rccm.2009-040GL (2011).

26 Brian D. Southern, M. Pirfenidone and Nintedanib: Novel Agents in the Treatment of Idiopathic Pulmonary Fibrosis. (Cleveland Clinic, 2015).

27 Scotton, C. J. & Chambers, R. C. Molecular targets in pulmonary fibrosis: the myofibroblast in focus. *Chest* **132**, 1311-1321, doi:10.1378/chest.06-2568 (2007).

28 Barker, T. H. *et al.* Thy-1 regulates fibroblast focal adhesions, cytoskeletal organization and migration through modulation of p190 RhoGAP and Rho GTPase activity. *Exp Cell Res* **295**, 488-496, doi:10.1016/j.yexcr.2004.01.026 (2004).

29 Cao, L. N., John; Larouche, Jacqueline; Zhang, Yuanyuan; Bachman, Haylee; Brown, Ashley; Holmgren, Lars; Barker, Thomas. Detection of an integrin binding mechanoswitch within fibronectin during tissue formation and fibrosis. *ACS Nano*.

30 Brown, A. C., Rowe, J. A. & Barker, T. H. Guiding epithelial cell phenotypes with engineered integrin-specific recombinant fibronectin fragments. *Tissue engineering. Part A* **17**, 139-150, doi:10.1089/ten.TEA.2010.0199 (2011).

31 Frantz, C., Stewart, K. M. & Weaver, V. M. The extracellular matrix at a glance. *J Cell Sci* **123**, 4195-4200, doi:10.1242/jcs.023820 (2010).

32 Mochitate, K., Pawelek, P. & Grinnell, F. Stress relaxation of contracted collagen gels: disruption of actin filament bundles, release of cell surface fibronectin, and down-regulation of DNA and protein synthesis. *Experimental cell research* **193**, 198-207 (1991).

33 Lo, C. M., Wang, H. B., Dembo, M. & Wang, Y. L. Cell movement is guided by the rigidity of the substrate. *Biophysical journal* **79**, 144-152, doi:10.1016/S0006-3495(00)76279-5 (2000).

34 Engler, A. J., Sen, S., Sweeney, H. L. & Discher, D. E. Matrix elasticity directs stem cell lineage specification. *Cell* **126**, 677-689, doi:10.1016/j.cell.2006.06.044 (2006).

35 Xian, X., Gopal, S. & Couchman, J. R. Syndecans as receptors and organizers of the extracellular matrix. *Cell and tissue research* **339**, 31-46, doi:10.1007/s00441-009-0829-3 (2010).

36 Leitinger, B. & Hohenester, E. Mammalian collagen receptors. *Matrix Biol* **26**, 146-155, doi:10.1016/j.matbio.2006.10.007 (2007).

37 Humphries, J., Byron, A, Humphries, M. Integrin ligands at a glance. *J Cell Sci* **119**, 3901-3903 (2006).

38 Harburger, D. S. & Calderwood, D. A. Integrin signalling at a glance. *J Cell Sci* **122**, 159-163, doi:10.1242/jcs.018093 (2009).

39 Pankov, R. & Yamada, K. M. Fibronectin at a glance. *J Cell Sci* **115**, 3861-3863 (2002).

40 Booth, A. J. *et al.* Acellular normal and fibrotic human lung matrices as a culture system for in vitro investigation. *Am J Respir Crit Care Med* **186**, 866-876, doi:10.1164/rccm.201204-0754OC (2012).

41 Huang, C. & Ogawa, R. Fibroproliferative disorders and their mechanobiology. *Connect Tissue Res* **53**, 187-196, doi:10.3109/03008207.2011.642035 (2012).

42 Brown, A. C., Fiore, V. F., Sulchek, T. A. & Barker, T. H. Physical and chemical microenvironmental cues orthogonally control the degree and duration of fibrosis-associated epithelial-to-mesenchymal transitions. *J Pathol* **229**, 25-35, doi:10.1002/path.4114 (2013).

43 Markowski, M. C., Brown, A. C. & Barker, T. H. Directing epithelial to mesenchymal transition through engineered microenvironments displaying orthogonal adhesive and mechanical cues. *J Biomed Mater Res A* **100**, 2119-2127, doi:10.1002/jbm.a.34068 (2012).

44 Raghu, G., Weycker, D., Edelsberg, J., Bradford, W. Z. & Oster, G. Incidence and prevalence of idiopathic pulmonary fibrosis. *Am J Respir Crit Care Med* **174**, 810-816, doi:10.1164/rccm.200602-163OC (2006).

45 Humphries, J. D., Byron, A. & Humphries, M. J. Integrin ligands at a glance. *Journal of cell science* **119**, 3901-3903, doi:10.1242/jcs.03098 (2006).

46 Humphries, M. J. The molecular basis and specificity of integrin-ligand interactions. *Journal of cell science* **97 (Pt 4)**, 585-592 (1990).

47 Watt, F. M. & Huck, W. T. S. Role of the extracellular matrix in regulating stem cell fate. *Nature Reviews Molecular Cell Biology* **14**, 467-473, doi:10.1038/nrm3620 (2013).

48 Schultz, G. S. & Wysocki, A. Interactions between extracellular matrix and growth factors in wound healing. *Wound repair and regeneration : official publication of the Wound Healing Society [and] the European Tissue Repair Society* **17**, 153-162, doi:10.1111/j.1524-475X.2009.00466.x (2009).

49 Herard, A. L. *et al.* Fibronectin and its alpha 5 beta 1-integrin receptor are involved in the wound-repair process of airway epithelium. *Am J Physiol* **271**, L726-733 (1996).

50 To, W. S. & Midwood, K. S. Plasma and cellular fibronectin: distinct and independent functions during tissue repair. *Fibrogenesis & tissue repair* **4**, 21, doi:10.1186/1755-1536-4-21 (2011).

51 Miyamoto, S., Katz, B. Z., Lafrenie, R. M. & Yamada, K. M. Fibronectin and integrins in cell adhesion, signaling, and morphogenesis. *Ann N Y Acad Sci* **857**, 119-129 (1998).

52 Hinz, B., Celetta, G., Tomasek, J. J., Gabbiani, G. & Chaponnier, C. Alpha-smooth muscle actin expression upregulates fibroblast contractile activity. *Mol Biol Cell* **12**, 2730-2741 (2001).

53 Goffin, J. M. *et al.* Focal adhesion size controls tension-dependent recruitment of alpha-smooth muscle actin to stress fibers. *J Cell Biol* **172**, 259-268, doi:10.1083/jcb.200506179 (2006).

54 Baron, M., Norman, D., Willis, A. & Campbell, I. D. STRUCTURE OF THE FIBRONECTIN TYPE 1 MODULE. *Nature* **345**, 642-646, doi:10.1038/345642a0 (1990).

55 Pickford, A. R., Potts, J. R., Bright, J. R., Phan, I. & Campbell, D. Solution structure of a type 2 module from fibronectin: Implications for the structure and function of the gelatin-binding domain. *Structure* **5**, 359-370, doi:10.1016/s0969-2126(97)00193-7 (1997).

56 Main, A. L., Harvey, T. S., Baron, M., Boyd, J. & Campbell, I. D. THE 3-DIMENSIONAL STRUCTURE OF THE 10TH TYPE-III MODULE OF FIBRONECTIN - AN INSIGHT INTO RGD-MEDIATED INTERACTIONS. *Cell* **71**, 671-678, doi:10.1016/0092-8674(92)90600-h (1992).

57 Gao, M. *et al.* Structure and functional significance of mechanically unfolded fibronectin type III1 intermediates. *Proceedings of the National Academy of Sciences* **100**, 14784-14789 (2003).

58 Krammer, A., Craig, D., Thomas, W. E., Schulten, K. & Vogel, V. A structural model for force regulated integrin binding to fibronectin's RGD-synergy site. *Matrix Biol* **21**, 139-147, doi:S0945053X01001974 [pii] (2002).

59 Yamada, K. M. *et al.* Recent advances in research on fibronectin and other cell attachment proteins. *Journal of cellular biochemistry* **28**, 79-97, doi:10.1002/jcb.240280202 (1985).

60 Akiyama, S. K., Nagata, K. & Yamada, K. M. Cell surface receptors for extracellular matrix components. *Biochimica et biophysica acta* **1031**, 91-110 (1990).

61 Dufour, S. *et al.* Attachment, spreading and locomotion of avian neural crest cells are mediated by multiple adhesion sites on fibronectin molecules. *EMBO J* **7**, 2661-2671 (1988).

62 Clark, E. A. & Brugge, J. S. Integrins and Signal Transduction Pathways: The Road Taken. *Science* **268**, 233-239, doi:10.2307/2886683 (1995).

63 Humphries, M. J. Integrin structure. *Biochemical Society Transactions* **28**, 311-340, doi:10.1042/0300-5127:0280311 (2000).

64 Hynes, R. O. Integrins: Bidirectional, allosteric signaling machines. *Cell* **110**, 673-687, doi:10.1016/s0092-8674(02)00971-6 (2002).

65 Ruoslahti, E. & Pierschbacher, M. D. New perspectives in cell adhesion: RGD and integrins. *Science* **238**, 491-497 (1987).

66 Pierschbacher, M. D. & Ruoslahti, E. CELL ATTACHMENT ACTIVITY OF FIBRONECTIN CAN BE DUPLICATED BY SMALL SYNTHETIC FRAGMENTS OF THE MOLECULE. *Nature* **309**, 30-33, doi:10.1038/309030a0 (1984).

67 Pierschbacher, M. D. & Ruoslahti, E. INFLUENCE OF STEREOCHEMISTRY OF THE SEQUENCE ARG-GLY-ASP-XAA ON BINDING-SPECIFICITY IN CELL-ADHESION. *Journal of Biological Chemistry* **262**, 17294-17298 (1987).

68 Smith, M. L. *et al.* Force-induced unfolding of fibronectin in the extracellular matrix of living cells. *PLoS biology* **5**, e268, doi:10.1371/journal.pbio.0050268 (2007).

69 Erickson, H. P. & Carrell, N. A. Fibronectin in extended and compact conformations. Electron microscopy and sedimentation analysis. *J Biol Chem* **258**, 14539-14544 (1983).

70 Soteriou, A., Clarke, A., Martin, S. & Trinick, J. Titin folding energy and elasticity. *Proc Biol Sci* **254**, 83-86, doi:10.1098/rspb.1993.0130 (1993).

71 Erickson, H. P. Reversible unfolding of fibronectin type III and immunoglobulin domains provides the structural basis for stretch and elasticity of titin and fibronectin. *Proc Natl Acad Sci U S A* **91**, 10114-10118 (1994).

72 Carr, P. A., Erickson, H. P. & Palmer, A. G., 3rd. Backbone dynamics of homologous fibronectin type III cell adhesion domains from fibronectin and tenascin. *Structure* **5**, 949-959 (1997).

73 Altroff, H. *et al.* Interdomain tilt angle determines integrin-dependent function of the ninth and tenth FIII domains of human fibronectin. *J Biol Chem* **279**, 55995-56003 (2004).

74 Oberhauser, A. F., Marszalek, P. E., Erickson, H. P. & Fernandez, J. M. The molecular elasticity of the extracellular matrix protein tenascin. *Nature* **393**, 181-185, doi:10.1038/30270 (1998).

75 Krammer, A., Lu, H., Isralewitz, B., Schulten, K. & Vogel, V. Forced unfolding of the fibronectin type III module reveals a tensile molecular recognition switch. *Proc Natl Acad Sci U S A* **96**, 1351-1356 (1999).

76 Craig, D., Krammer, A., Schulten, K. & Vogel, V. Comparison of the early stages of forced unfolding for fibronectin type III modules. *Proc Natl Acad Sci U S A* **98**, 5590-5595, doi:10.1073/pnas.101582198 (2001).

77 Oberhauser, A. F., Badilla-Fernandez, C., Carrion-Vazquez, M. & Fernandez, J. M. The mechanical hierarchies of fibronectin observed with single-molecule AFM. *J Mol Biol* **319**, 433-447, doi:10.1016/S0022-2836(02)00306-6 (2002).

78 Grant, R. P., Spitzfaden, C., Altroff, H., Campbell, I. D. & Mardon, H. J. Structural requirements for biological activity of the ninth and tenth FIII domains of human fibronectin. *The Journal of biological chemistry* **272**, 6159-6166 (1997).

79 Baneyx, G., Baugh, L. & Vogel, V. Coexisting conformations of fibronectin in cell culture imaged using fluorescence resonance energy transfer. *Proc Natl Acad Sci U S A* **98**, 14464-14468, doi:10.1073/pnas.251422998 (2001).

80 Baneyx, G., Baugh, L. & Vogel, V. Fibronectin extension and unfolding within cell matrix fibrils controlled by cytoskeletal tension. *Proc Natl Acad Sci U S A* **99**, 5139-5143, doi:10.1073/pnas.072650799

99/8/5139 [pii] (2002).

81 Chabria, M., Hertig, S., Smith, M. L. & Vogel, V. Stretching fibronectin fibres disrupts binding of bacterial adhesins by physically destroying an epitope. **1**, 135, doi:10.1038/ncomms1135

https://www.nature.com/articles/ncomms1135#supplementary-information (2010).

82 Cao, L. Z. *et al.* Phage-based molecular probes that discriminate force-induced structural states of fibronectin in vivo. *Proceedings of the National Academy of Sciences of the United States of America* **109**, 7251-7256, doi:DOI 10.1073/pnas.1118088109 (2012).

83 Cao, L. *et al.* Phage-based molecular probes that discriminate force-induced structural states of fibronectin in vivo. *Proc Natl Acad Sci U S A* **109**, 7251-7256, doi:10.1073/pnas.1118088109 (2012).

84 Morla, A., Zhang, Z. & Ruoslahti, E. Superfibronectin is a functionally distinct form of fibronectin. *Nature* **367**, 193-196, doi:10.1038/367193a0 (1994).

85 Hocking, D. C., Sottile, J. & McKeown-Longo, P. J. Fibronectin's III-1 module contains a conformation-dependent binding site for the amino-terminal region of fibronectin. *J Biol Chem* **269**, 19183-19187 (1994).

86 Ingham, K. C., Brew, S. A., Huff, S. & Litvinovich, S. V. Cryptic self-association sites in type III modules of fibronectin. *J Biol Chem* **272**, 1718-1724 (1997).

87 Zhong, C. *et al.* Rho-mediated contractility exposes a cryptic site in fibronectin and induces fibronectin matrix assembly. *J Cell Biol* **141**, 539-551 (1998).

88 Ohashi, T., Kiehart, D. P. & Erickson, H. P. Dynamics and elasticity of the fibronectin matrix in living cell culture visualized by fibronectin-green fluorescent protein. *Proc Natl Acad Sci U S A* **96**, 2153-2158 (1999).

89 Klotzsch, E. *et al.* Fibronectin forms the most extensible biological fibers displaying switchable force-exposed cryptic binding sites. *Proc Natl Acad Sci U S A* **106**, 18267-18272, doi:10.1073/pnas.0907518106 (2009).

90 Martino, M. M. & Hubbell, J. A. The 12th-14th type III repeats of fibronectin function as a highly promiscuous growth factor-binding domain. *FASEB journal : official publication of the Federation of American Societies for Experimental Biology* **24**, 4711-4721, doi:10.1096/fj.09-151282 (2010).

91 Martino, M. M. *et al.* Engineering the growth factor microenvironment with fibronectin domains to promote wound and bone tissue healing. *Science translational medicine* **3**, 100ra189, doi:10.1126/scitranslmed.3002614 (2011).

92 Martino, M. M. *et al.* Controlling integrin specificity and stem cell differentiation in 2D and 3D environments through regulation of fibronectin domain stability. *Biomaterials* **30**, 1089-1097 (2009).

93 Ng, S. P. *et al.* Designing an extracellular matrix protein with enhanced mechanical stability. *Proceedings of the National Academy of Sciences* **104**, 9633-9637, doi:10.1073/pnas.0609901104 (2007).

94 Akiyama, S. K., Yamada, S. S., Chen, W. T. & Yamada, K. M. Analysis of fibronectin receptor function with monoclonal antibodies: roles in cell adhesion, migration, matrix assembly, and cytoskeletal organization. *J Cell Biol* **109**, 863-875 (1989).

95 Zhang, Z. *et al.* The alpha v beta 1 integrin functions as a fibronectin receptor but does not support fibronectin matrix assembly and cell migration on fibronectin. *J Cell Biol* **122**, 235-242 (1993).

96 Zhang, Z., Vuori, K., Reed, J. C. & Ruoslahti, E. The alpha 5 beta 1 integrin supports survival of cells on fibronectin and up-regulates Bcl-2 expression. *Proc Natl Acad Sci U S A* **92**, 6161-6165 (1995).

97 Gronthos, S., Simmons, P. J., Graves, S. E. & Robey, P. G. Integrin-mediated interactions between human bone marrow stromal precursor cells and the extracellular matrix. *Bone* **28**, 174-181 (2001).

98 Stephansson, S. N., Byers, B. A. & Garcia, A. J. Enhanced expression of the osteoblastic phenotype on substrates that modulate fibronectin conformation and integrin receptor binding. *Biomaterials* **23**, 2527-2534 (2002).

99 Koistinen, P. *et al.* Depletion of alphaV integrins from osteosarcoma cells by intracellular antibody expression induces bone differentiation marker genes and suppresses gelatinase (MMP-2) synthesis. *Matrix biology : journal of the International Society for Matrix Biology* **18**, 239-251 (1999).

100 Cheng, S. L., Lai, C. F., Blystone, S. D. & Avioli, L. V. Bone mineralization and osteoblast differentiation are negatively modulated by integrin alpha(v)beta3. *Journal of bone and mineral research : the official journal of the American Society for Bone and Mineral Research* **16**, 277-288, doi:10.1359/jbmr.2001.16.2.277 (2001).

101 Keselowsky, B. G., Collard, D. M. & Garcia, A. J. Surface chemistry modulates focal adhesion composition and signaling through changes in integrin binding. *Biomaterials* **25**, 5947-5954, doi:10.1016/j.biomaterials.2004.01.062 (2004).

102 Roy, D. C. & Hocking, D. C. Recombinant fibronectin matrix mimetics specify integrin adhesion and extracellular matrix assembly. *Tissue Eng Part A* **19**, 558-570, doi:10.1089/ten.TEA.2012.0257 (2013).

103 Petrie, T. A., Capadona, J. R., Reyes, C. D. & Garcia, A. J. Integrin specificity and enhanced cellular activities associated with surfaces presenting a recombinant fibronectin fragment compared to RGD supports. *Biomaterials* **27**, 5459-5470, doi:S0142-9612(06)00585-0 [pii]

10.1016/j.biomaterials.2006.06.027 (2006).

104 Ochsenhirt, S. E., Kokkoli, E., McCarthy, J. B. & Tirrell, M. Effect of RGD secondary structure and the synergy site PHSRN on cell adhesion, spreading and specific integrin engagement. *Biomaterials* **27**, 3863-3874, doi:10.1016/j.biomaterials.2005.12.012 (2006).

105 Moursi, A. M., Globus, R. K. & Damsky, C. H. Interactions between integrin receptors and fibronectin are required for calvarial osteoblast differentiation in vitro. *J Cell Sci* **110 (Pt 18)**, 2187-2196 (1997).

106 Garcia, A. J., Vega, M. D. & Boettiger, D. Modulation of cell proliferation and differentiation through substrate-dependent changes in fibronectin conformation. *Mol Biol Cell* **10**, 785-798 (1999).

107 Keselowsky, B. G., Collard, D. M. & Garcia, A. J. Integrin binding specificity regulates biomaterial surface chemistry effects on cell differentiation. *Proc Natl Acad Sci U S A* **102**, 5953-5957, doi:10.1073/pnas.0407356102 (2005).

108 Hamidouche, Z. *et al.* Priming integrin alpha5 promotes human mesenchymal stromal cell osteoblast differentiation and osteogenesis. *Proc Natl Acad Sci U S A* **106**, 18587-18591, doi:10.1073/pnas.0812334106 (2009).

109 Lee, S. T. *et al.* Engineering integrin signaling for promoting embryonic stem cell self-renewal in a precisely defined niche. *Biomaterials* **31**, 1219-1226, doi:10.1016/j.biomaterials.2009.10.054 (2010).

110 Grose, R. *et al.* A crucial role of beta 1 integrins for keratinocyte migration in vitro and during cutaneous wound repair. *Development* **129**, 2303-2315 (2002).

111 Roy, D. C., Mooney, N. A., Raeman, C. H., Dalecki, D. & Hocking, D. C. Fibronectin matrix mimetics promote full-thickness wound repair in diabetic mice. *Tissue Eng Part A* **19**, 2517-2526, doi:10.1089/ten.TEA.2013.0024 (2013).

112 Lutolf, M. P. & Hubbell, J. A. Synthetic biomaterials as instructive extracellular microenvironments for morphogenesis in tissue engineering. *Nature biotechnology* **23**, 47-55, doi:10.1038/nbt1055 (2005).

113 Petrie, T. A. *et al.* The effect of integrin-specific bioactive coatings on tissue healing and implant osseointegration. *Biomaterials* **29**, 2849-2857, doi:10.1016/j.biomaterials.2008.03.036 (2008).

114 Kisiel, M. *et al.* Improving the osteogenic potential of BMP-2 with hyaluronic acid hydrogel modified with integrin-specific fibronectin fragment. *Biomaterials* **34**, 704-712, doi:10.1016/j.biomaterials.2012.10.015 (2013).

115 Paluch, E. K. *et al.* Mechanotransduction: use the force(s). *BMC Biology* **13**, 47, doi:10.1186/s12915-015-0150-4 (2015).

116 Vogel, V. & Sheetz, M. Local force and geometry sensing regulate cell functions. *Nat Rev Mol Cell Biol* **7**, 265-275, doi:10.1038/nrm1890 (2006).

117 Brown, A. E. & Discher, D. E. Conformational changes and signaling in cell and matrix physics. *Curr Biol* **19**, R781-789, doi:10.1016/j.cub.2009.06.054 (2009).

118 Riveline, D. *et al.* Focal contacts as mechanosensors: externally applied local mechanical force induces growth of focal contacts by an mDia1-dependent and ROCK-independent mechanism. *J Cell Biol* **153**, 1175-1186 (2001).

119 Balaban, N. Q. *et al.* Force and focal adhesion assembly: a close relationship studied using elastic micropatterned substrates. *Nat Cell Biol* **3**, 466-472, doi:10.1038/35074532 (2001).

120 Gardel, M. L., Schneider, I. C., Aratyn-Schaus, Y. & Waterman, C. M. Mechanical integration of actin and adhesion dynamics in cell migration. *Annu Rev Cell Dev Biol* **26**, 315-333, doi:10.1146/annurev.cellbio.011209.122036 (2010).

121 Geiger, B. & Yamada, K. M. Molecular Architecture and Function of Matrix Adhesions. *Cold Spring Harbor Perspectives in Biology* **3**, 10.1101/cshperspect.a005033 a005033, doi:10.1101/cshperspect.a005033 (2011).

122 Dumbauld, D. W. *et al.* How vinculin regulates force transmission. *Proc Natl Acad Sci U S A* **110**, 9788-9793, doi:10.1073/pnas.1216209110 (2013).

123 Wang, Y. *et al.* Visualizing the mechanical activation of Src. *Nature* **434**, 1040-1045, doi:10.1038/nature03469 (2005).

124 Friedland, J. C., Lee, M. H. & Boettiger, D. Mechanically activated integrin switch controls alpha5beta1 function. *Science* **323**, 642-644, doi:10.1126/science.1168441 (2009).

125 Wang, N., Butler, J. P. & Ingber, D. E. Mechanotransduction across the cell surface and through the cytoskeleton. *Science* **260**, 1124-1127 (1993).

126 Kong, F. *et al.* Cyclic mechanical reinforcement of integrin-ligand interactions. *Mol Cell* **49**, 1060-1068, doi:10.1016/j.molcel.2013.01.015 (2013).

127 Kong, F., García, A. J., Mould, A. P., Humphries, M. J. & Zhu, C. Demonstration of catch bonds between an integrin and its ligand. *The Journal of Cell Biology* **185**, 1275 (2009).

128 Thomas, S. M. & Brugge, J. S. Cellular functions regulated by Src family kinases. *Annu Rev Cell Dev Biol* **13**, 513-609, doi:10.1146/annurev.cellbio.13.1.513 (1997).

129 Shattil, S. J. Integrins and Src: dynamic duo of adhesion signaling. *Trends Cell Biol* **15**, 399-403, doi:10.1016/j.tcb.2005.06.005 (2005).

130 Legate, K. R. & Fassler, R. Mechanisms that regulate adaptor binding to beta-integrin cytoplasmic tails. *J Cell Sci* **122**, 187-198, doi:10.1242/jcs.041624 (2009).

131 Arias-Salgado, E. G., Lizano, S., Shattil, S. J. & Ginsberg, M. H. Specification of the direction of adhesive signaling by the integrin beta cytoplasmic domain. *J Biol Chem* **280**, 29699-29707, doi:10.1074/jbc.M503508200 (2005).

132 Moore, S. W., Roca-Cusachs, P. & Sheetz, M. P. Stretchy proteins on stretchy substrates: the important elements of integrin-mediated rigidity sensing. *Dev Cell* **19**, 194-206, doi:10.1016/j.devcel.2010.07.018 (2010).

133 Levental, K. R. *et al.* Matrix crosslinking forces tumor progression by enhancing integrin signaling. *Cell* **139**, 891-906, doi:10.1016/j.cell.2009.10.027 (2009).

134 Sorrell, J. M. & Caplan, A. I. Fibroblasts-a diverse population at the center of it all. *Int Rev Cell Mol Biol* **276**, 161-214, doi:10.1016/s1937-6448(09)76004-6 (2009).

135 Kuhn, C. & McDonald, J. A. The roles of the myofibroblast in idiopathic pulmonary fibrosis. Ultrastructural and immunohistochemical features of sites of active extracellular matrix synthesis. *Am J Pathol* **138**, 1257-1265 (1991).

136 Ramos, C. *et al.* Fibroblasts from idiopathic pulmonary fibrosis and normal lungs differ in growth rate, apoptosis, and tissue inhibitor of metalloproteinases expression. *Am J Respir Cell Mol Biol* **24**, 591-598, doi:10.1165/ajrcmb.24.5.4333 (2001).

137 Miki, H. *et al.* Fibroblast contractility: usual interstitial pneumonia and nonspecific interstitial pneumonia. *Am J Respir Crit Care Med* **162**, 2259-2264, doi:10.1164/ajrccm.162.6.9812029 (2000).

138 Zhang, H. Y., Gharaee-Kermani, M. & Phan, S. H. Regulation of lung fibroblast alpha-smooth muscle actin expression, contractile phenotype, and apoptosis by IL-1beta. *J Immunol* **158**, 1392-1399 (1997).

139 Danowski, B. A. Fibroblast contractility and actin organization are stimulated by microtubule inhibitors. *J Cell Sci* **93 (Pt 2)**, 255-266 (1989).

140 Sixt, M. Cell migration: Fibroblasts find a new way to get ahead. *The Journal of Cell Biology* **197**, 347-349, doi:10.1083/jcb.201204039 (2012).

141 Li, S. *et al.* Hydrogels with precisely controlled integrin activation dictate vascular patterning and permeability. *Nature Materials* **advance online publication**, doi:10.1038/nmat4954

http://www.nature.com/nmat/journal/vaop/ncurrent/abs/nmat4954.html#supplementary-information (2017).

142 Plow, E. F., Haas, T. A., Zhang, L., Loftus, J. & Smith, J. W. Ligand binding to integrins. *J Biol Chem* **275**, 21785-21788, doi:10.1074/jbc.R000003200 (2000).

143 Akiyama, S. K. Integrins in cell adhesion and signaling. *Hum Cell* **9**, 181-186 (1996).

144 Boregowda, R. K., Krovic, B. M. & Ritty, T. M. Selective integrin subunit reduction disrupts fibronectin extracellular matrix deposition and fibrillin 1 gene expression. *Mol Cell Biochem* **369**, 205-216, doi:10.1007/s11010-012-1383-y (2012).

145 Girós, A., Grgur, K., Gossler, A. & Costell, M. α5β1 Integrin-Mediated Adhesion to Fibronectin Is Required for Axis Elongation and Somitogenesis in Mice. *PLOS ONE* **6**, e22002, doi:10.1371/journal.pone.0022002 (2011).

146 Mittal, A., Pulina, M., Hou, S.-Y. & Astrof, S. Fibronectin and integrin alpha 5 play requisite roles in cardiac morphogenesis. *Developmental Biology* **381**, 73-82, doi:https://doi.org/10.1016/j.ydbio.2013.06.010 (2013).

147 Pankov R, Y. K. Fibronectin at a glance. *J Cell Sci* **115**, 3861-3863 (2002).

148 Schiller, H. B. *et al.* beta1- and alphav-class integrins cooperate to regulate myosin II during rigidity sensing of fibronectin-based microenvironments. *Nat Cell Biol* **15**, 625-636, doi:10.1038/ncb2747 (2013).

149 Altroff, H. *et al.* Interdomain tilt angle determines integrin-dependent function of the ninth and tenth FIII domains of human fibronectin. *J Biol Chem* **279**, 55995-56003, doi:Doi 10.1074/Jbc.M406976200 (2004).

150 Brown, A. C., Dysart, M. M., Clarke, K. C., Stabenfeldt, S. E. & Barker, T. H. Integrin alpha3beta1 Binding to Fibronectin Is Dependent on the Ninth Type III Repeat. *J Biol Chem* **290**, 25534-25547, doi:10.1074/jbc.M115.656702 (2015).

151 Bryksin, A. V. *et al.* One Primer To Rule Them All: Universal Primer That Adds BBa_B0034 Ribosomal Binding Site to Any Coding Standard 10 BioBrick. *ACS Synthetic Biology* **3**, 956-959, doi:10.1021/sb500047r (2014).

152 Schense, J. C. & Hubbell, J. A. Cross-linking exogenous bifunctional peptides into fibrin gels with factor XIIIa. *Bioconjug Chem* **10**, 75-81 (1999).

153 Humphries, M. J. in *Extracellular Matrix Protocols* Vol. 522 *Methods in Molecular Biology* (eds Sharona Even-Ram & Vira Artym) Ch. 14, 203-210 (Humana Press, 2009).

154 Altroff, H. *et al.* The Eighth FIII Domain of Human Fibronectin Promotes Integrin α5β1 Binding via Stabilization of the Ninth FIII Domain. *Journal of Biological Chemistry* **276**, 38885-38892, doi:10.1074/jbc.M105868200 (2001).

155 Carlsson, J., AxÉN, R. & Unge, T. Reversible, Covalent Immobilization of Enzymes by Thiol-Disulphide Interchange. *European Journal of Biochemistry* **59**, 567-572, doi:10.1111/j.1432-1033.1975.tb02483.x (1975).

156 Nurden, A. T., Nurden, P., Sanchez, M., Andia, I. & Anitua, E. Platelets and wound healing. *Front Biosci* **13**, 3532-3548 (2008).

157 Kendall, R. T. & Feghali-Bostwick, C. A. Fibroblasts in fibrosis: novel roles and mediators. *Frontiers in Pharmacology* **5**, 123, doi:10.3389/fphar.2014.00123 (2014).

158 Klingberg, F., Hinz, B. & White, E. S. The myofibroblast matrix: implications for tissue repair and fibrosis. *J Pathol* **229**, 298-309, doi:10.1002/path.4104 (2013).

159 Ye, F., Kim, C. & Ginsberg, M. H. Reconstruction of integrin activation. *Blood* **119**, 26-33, doi:10.1182/blood-2011-04-292128 (2012).

160 Katsumi, A., Orr, A. W., Tzima, E. & Schwartz, M. A. Integrins in mechanotransduction. *J Biol Chem* **279**, 12001-12004, doi:10.1074/jbc.R300038200 (2004).

161 Obara, M., Kang, M. S. & Yamada, K. M. Site-directed mutagenesis of the cell-binding domain of human fibronectin: Separable, synergistic sites mediate adhesive function. *Cell* **53**, 649-657, doi:http://dx.doi.org/10.1016/0092-8674(88)90580-6 (1988).

162 Frank, A. O. *et al.* Conformational Control of Integrin-Subtype Selectivity in isoDGR Peptide Motifs: A Biological Switch. *Angewandte Chemie International Edition* **49**, 9278-9281, doi:10.1002/anie.201004363 (2010).

163 Kuo, J.-C., Han, X., Hsiao, C.-T., Yates, J. R. & Waterman, C. M. Analysis of the myosinII-responsive focal adhesion proteome reveals a role for β-Pix in negative regulation of focal adhesion maturation. *Nature cell biology* **13**, 383-393, doi:10.1038/ncb2216 (2011).

164 Pasapera, A. M., Schneider, I. C., Rericha, E., Schlaepfer, D. D. & Waterman, C. M. Myosin II activity regulates vinculin recruitment to focal adhesions through FAK-mediated paxillin phosphorylation. *The Journal of Cell Biology* **188**, 877-890, doi:10.1083/jcb.200906012 (2010).

165 Choquet, D., Felsenfeld, D. P. & Sheetz, M. P. Extracellular matrix rigidity causes strengthening of integrin-cytoskeleton linkages. *Cell* **88**, 39-48 (1997).

166 Huang, X. *et al.* Matrix Stiffness–Induced Myofibroblast Differentiation Is Mediated by Intrinsic Mechanotransduction. *American Journal of Respiratory Cell and Molecular Biology* **47**, 340-348, doi:10.1165/rcmb.2012-0050OC (2012).

167 Velasquez, L. S. *et al.* Activation of MRTF-A–dependent gene expression with a small molecule promotes myofibroblast differentiation and wound healing. *Proceedings of the National Academy of Sciences of the United States of America* **110**, 16850-16855, doi:10.1073/pnas.1316764110 (2013).

168 Olson, E. N. & Nordheim, A. Linking actin dynamics and gene transcription to drive cellular motile functions. *Nat Rev Mol Cell Biol* **11**, 353-365, doi:10.1038/nrm2890 (2010).

169 Fiore, V. F. *et al.* Conformational coupling of integrin and Thy-1 regulates Fyn priming and fibroblast mechanotransduction. *J Cell Biol* **211**, 173-190, doi:10.1083/jcb.201505007 (2015).

170 Lygoe, K. A., Norman, J. T., Marshall, J. F. & Lewis, M. P. αv integrins play an important role in myofibroblast differentiation. *Wound Repair and Regeneration* **12**, 461-470, doi:10.1111/j.1067-1927.2004.12402.x (2004).

171 Asano, Y., Ihn, H., Yamane, K., Jinnin, M. & Tamaki, K. Increased Expression of Integrin αvβ5 Induces the Myofibroblastic Differentiation of Dermal Fibroblasts. *The American Journal of Pathology* **168**, 499-510, doi:http://dx.doi.org/10.2353/ajpath.2006.041306 (2006).

172 Stutchbury, B., Atherton, P., Tsang, R., Wang, D.-Y. & Ballestrem, C. Distinct focal adhesion protein modules control different aspects of mechanotransduction. *Journal of Cell Science* **130**, 1612 (2017).

173 Roca-Cusachs, P., Gauthier, N. C., del Rio, A. & Sheetz, M. P. Clustering of α(5)β(1) integrins determines adhesion strength whereas α(v)β(3) and talin enable mechanotransduction. *Proceedings of the National Academy of Sciences of the United States of America* **106**, 16245-16250, doi:10.1073/pnas.0902818106 (2009).

174 Galbraith, C. G., Yamada, K. M. & Sheetz, M. P. The relationship between force and focal complex development. *The Journal of Cell Biology* **159**, 695 (2002).

175 Chang, Y. *et al.* A General Approach for Generating Fluorescent Probes to Visualize Piconewton Forces at the Cell Surface. *Journal of the American Chemical Society* **138**, 2901-2904, doi:10.1021/jacs.5b11602 (2016).

176 Stabley, D. R., Jurchenko, C., Marshall, S. S. & Salaita, K. S. Visualizing mechanical tension across membrane receptors with a fluorescent sensor. *Nat Meth* **9**, 64-67, doi:10.1038/nmeth.1747

http://www.nature.com/nmeth/journal/v9/n1/abs/nmeth.1747.html#supplementary-information (2012).

177 Jurchenko, C., Chang, Y., Narui, Y., Zhang, Y. & Salaita, K. S. Integrin-generated forces lead to streptavidin-biotin unbinding in cellular adhesions. *Biophysical journal* **106**, 1436-1446 (2014).

178 Henderson, N. C. *et al.* Targeting of alphav integrin identifies a core molecular pathway that regulates fibrosis in several organs. *Nature medicine* **19**, 1617-1624, doi:10.1038/nm.3282 (2013).

179 Patan, S. Vasculogenesis and angiogenesis. *Cancer Treat Res* **117**, 3-32 (2004).

180 Jiang, B., Liou, G. I., Behzadian, M. A. & Caldwell, R. B. Astrocytes modulate retinal vasculogenesis: effects on fibronectin expression. *Journal of cell science* **107 (Pt 9)**, 2499-2508 (1994).